ENHANCING RETAIL INVESTOR PORTFOLIOS WITH BEHAVIOR-BASED MODELS AND PARTICLE SWARM OPTIMIZATION

WANG XIANHE

PhD

The Hong Kong Polytechnic University

2026

The Hong Kong Polytechnic University

Department of Industrial and Systems Engineering

Enhancing Retail Investor Portfolios with Behavior-based Models and Particle Swarm Optimization

WANG Xianhe

A thesis submitted in partial fulfillment of the requirements for the degree of Doctor of Philosophy

August 2025

CERTIFICATE OF ORIGINALITY

I hereby declare that this thesis is my own work and that, to the best of my knowledge and belief, it reproduces no material previously published or written, nor material that has been accepted for the award of any other degree or diploma, except where due acknowledgment has been made in the text.

______________________________(Signed)

WANG Xianhe (Name of student)

Abstract

Portfolio selection is a critical decision-making problem in financial engineering, where investors strive to optimize the balance between risk and return. While classical models, such as Markowitz's mean-variance theory, have laid the foundation for portfolio optimization, they often fail to account for the psychological biases and complex behaviors exhibited by real-world investors, particularly retail investors. These models also struggle under extreme market conditions and high-dimensional, non-convex optimization spaces, where computational challenges such as premature convergence and local optima arise. This research addresses these significant limitations by developing innovative portfolio selection models and enhanced optimization algorithms.

The novelty of this work lies in its integration of behavioral finance with advanced optimization techniques, specifically tailored to the needs of retail investors. First, a multi-objective portfolio selection model which simultaneously incorporates prospect theory, disappointment theory, and expected utility theory is proposed. This novel combination allows the model to better reflect investor behavior under uncertainty by balancing the pursuit of returns with the avoidance of extreme losses. Additionally, a second portfolio model incorporates multiple fuzzy reference points to capture the dynamic behavior of return chasing, a common phenomenon in investor decision-making. This model offers a more adaptive approach, avoiding overly conservative or aggressive investment strategies and improving risk control.

To address the computational challenges of local optimal and premature convergence, two

advanced variants of the particle swarm optimization algorithm will be introduced. These algorithms overcome the common problems of premature convergence and local optima by decomposing the swarm into sub-swarms with distinct iteration strategies and introducing adaptive parameter optimization via deep deterministic policy gradient techniques. These enhancements significantly improve the efficiency and accuracy of particle swarm optimization in solving complex optimization problems in behavioral portfolio selection.

The results of this study show that the proposed portfolio models outperform traditional approaches in terms of return-risk balancing, particularly under extreme market conditions. The enhanced particle swarm optimization algorithms demonstrate superior performance in high-dimensional, non-convex problems, consistently finding optimal solutions more efficiently than standard particle swarm optimization methods. The effectiveness of the models and algorithms is verified through extensive comparisons with state-of-the-art techniques, proving their practical applicability and advancing the state of knowledge in portfolio selection and optimization.

The contributions of this study lie in how a behaviorally ground, multi-objective portfolio selection model, a multi-reference point extension of prospect theory, and two collaborative-adaptive particle swarm algorithms collectively address the empirical gaps of investor irrationality and algorithmic premature convergence. Case studies on real-market data validate that the proposed portfolio selection models consistently deliver higher risk-adjusted returns than classical and contemporary benchmarks, while computational studies demonstrate the superiority and generality of the proposed particle swarm algorithm variants. This study charts future research on real-time reference point calibration, hybrid heuristic-convex optimization, and resource-aware optimization algorithms, laying a roadmap for more adaptive and resilient portfolio selection framework under uncertainty.

Acknowledgments

I would extend profound appreciation to Prof. Chak Yin Tang and Prof. Nick Chung for their invaluable guidance, sustained support, and unwavering patience throughout the doctoral program. Their perceptive advice and rigorous academic training were pivotal in shaping the research direction and fostering intellectual growth. Deep gratitude is also owed to Prof. Bo Wang for the encouragement offered during the most challenging stages of the Ph.D. journey and for the substantial assistance that enabled the completion of the Ph.D. studies.

I am also deeply grateful to the faculty members and research fellows at The Hong Kong Polytechnic University— Zichun Wei, Guochong Qiu, Chi Sun, Zijie Sun, and Ziqi Wu—whose meticulous comments, generous sharing of data, and sustained encouragement have sharpened both the theoretical underpinnings and empirical analyses of this dissertation. I owe special thanks to my former chief supervisor, Dr. Long Teng, for his unwavering mentorship, strategic insight, and patient guidance during the formative stages of my doctoral journey. Beyond PolyU, I have been fortunate to collaborate with a circle of colleagues and friends whose spirited discussions, timely advice, and warm companionship provided intellectual stimulation and emotional balance, transforming this academic pursuit into a truly rewarding experience.

Heartfelt appreciation is extended to my family for their unwavering love, support, and understanding. Their steady encouragement has been a constant source of strength, especially throughout the most challenging phases of the Ph.D. journey.

Contents

List of Figures

List of Tables

Chapter 1

INTRODUCTION

1.1 Background

Portfolio selection, as a cornerstone of modern financial theory, involves the strategic allocation of assets to achieve specific investment goals, balancing risk and return through diversification. The seminal work of Harry Markowitz [1] in the 1950s introduced the mean-variance optimization framework, revolutionizing portfolio selection by quantifying risk-return tradeoffs mathematically [2]. Markowitz's model assumes rational investors who maximize expected utility based on normally distributed returns—a paradigm that dominated financial theory for decades. Subsequent developments, such as the capital asset pricing model [3] and arbitrage pricing theory [4], extended this framework by incorporating systematic risk factors and macroeconomic variables. However, these models retain foundational assumptions of investor rationality and market efficiency, which increasingly clash with empirical observations of real-world market behavior.

The rise of behavioral finance in the late 20th century challenged these classical assumptions [5], demonstrating that investors often deviate from rational decision-making due to cognitive biases and emotional responses. Retail investors, who constitute over 40% of global equity market participation, exemplify this divergence. In emerging markets like China, retail investors dominate trading volumes, accounting for approximately 85% of daily transactions on the Shanghai Stock Exchange [6]. In contrast to institutional investors, individual investors commonly display return-chasing behavior — tilting portfolios toward assets with recent outperformance — and marked loss aversion, whereby the disutility from losses exceeds the utility derived from gains of equal magnitude [7]. These behaviors are amplified during market volatility, as seen in the 2015 Chinese stock market crash, where panic selling triggered by breaching psychological price thresholds exacerbated systemic risks.

Behavioral anomalies are not confined to emerging markets. Even in mature markets like the U.S., retail investors display overconfidence in their ability to time markets and anchoring bias, clinging to historical price levels despite new information. Such biases distort portfolio decisions, leading to suboptimal diversification, excessive trading, and vulnerability to market shocks. For instance, during the 2020 COVID-19 market downturn, retail investors disproportionately poured capital into speculative assets like "meme stocks" (e.g., GameStop [8]), driven by social media influence and herd mentality - a phenomenon poorly captured by traditional models.

The limitations of conventional portfolio frameworks extend beyond behavioral oversight. Mathematically, high-dimensional optimization — essential for managing portfolios with hundreds of assets — faces the curse of dimensionality, where computational complexity escalates exponentially [9]. Non-convex objective functions, arising from transaction costs, liquidity constraints, or behavioral utility functions, further complicate optimization [10]. Heuristic algorithms like particle swarm optimization [11] have gained traction for solving such problems, yet their application remains constrained by premature convergence and susceptibility to local optima, particularly in noisy financial datasets.

Technological advancements, such as algorithmic trading and big data analytics, have reshaped market dynamics, introducing new challenges. High-frequency trading amplifies short-term volatility, while environmental, social, and governance investing introduces non-financial criteria into portfolio decisions [12]. These shifts demand adaptive models that reconcile quantitative rigor with behavioral realism — a gap this research seeks to address by integrating prospect theory, multi-objective optimization, and enhanced algorithms.

By bridging behavioral insights with computational advances, this study aims to redefine portfolio selection for an era where human psychology and algorithmic complexity coexist. The following sections elaborate on the research gaps, significance, objectives and methodologies developed to achieve this synthesis.

1.2 Research Gaps

Most existing portfolio selection studies are grounded in expected utility theory, a framework that assumes rational decision-making and often fails to account for the behavioral biases of investors, particularly in the presence of asset value volatility [13]. While some research has incorporated prospect theory to address behavioral factors under conditions of risk and uncertainty [14, 15, 16, 17, 18], there remains a significant gap in understanding how extreme market scenarios influence investor behavior. Specifically, the impact of events where investment returns fall below an investor's psychological thresholds — referred to as the "psychological lower bounds" — has not been adequately explored. This oversight limits the robustness and practical applicability of existing portfolio selection models, especially in scenarios characterized by significant market stress or downturns.

Loss aversion is the most prominent finding in prospect theory, which captures decision-makers' over-reactions to losses compared with gains of the same magnitude [19]. However, an exclusive focus on loss aversion in portfolio models can lead to overly conservative strategies. The behavioral phenomenon of return chasing, where investors disproportionately favor assets with recent positive performance, is often neglected [3]. This omission risks underestimating the dynamic interplay of behavioral factors, leading to models that do not fully reflect the complexities of real-world investor behavior.

In summary, the first research gap identified in this study lies in the incomplete characterization of retail investors' behavioral patterns within existing prospect theory-based portfolio models, particularly under market conditions marked by uncertainty and risk. These models exhibit limited predictive capacity for investor decision-making when confronted with unanticipated events. From a practical perspective, current frameworks demonstrate a polarized tendency: they either adopt excessively aggressive strategies vulnerable to low-probability market shocks, or overly conservative approaches that fail to deliver satisfactory returns for investors.

On the other hand, recent advancements in prospect theory and portfolio selection research have led to behaviorally-based portfolio models with mathematically complex structures — often non-convex and non-smooth — that defy efficient numerical resolution using existing methods [20]. Compounding this challenge, real-world equity pools typically entail high-dimensional portfolio selection optimization, imposing prohibitive computational burdens. Collectively, these factors constitute the second research gap: From a methodological perspective, high-dimensional optimization problems, particularly those that are non-convex or non-smooth, pose significant challenges. PSO, despite its wide use as a heuristic, is prone to premature convergence and to becoming trapped in local optima when tackling highly complex optimization landscapes. These challenges hinder the efficacy of PSO in consistently identifying optimal solutions for behavioral portfolio selection models, especially in high-stakes scenarios.

1.3 Significance

Portfolio selection is a critical area of study within decision-making and management engineering, addressing the complex interplay between capital market dynamics and investor decision-making paradigms [21]. The intrinsic complexity of financial markets, coupled with pervasive behavioral biases, renders the attainment of predefined investment objectives a persistent challenge for both retail and institutional investors. Behavioral finance has highlighted the profound impact of psychological biases on investment decisions, underscoring the need for models and strategies that not only accommodate these biases but also leverage them to optimize portfolio outcomes [22].

The significance of portfolio selection research lies in its ability to provide both theoretical and practical frameworks for constructing diversified, risk-adjusted investment portfolios [23]. These contributions are essential for enhancing investment efficiency and resilience when confronting of evolving market dynamics, technological advancements, and shifting investor behaviors. By bridging the gap between behavioral insights and quantitative methods, progress in portfolio selection research is essential for advancing financial management practices and improving decision making processes [24].

Optimization techniques are indispensable across various engineering and scientific domains, including electrical power systems, signal processing, and financial engineering. Among these, PSO stands out due to its simplicity, computational efficiency, and adaptability to numerous optimization problems, particularly those that are high-dimensional, non-convex, or non-smooth [25].

PSO's continued relevance stems from its ability to tackle complex problems effectively, offering a robust alternative to traditional optimization methods. Its significance extends beyond its current applications, as ongoing research seeks to enhance its performance, address challenges such as premature convergence, and expand its applicability to new and emerging fields [26]. By improving the reliability and scalability of PSO, this research contributes to the broader goal of solving intricate optimization problems across disciplines, thereby reinforcing its value as a versatile and practical computational tool.

1.4 Research Objectives

The overall goal of this research is to develop innovative portfolio selection models that integrate behavioral insights and advanced optimization techniques, with the aim of improving investment strategies, particularly for retail investors, in the context of market volatility and uncertainty. Traditional portfolio selection models fail to adequately account for behavioral biases such as loss aversion, return chasing, and the psychological lower bounds that influence investor decisions under extreme market conditions. This research seeks to bridge these gaps by proposing two new models that better reflect the complexities of real-world investor behavior while providing robust solutions to high-dimensional portfolio optimization problems. In response to the research gaps identified earlier, this study establishes three research objectives. The specific objectives of this research are as follows:

To address the first research gap: behavioral-based portfolio models' incompleteness and narrowness, this study tries to provide comprehensive explanatory frameworks for retail investors' decision-making behavioral in investment markets characterized by uncertainty and risk. The first research gap will be filled in by pursing the first and second research objectives. And the second research gap will be filled in by pursing the third research objective.

1. The first research objective is development of multi-objective portfolio selection model by integrating multiple retail investor behavioral decision theories. Leveraging cutting-edge insights from retail investor portfolios, a multi-objective portfolio selection framework will be adopted to strengthen the model's reliability while balancing profits and risks. The goal of this research is to offer a more comprehensive explanatory framework for investor preferences, based on widely observed and confirmed behavioral biases such as loss aversion.

2. The second research objective is enhancement of prospect theory by encompassing diverse decision biases. Develop a prospect theory-based multiple reference points model to capture return chasing, address dynamic investor behavior, and mitigate loss aversion-driven conservatism. Integrate risk constraints into portfolio selection for diversification and enhanced risk control.

3. To address the second research gap: premature convergence and local minima in solution algorithms, the third research objective focuses on algorithmic innovation by optimizing

the architecture and parameters of the PSO algorithm. The third objective enhances PSO for high-dimensional non-convex portfolio optimization, addressing local optima and premature convergence via collaborative-adaptive mechanisms. This objective aims to deliver rapid precision for portfolio selection while serving as a general tool for similar problems.

1.5 Thesis Outlines

An overview of the research project of this study is illustrated in Figure 1.1, which visually elucidates the organizational architecture and the logical interdependencies among its constituent components. The thesis commences with an introductory chapter (Chapter 1) that contextualizes the challenges inherent in modern portfolio selection, particularly the dual imperatives of balancing financial returns with risk management while addressing behavioral phenomena such as return chasing. Traditional models, while foundational, often struggle with high-dimensional, non-convex optimization problems and fail to account for extreme risks or investor psychology.

The two research gaps were introduced in Section 1.2, the first will be discussed further in Section 2.1 and Section 2.2 while the other will be discussed further in Section 2.3. This study intends to provide comprehensive portfolio selection frameworks to capture retail investors' diverse decision behaviors through dual perspectives to resolve to resolve the first research gap: 1. Development of multi-objective model integrating multiple behavioral decision theories, formalized as the first research objective. 2. Enhancement of prospect theory encompassing diverse decision biases, designated as the second research objective. To address the second research gap, this study intends to develop PSO algorithm through iterative strategy optimizing, which constitutes the third research objective.

The subsequent chapter (Chapter 2) delves into a comprehensive literature review, tracing the evolution of portfolio theory from the Markowitz mean-variance paradigm to behavioral finance approaches. It critiques existing methodologies for their limited scalability

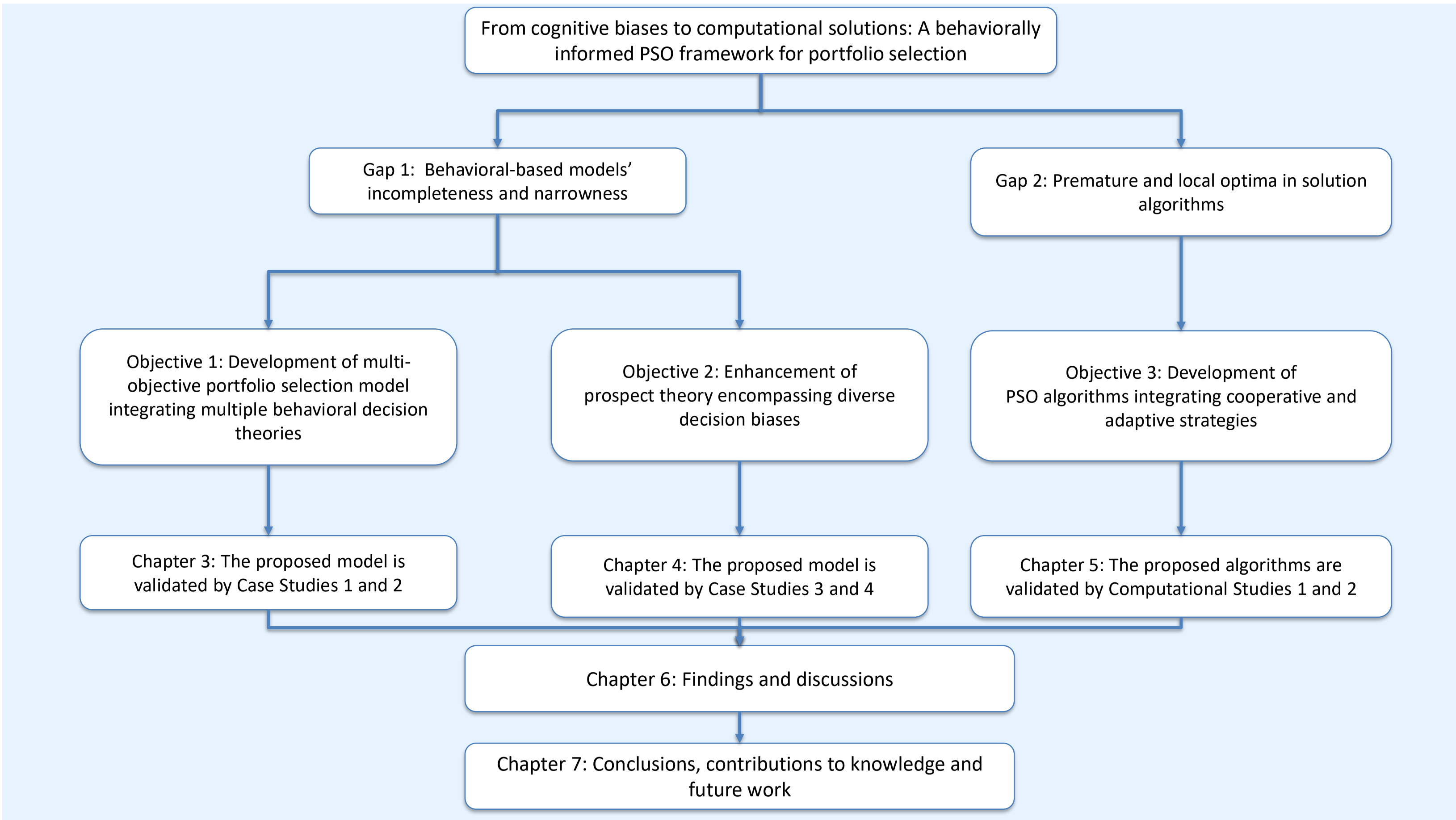

Figure 1.1: Overview of the research project.

in high-dimensional contexts and their oversight of behavioral biases, thereby justifying the need for the proposed frameworks. This critique highlights the innovation of incorporating multi-reference points — investor-specific benchmarks — and extreme risk metrics, which collectively address both computational and psychological dimensions of portfolio selection.

Chapter 3 corresponds to the first research objective , a multi-objective portfolio selection model will be provided and its effectiveness in balancing return and risk will be validated by Case Studies 1 and 2. The specific research methodology of this multi-objective portfolio selection model will be presented in Chapter 3. Chapter 4 corresponds to the second research objective, a two reference points portfolio selection model will be provided and its effectiveness in balancing return and risk will be validated by Case Studies 3 and 4. The specific research methodology of this multiple reference points framework will be presented in Chapter 4. Chapter 5 corresponds to the third research objective, two PSO algorithms serve as the solver to the proposed portfolio selection models will be provided and their effectiveness in finding reliable solutions will be validated by Computational Studies 1 and 2. The specific research methodology of these two algorithms will be presented in Chapter 5.

Chapter 6 synthesizes the findings and discusses how the proposed models and algorithms advance portfolio theory and practice. The final chapter (Chapter 7) systematically reviews and synthesizes the entirety of the study, while critically delineating the substantive contributions from this study and explores practical implications for investors and financial institutions, particularly in volatile markets. The thesis concludes by outlining future research trajectories, such as extending the frameworks to dynamic market conditions or incorporating additional behavioral factors, ensuring its relevance in an ever-evolving financial landscape. This structure ensures a cohesive narrative, blending theoretical rigor with empirical validation to address critical gaps in portfolio optimization.

Chapter 2

LITERATURE REVIEW

This chapter forms the vital link between the foundational context established in Chapter 1 and the dissertation's original contributions. It is divided into three mutually reinforcing sections. Section 2.1 reviews traditional portfolio theories—including Markowitz's mean–variance model and capital asset pricing model—and clarifies why they fall short in explaining real-world retail investor behavior. Section 2.2 turns to behavioral finance, summarizing core psychological biases such as loss aversion, overconfidence, and herding, and showing how these biases help explain market anomalies and inconsistent portfolio choices. Section 2.3 introduces modern computational techniques capable of incorporating those behavioral nuances while tackling the non-convex optimization challenges they create. Together, these sections set the stage for the dissertation's central goal: developing a behaviorally enriched portfolio-selection framework that combines psychological realism with computational practicality, laying the groundwork for the model development, empirical tests, and policy insights presented in later chapters.

2.1 Portfolio Selection: Markowitz to Behavioral-based Models

Diversification and optimization to portfolio have always been pivotal to the evolution of financial engineering and to the direction of investment decision-making. This section presents a review of various methods that have been proposed to tackle the practical difficulties associated with applying portfolio optimization techniques.

This section provides a systematic review of classical portfolio selection frameworks, focusing on their theoretical underpinnings, methodological assumptions, and practical applications. By critically examining these foundational models, the section lays the groundwork for understanding the limitations that motivate modern portfolio selection theory integrates the insights from behavioral finance. The section is organized into three interconnected subsections. Section 2.1.1 opens by outlining the foundational tenets of classical portfolio selection models. These models form the bedrock of quantitative finance and remain widely used despite their assumptions of rationality, market efficiency, and static risk preferences. Section 2.1.2 then shifts focus to the empirical and theoretical critiques of these models, highlighting key shortcomings such as their inability to account for investor psychology, market inefficiencies, and dynamic risk perceptions. This subsection demonstrates how classical frameworks often fail to align with real-world investment behaviors, particularly in volatile or crisis-driven markets. Finally, Section 2.1.3 synthesizes the most pressing unresolved challenges and emerging research directions of portfolio selection. This subsection not only identifies the hottest topics — such as adaptive portfolio optimization, machine learning integration, and behavioral risk modeling — but also explicitly outlines the specific contributions of this dissertation. By linking the limitations of existing models to the opportunities for innovation, this subsection bridges the gap between theoretical critiques and the practical advancements proposed in subsequent chapters. Together, these subsections create a cohesive narrative that transitions from foundational knowledge to critical analysis and forward-looking insights, setting the stage for the dissertation's novel contributions to behaviorally enriched portfolio selection.

2.1.1 Origin and Background Information of Portfolio Selection

In recent decades, academia have seen an accelerated evolution in portfolio selection since it was first proposed by Markowitz in 1952 [1]. Commonly known as modern portfolio theory, this framework addressed a key issue in finance: how investors should distribute their capital across various investment opportunities. Markowitz pioneered a quantitative framework in which a financial asset's performance and uncertainty are captured by two statistics: expected return to represent the level of payoff meanwhile the level of risk is quantified by standard deviation. He then emphasized that investors ought to evaluate return and risk jointly, selecting investment allocations based on the trade-off between the two [2]. The resulting mean–variance optimization model proposes that, given numerous portfolios achieving the same expected return, the optimal choice is the one with the lowest associated variance. The efficient frontier in its feasible plane is formed by the set of efficient strategies. Figure 2.1 illustrates this frontier for portfolios composed of risky assets. Any portfolio lying off the frontier is "inefficient", since for a given expected return it entails strictly higher variance — and therefore greater risk [21].

Consider a financial market consisting of n assets $S_1, S_2, \cdots, S_n$, each associated with an uncertain return $r_1, r_2, \cdots, r_n$. Let the return vector be denoted by $\mathbf{r} = [r_1, r_2, \cdots, r_n]^\top$. A portfolio is denoted by its allocation $\mathbf{x} = [x_1, x_2, \cdots, x_n]^\top$, where x_i indicates the investment proportion of asset i. Then the portfolio return r_p can be expressed as:

$$r_p = x_1 r_1 + x_2 r_2 + \cdots + x_n r_n = \mathbf{x}^\top \mathbf{r}. \tag{2.1}$$

Standard deviation of r_i is denoted by σ_i, and correlation coefficient between r_i and r_j is ρ_{ij}. Then a symmetric $n \times n$ matrix Σ could denote the covariance relations between asset

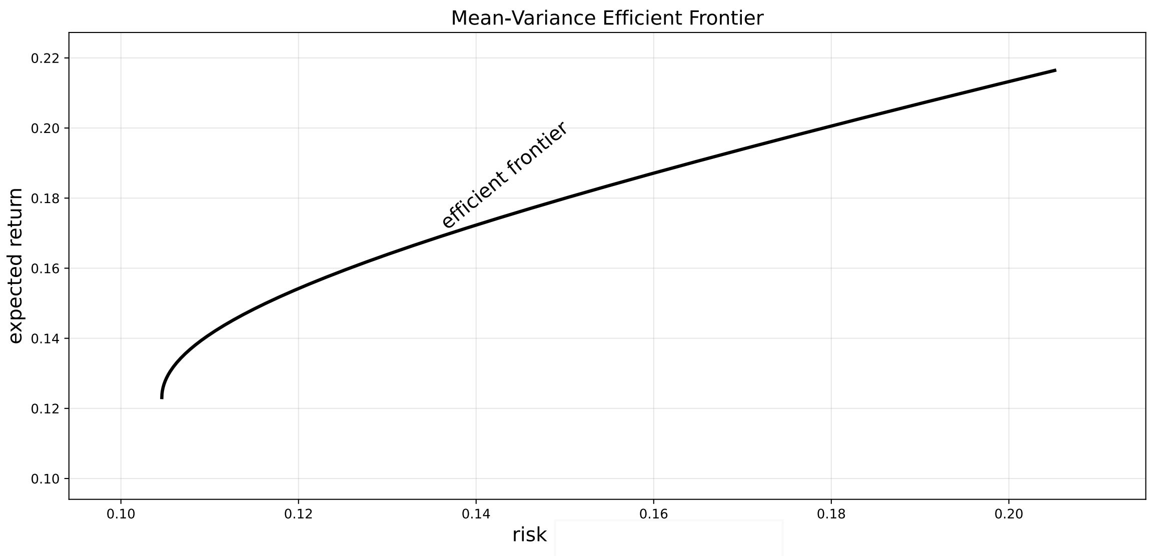

Figure 2.1: Mean-variance efficient frontier.

returns.

$$\Sigma = \begin{bmatrix} \sigma_{11} & \sigma_{12} & \cdots & \sigma_{1n} \\ \sigma_{21} & \sigma_{22} & \cdots & \sigma_{2n} \\ \vdots & \vdots & \ddots & \vdots \\ \sigma_{n1} & \sigma_{n2} & \cdots & \sigma_{nn} \end{bmatrix}, \tag{2.2}$$

where $\sigma_{ii} = \sigma_i^2$ and $\sigma_{ij} = \sigma_{ji} = \rho_{ij}\sigma_i\sigma_j$ for $i \neq j$. The covariance matrix satisfies $\mathbf{x}^\top \Sigma \mathbf{x} \geq 0$, $\forall \mathbf{x}$, or equivalently, all its eigenvalues must be nonnegative.

For a given portfolio allocation $\mathbf{x}$, its variance and standard deviation are given by:

$$V(\mathbf{x}) = \mathbf{x}^\top \Sigma \mathbf{x}, \qquad \sigma(\mathbf{x}) = \sqrt{\mathbf{x}^\top \Sigma \mathbf{x}}. \tag{2.3}$$

$\sigma(\mathbf{x})$ represents the portfolio's volatility, is a commonly adopted metric for the risk borne by portfolio $\mathbf{x}$.

Based on these definitions, the mean–variance scheme can be formulated as:

$$\max_{\mathbf{x} \in \Omega} \mathbf{x}^\top \mathbf{r} - \lambda \cdot \mathbf{x}^\top \Sigma \mathbf{x}, \tag{2.4}$$

where the risk aversion parameter λ balances return and risk.

Alternative formulations are also available. One approach is to maximize the expected return while subject to a portfolio variance constraint:

$$\max_{\mathbf{x}\in\Omega} \mathbf{x}^\top \mathbf{r}, \quad \text{s.t.} \quad \mathbf{x}^\top \Sigma \mathbf{x} \leq \sigma_{\max}^2, \tag{2.5}$$

or to minimize the variance while ensuring that the portfolio return exceeds a threshold:

$$\min_{\mathbf{x}\in\Omega} \mathbf{x}^\top \Sigma \mathbf{x}, \quad \text{s.t.} \quad \mathbf{x}^\top \mathbf{r} \geq R_{\min}. \tag{2.6}$$

When the feasible region Ω contains only linear equality and inequality constraints, the mean-variance portfolio selection model specializes to a convex quadratic program which can be solved efficiently by standard numerical solvers. Modern portfolio optimization packages also accommodate richer specifications with non-linear constraints, like contribution caps and group-based risk limits.

In addition, these tools can impose discrete requirements, e.g., cardinality limits on the trading frequency or holding number. Dealing with similar type formulations typically calls for optimizers that support conic and mixed-integer programming; for an extensive discussion of numerical methods for portfolio selection models, see Fabozzi et al. [27].

2.1.2 Advances in Portfolio Selection

In this section, I will survey the most significant advances in portfolio selection in recent years, including incorporating transaction costs in portfolio selection, constraints in portfolio construction and mitigating the impacts of estimation errors.

Portfolio selection with transaction costs

Historically, trading costs were often excluded from this process and treated independently by trading desks. Decoupling allocation from cost considerations can yield portfolio weights that induce substantial turnover and, consequently, sizable transaction costs, thereby eroding risk-adjusted returns. Portfolio allocation procedure with transaction costs produces more cost-efficient portfolios and improves realized performance.

However, accounting for transaction costs increases the complexity of the optimization, especially in high-dimensional or dynamic settings. For example, Dai et al. [28] analyze a dynamic mean–variance portfolio selection framework considering transaction costs using a game-theoretical framework. Their results show that constant risk aversion in classical mean–variance models may lead to irrational strategies under transaction cost environments.

Transaction costs include both direct fees — like taxes, bid-ask spreads and commissions — and indirect costs like slippage. These vary across assets depending on liquidity. Typically, more liquid securities result in better post-cost performance. Ignoring transaction costs often results in inefficient portfolios. Therefore, modern portfolio managers integrate cost forecasting techniques when constructing portfolios.

Numerous models have been proposed to address transaction costs in the literature [29]. Many realistic formulations are nonlinear and non-quadratic. While cost-free models often lead to quadratic programs, the inclusion of transaction costs turns the mathematical model into a nonlinear program, which increases computational effort.

There are generally two solution strategies. The first, as in Ceria et al. [30], applies second-order cone programming (SOCP) to solve the nonlinear problem directly. The second approach relaxes the problem into a quadratic form, typically by approximating market impact functions using linear or quadratic expressions. Though such approximations introduce estimation errors, they benefit from faster computation with minimal loss in solution accuracy.

For instance, the following equivalence is used to handle square-root-based market impact models:

$$\min_{x_1,\cdots,x_N} \sum_{i=1}^{N} a_i x_i^{3/2} \tag{2.7}$$

is equivalent to:

$$\min_{x_1,\cdots,x_N,y_1,\cdots,y_N} \sum_{i=1}^{N} a_i y_i \quad \text{s.t.} \quad x_1^{3/2} \le y_1, \cdots, x_N^{3/2} \le y_N. \tag{2.8}$$

Additional discussions on transaction cost models can be found in [31].

Transaction costs significantly influence multi-period investment planning [2]. Realistic investors often focus on long-term performance, prompting the shift from static single-period models to dynamic multi-period frameworks. As market conditions evolve, investment strategies must adapt accordingly.

This growing need for dynamic rebalancing has spurred extensive research. Fu et al. [32] derived closed-form solutions for dynamic mean–variance problems under borrowing constraints. Li and Ng [33] offered an analytical formulation for multi-period optimization. Yao et al. [34] modeled interest rate changes using a discrete-time Vasicek process.

The differentiation between long-term and short-term optimization is well documented [35, 36]. Over long horizons, accurate forecasts become infeasible, leading to the adoption of rolling-horizon methods or step-wise optimization. This shift aligns with investor behavior in volatile environments [37, 38], pushing the field toward multi-period frameworks [39].

Multi-period models are often framed as stochastic control problems [38]. Investors must make daily allocation decisions, constantly revisited as new information arrives. Let $\mathbf{x}_t \in \mathbb{R}^{n+1}$ be the portfolio weights at time t, where the final component denotes the risk-free asset. The sum of weights is one.

A standard objective is to maximize the discounted, risk-adjusted return net of transaction and holding costs over a planning horizon T^{invest}:

$$\mathbb{E}\left[\sum_{t=0}^{T^{\text{invest}}-1} \eta^{t+1}\left(\mathbf{r}_{t+1}^{\top}\mathbf{x}_{t+1} - \gamma_{t+1}\phi_t(\mathbf{x}_{t+1})\right) - \eta^t\left(\phi_t^{\text{trade}}(\omega_{t+1}-\omega_t) + \phi_t^{\text{hold}}(\omega_{t+1})\right)\right], \tag{2.9}$$

where ϕ_t is a risk function, ϕ_t^{trade} is a transaction cost function, ϕ_t^{hold} is a holding cost function,

γ_t is a risk aversion coefficient, and $\eta \in (0, 1)$ is the discount factor.

Classic mean–variance insights, such as the Sharpe ratio and the One-Fund Theorem, may not hold in multi-period settings. For instance, incorporating a risk-free asset across time enhances cumulative returns, a concept known as the premium of dynamic trading [40].

Figure 2.2 shows how the efficient frontier shifts under various time horizons and portfolio constraints. As the investment period lengthens, the deviation between models with and without a risk-free asset becomes more evident.

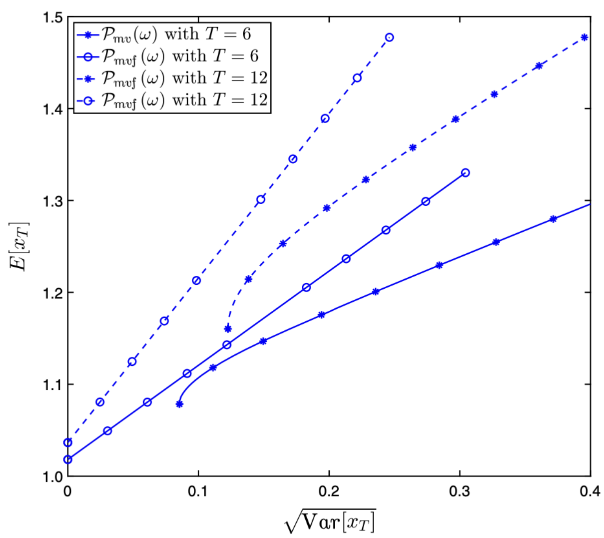

Figure 2.2: Comparison of efficient frontiers

Notes: $\mathcal{P}_{mv}$ represents the investment policy generated from multi-period mean-variance framework, $\mathcal{P}_{mvf}$ represents the policy from the same framework but includes risk-free asset. The horizontal axis is the risk indicator while the vertical axis is the return indicator.

Constraints in portfolio construction

Following Markowitz's seminal contribution, the mean–variance paradigm has been progressively extended to embed practical implementation restrictions, including long-only requirements. One of the notable strengths of this framework lies in its flexibility to handle diverse constraint types in quantitative portfolio construction.

These constraints may reflect investor preferences, regulatory requirements, or the discretion of portfolio managers. The algorithms and software implementations used within the mean–variance approach are equipped to manage such constraints in a robust and systematic manner. This adaptability allows portfolio customization based on client needs, risk tolerance, and regulatory rules, without modifying the core alpha or risk estimation models.

In the classical mean–variance setting, expected return is modeled as the portfolio's expected value, while risk is quantified via its variance — the average squared deviation from the expected value [2]. Building on this foundational concept, researchers have developed alternative risk measures. For example, Markowitz et al. [1] advanced the mean–semivariance formulation, which concentrates on downside risk by penalizing only returns falling below the expectation while disregarding favorable deviations. In a complementary direction, the mean–absolute deviation model [41] provides a robust dispersion measure that serves as an effective alternative to variance. Empirical studies indicate that mean-absolute deviation models often yield solutions similar to mean–variance portfolios but require significantly less computational time. The broader literature continues to address challenges arising from return uncertainty and market fluctuations [42].

Recent advances in portfolio optimization include the application of artificial intelligence (AI) methods. These range from neural network architectures — such as recurrent neural networks [43], variational recurrent neural networks [44], and long short-term memory networks [45] — to asset allocation tasks. Such models are particularly valuable in multi-criteria decision-making contexts, where they can handle complex nonlinearities and interdependencies.

To address the limitation of variance for failing to capture downside losses explicitly, the Value-at-Risk (VaR) metric [46, 47] is widely adopted to estimate potential losses with a specified probability level γ. VaR identifies the threshold loss level λ such that the probability of losses exceeding λ does not surpass $1-\gamma$:

$$\mathbf{VaR}_{1-\gamma}(\vec{L}) = \sup\{\lambda \mid \Pr(\vec{L} \geq \lambda) \geq \gamma\}. \tag{2.10}$$

Here, $\vec{L}$ denotes the loss variable. Although VaR is popular, it is often criticized for lacking smoothness, convexity, and being prone to local minima.

As an alternative, a coherent and convex risk measure Conditional Value-at-Risk (CVaR) [48] is proposed. CVaR represents the expected loss exceeding the VaR threshold, providing a more informative assessment:

$$\mathbf{CVaR}_{1-\gamma}(\vec{L}) = \mathbb{E}[x \mid x > \mathbf{VaR}_{1-\gamma}(\vec{L})]. \tag{2.11}$$

Alternatively, CVaR can also be computed without directly using the VaR:

$$\mathbf{CVaR}_{1-\gamma}(\vec{L}) = \max_{z} \left\{ z + \frac{1}{\gamma}\mathbb{E}[(x-z)^{+}] \right\}, \tag{2.12}$$

where $(x - z)^{+} = \max\{x - z, 0\}$.

Figure 2.3 provides an intuitive representation of VaR and CVaR for continuous distribution function. For details on CVaR under discontinuous distributions, see Rockafellar and Uryas [49]. Pflug [50] proves that CVaR satisfies key properties of a coherent risk measure, such as convexity. This makes CVaR not only theoretically appealing but also practically easier to optimize than VaR. As a result, many studies adopt CVaR in risk-based portfolio design [51, 52, 53].

Mitigating the impacts of estimation errors

Under the traditional mean–variance framework, investors are expected to provide estimations to the expected values and covariance matrix for all assets considered in the portfolio. However, given the large number of available financial instruments, this task becomes highly complex. Portfolio managers often lack detailed insights into every company, industry, or sector they are exposed to. Instead, they tend to specialize in specific areas to optimize performance.

This limitation is one of the reasons why the mean–variance optimization model has not

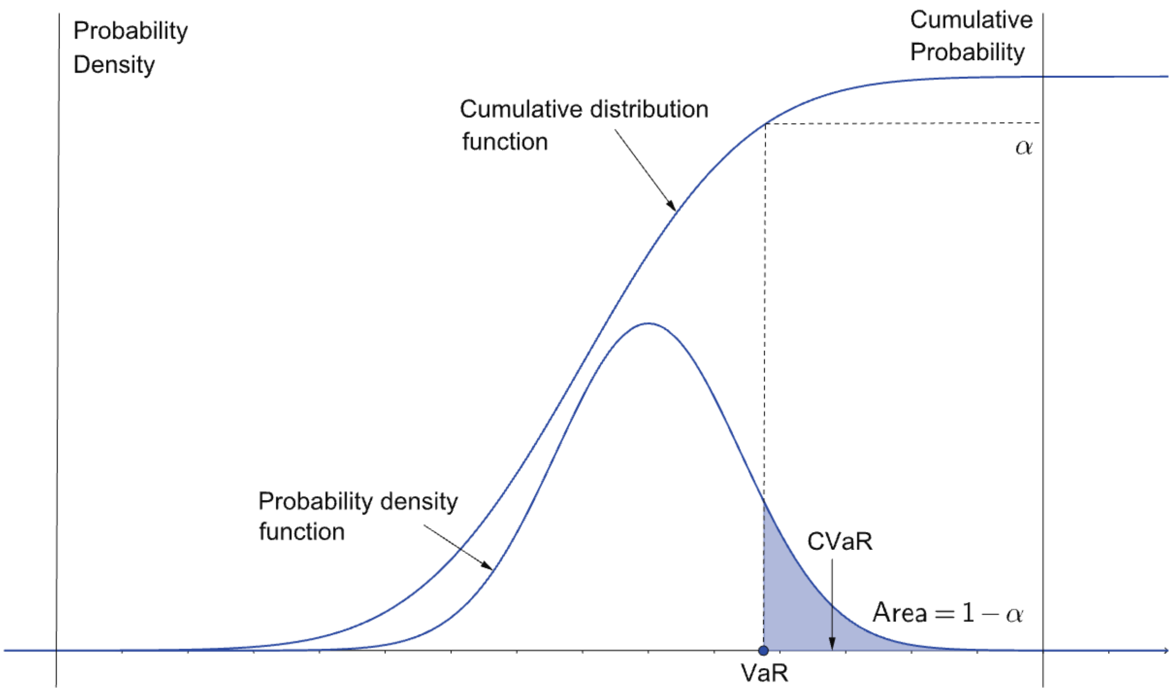

Figure 2.3: Comparison of VaR and CVaR

been more widely adopted in practice. Expecting managers to provide accurate parameter estimates is unrealistic—especially considering the potential estimation errors involved [21]. Moreover, most portfolio optimization models treat these estimates as deterministic and ignore their inherent uncertainty. Relying solely on point estimates for expected returns and covariances, without accounting for estimation risk, can lead to unreliable allocations [54].

To mitigate these limitations, contemporary portfolio optimization explicitly incorporates uncertainty in both expected returns and risk measures within the model, leading to more realistic formulations. One prominent avenue is the adoption of fuzzy set theory, which offers a non-probabilistic framework for representing imprecise and vague information as an alternative to classical probability theory [55].

Fuzzy models are particularly helpful when historical data is limited or when returns follow nonstatistical patterns. In such cases, linguistic and heuristic knowledge can supplement missing data [56]. Consequently, fuzzy set theory has emerged as a practical tool for modeling return uncertainty in financial decision-making.

For example, a bi-criteria fuzzy portfolio model is proposed by Dymova et al. [57], questioning the reliability of variance as a sole risk measure. Liu et al. [58] focused on multi-period fuzzy portfolio selection, considering factors like return, transaction cost, and skewness. Mehlawat et al. [59] developed credibility-based fuzzy models to better reflect investor preferences. Mansour et al. [60] also integrated satisfaction functions to capture human judgment. Dymova et al. [57] further proposed a two-stage fuzzy model using trading signals and parameter fuzzification.

While early work in behavioral finance relied on precise numerical evaluations [19, 54], it is now recognized that decision-making often involves qualitative assessments. Thus, fuzzy logic models, including intuitionistic [15], hesitant [61], and linguistic fuzzy sets [62], have been increasingly used.

Fuzzy decision theory, originally introduced by Bellman and Zadeh [63], defines decisions over fuzzy alternatives and constraints. Let A denote the set of alternatives, $\bar{g}_m$ the M fuzzy goals, and $\bar{c}_n$ the N fuzzy constraints. Then the feasible fuzzy decision set is:

$$\bar{S} = \bar{g}_1 \cap \bar{g}_2 \cap \cdots \cap \bar{g}_M \cap \bar{c}_1 \cap \bar{c}_2 \cap \cdots \cap \bar{c}_N. \tag{2.13}$$

The associated membership function is defined as:

$$\xi_{\bar{S}} = \min\{\xi_{\bar{g}_1} \cap \xi_{\bar{g}_2} \cap \cdots \cap \xi_{\bar{g}_M} \cap \xi_{\bar{c}_1} \cap \xi_{\bar{c}_2} \cap \cdots \cap \xi_{\bar{c}_N}\}. \tag{2.14}$$

The optimal (crisp) decision is then determined by:

$$S^O = \{a^* \in A \mid a^* \in \arg\max \xi_{\bar{S}}(x)\}. \tag{2.15}$$

A visual representation is given in Figure 2.4. For more detailed exposition, refer to Bellman and Zadeh [63] and Zimmermann [64].

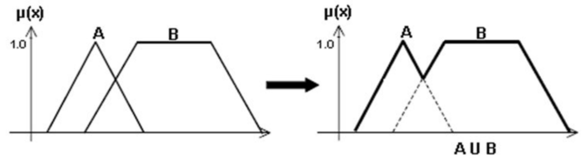

Figure 2.4: Fuzzy decision.

2.1.3 Research Gaps in Portfolio Selection

As what have been discussed earlier, while real-world financial markets are inherently uncertain and complex, most theoretical models remain relatively simplistic. Therefore, further efforts are needed to bridge this gap and improve the practical applicability of these models. One such improvement involves considering the variation in investment horizons across different securities in dynamic portfolio selection. Moreover, current research often assumes that returns of risky assets follow a normal distribution. In contrast, elliptical distributions may offer a more accurate representation of return behavior under real-world uncertainty.

In actual investment scenarios, investors are concerned with understanding current market conditions, anticipating future developments, and identifying strategies for constructing optimal portfolios. Thus, integrating forecasting methodologies with investors' subjective beliefs presents a promising research avenue. Existing studies [17, 65] primarily emphasize earnings prediction as an input for portfolio optimization, typically incorporating both fundamental and statistical risk models. Additionally, forecasting stock prices using financial statements is gaining attention, as it allows investors to complement objective technical indicators with personal judgment.

Notably, while existing behavioral-based portfolio selection models demonstrate theoretical rigor, they predominantly focus on decision-making within singular market regimes. However, real-world retail investors face significant challenges in predicting future market conditions. Therefore, developing a comprehensive portfolio selection framework that systematically accommodates investor behavior across diverse potential market conditions remains an imperative research endeavor. In this study, a model-driven approach by structurally refining portfolio models to develop the comprehensive portfolio selection framework. The detailed descriptions of this framework will be provided in Chapter 3.

2.2 Prospect Theory and Retail Investor Portfolio

Retail investor portfolio research focuses on understanding investor behavior and its influence on financial markets. It enhances the field of investor psychology by incorporating behavioral traits of retail investors into asset pricing frameworks. This line of research explores how retail investors form their investment decisions, interpret fundamental information, and respond to both financial and non-financial influences that shape their actions [5].

This section delves into the integration of retail investor portfolio principles, particularly prospect theory, into portfolio selection models, aiming to provide a more realistic framework that accounts for psychological biases and emotional influences on retail investor decision-making. Section 2.2.1 introduces the foundational concepts and theoretical underpinnings of retail investor portfolio, highlighting why market anomalies and irrational decisions can find a clue in mental schemes and emotions. This subsection highlights the shortcomings of conventional frameworks by juxtaposing classical asset–pricing models—focused solely on utilitarian payoffs—with behavioral asset–pricing approaches that also account for expressive and affective benefits, as well as cognitive and emotional biases. Section 2.2.2 builds upon this foundation by examining the application of prospect theory in portfolio selection, focusing on key psychological phenomena like loss aversion, probability distortion, and reference dependency. It discusses how these elements influence risk perception and decision-making under uncertainty, and evaluates existing models' effectiveness in capturing these complex behaviors. Finally, Section 2.2.3 identifies the most pressing issues and promising research directions in the field of prospect theory and retail investor portfolios. This subsection not only lists the hottest topics—such as dynamic modeling, alternative risk measures, and real-world validations—but also highlights specific contributions from this dissertation, including innovative approaches to addressing behavioral biases and optimizing portfolio strategies. Through this structured exploration, the section bridges the gap between theoretical insights and practical applications, laying the groundwork for subsequent chapters that will propose and validate new models integrating behavioral finance with advanced optimization techniques.

By logically progressing from foundational concepts to critical analysis and future directions, this section provides a comprehensive overview of how retail investor portfolio and prospect theory can enhance our understanding of retail investor behavior and improve portfolio management practices.

2.2.1 Origin and Background Information of Prospect Theory and Retail Investor Portfolio

One core premise in conventional financial theory is that investors behave rationally. However, empirical findings have consistently demonstrated that real-world investors often fail to act in line with this assumption, even though they aim to maximize returns and minimize risk. The foundational work of Kahneman and Tversky [19, 66] in judgment and decision-making marked a significant shift, initiating the emergence of behavioral finance by bridging finance with psychology. Behavioral finance incorporates psychological influences, such as heuristic-driven decisions and irrational arbitrage constraints [13].

Empirical analyses of modern portfolio theory applied to actual investment scenarios often reveal discrepancies and anomalies. Due to these discrepancies, communication between financial advisors and clients becomes challenging when utilizing modern portfolio theory structures, as its assumptions may not align with real-world investor behavior [7]. Within this context, retail investor portfolio models seek to manage consumption risk based on both initial wealth and uncertain labor income streams [20].

Shefrin and Statman [67] introduced a retail investor model grounded in Roy's [68] safety-first principle. Unlike the variance-based risk assessment in traditional models, this approach defines risk as the probability that final wealth falls below a critical threshold — termed ruin. Roy's model suggests that investors seek to reduce this probability. Building on this, Telser [69] proposed an acceptable upper limit for ruin probability, defining a portfolio as safe when this threshold is not exceeded. This retail investor model not only embraces Roy's safety-first paradigm but also incorporates behavioral components. Specifically, it integrates Lopes' [70] security potential aspiration theory and the mental accounting framework rooted in prospect theory. Security potential aspiration theory claims that investment decisions are guided by three components—security, potential, and aspiration — which are emotionally driven by fear and hope. Fear encourages preservation of wealth, while hope motivates risk-taking in pursuit of higher returns. The model embeds these two affective factors by applying a probability–weighting transformation to the outcome distribution, thereby producing a distorted distribution that reflects their influence. The presence of fear or hope modifies the perception of probabilities by overweighting the likelihood of extreme outcomes—either very bad or very good. As a consequence, expected wealth is assessed under an inverse S-shaped probability-weighting function that converts the objective probability into its subjectively perceived counterpart. This transformation replaces the traditional expectation $\mathbb{E}(W)$ with a distorted expectation $\mathbb{E}_\pi(W)$, where π is a probability distortion function. Under Lopes' framework, the notion of aspiration generalizes the subsistence threshold into a broader target level that investors strive to achieve.

Accordingly, portfolio risk is interpreted as the probability of lower than its aspiration level. Behavioral portfolio models, aligned with prospect theory, employ mental accounting mechanisms, in which retail investors compartmentalize their financial goals (e.g., retirement, education, inheritance) into sub-portfolios, each governed by its own aspiration level. Rather than viewing the portfolio holistically, investors manage separate mental accounts with individual risk tolerances. Hence, the objective becomes maximizing the weighted expected wealth across these accounts, subject to maintaining the probability of lower than its allowable aspiration level α:

$$\max \mathbb{E}_\pi(W) \\ \text{s.t.} \quad \mathbb{P}(W < A) < \alpha, \tag{2.16}$$

Prospects are mathematically modeled as a set of outcomes $A = \{(p_1, m_1), \ldots, (p_n, m_n)\}$, where each outcome m_i occurs with probability p_i for $i = 1, \ldots, n$. Outcomes are interpreted with a comparison to its reference point r, such that $m > r$ represents a gain, whereas $m < r$ indicates a loss.

Within the framework of prospect theory, a weighted probability function $\mathbf{w}$ and a distorted utility function $\mathbf{U}$ are employed to represent how individuals evaluate prospects. The overall subjective value of a prospect A under prospect theory is expressed as:

$$A \to \mathrm{PT}_r[A] = \int_{m \le r} \mathbf{U}(m)\, d\mathbf{w}(A) + \int_{m > r} \mathbf{U}(m)\, d\mathbf{w}(1 - A). \tag{2.17}$$

If the weighting function $\mathbf{w}$ is linear, this formulation collapses into the conventional expected utility model:

$$A \to \mathrm{RU}(A) = \int m\, dA. \tag{2.18}$$

This study adopts the utility and weighting functions proposed by Kahneman and Tversky in their prospect theory. The utility function is asymmetric and decides how an outcome is a gain or a loss. Specifically, the value function $\mathbf{U}(m)$ is defined as:

$$\mathbf{U}(m) = \begin{cases} (m - r)^\alpha, & \text{if } m \ge r, \\ \lambda \cdot (r - m)^\alpha, & \text{if } m < r, \end{cases} \tag{2.19}$$

where $\alpha = 0.88$ controls the curvature of the function, and $\lambda = -2.25$ reflects the loss aversion parameter. The gain and loss utilities are represented in Figure 2.5, where the red and green curves illustrate the respective cases, intersecting at the reference point.

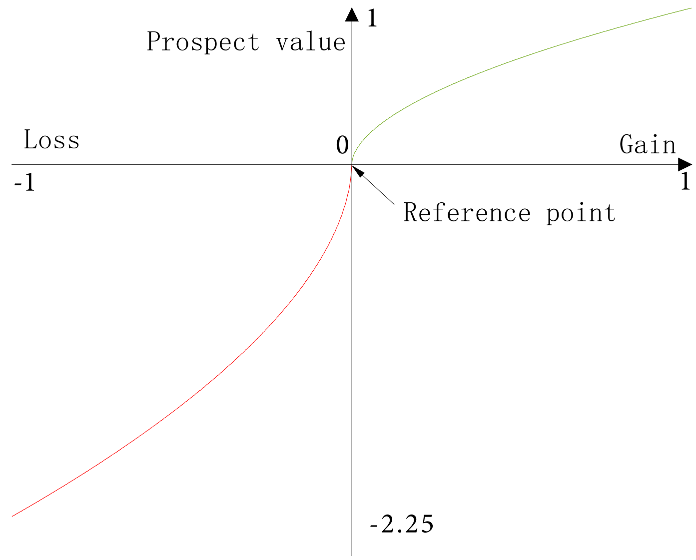

Figure 2.5: Gain-loss utility function.

Reference dependency means the investor evaluates portfolio outcomes through comparison with reference point r, not through outcome m alone. Hence, the same terminal wealth distribution can be perceived as containing more losses (or fewer gains) depending on reference point. In portfolio selection, reference point is often modeled as (i) the risk-free benchmark, (ii) a target/goal wealth level, or (iii) an expectations-based benchmark (endogenized reference point).

Loss aversion is the kink at $m - r = 0$: for equal-magnitude deviations, losses receive multiplicatively larger disutility than gains provide utility, goverened by $\lambda > 1$. In portfolio selection, this typically increases aversion to downside risk around the reference point and can lower optimal exposure to risky assets (or increase demand for downside protection), even when expected returns are attractive. In the perspective of portfolio selection, if a marginal increase in risky weight produces a roughly symmetric $\pm$ change in benchmark-relative wealth, loss aversion implies the investor will require substantially higher upside to justify that exposure.

Under prospect theory, the value function has an S-shaped curve with a noticeably steeper tend on the loss section, capturing loss aversion. This asymmetry reflects a robust behavioral regularity: decision makers are typically risk sensitive over gains but gambling over losses, exhibiting disproportionate sensitivity to losses relative to equivalent gains.

The corresponding weighted probability functions with respect to gain and loss are given by:

$$\begin{cases} w^{+}(\mathrm{Pr}_g) = \dfrac{\mathrm{Pr}_g^{\sigma}}{\left(\mathrm{Pr}_g^{\sigma} + (1 - \mathrm{Pr}_g)^{\sigma}\right)^{1/\sigma}}, \\ w^{-}(\mathrm{Pr}_l) = \dfrac{\mathrm{Pr}_l^{\delta}}{\left(\mathrm{Pr}_l^{\delta} + (1 - \mathrm{Pr}_l)^{\delta}\right)^{1/\delta}}, \end{cases} \tag{2.20}$$

where w^{+} and w^{-} are the decision weights assigned to gain and loss outcomes, respectively. Pr_g and Pr_l denote the objective probabilities of gain and loss, while σ and δ are the gan and loss curvature parameters.

Figure 2.6 illustrates the nonlinear shape of the probability weighting function. This function is continuous and strictly increasing, enabling flexible modeling of perceived probabilities. In practice, decision-makers are used to overweight low-probability outcomes and underweight high-probability ones, which supports the inclusion of nonlinear transformations in modeling decision behavior.

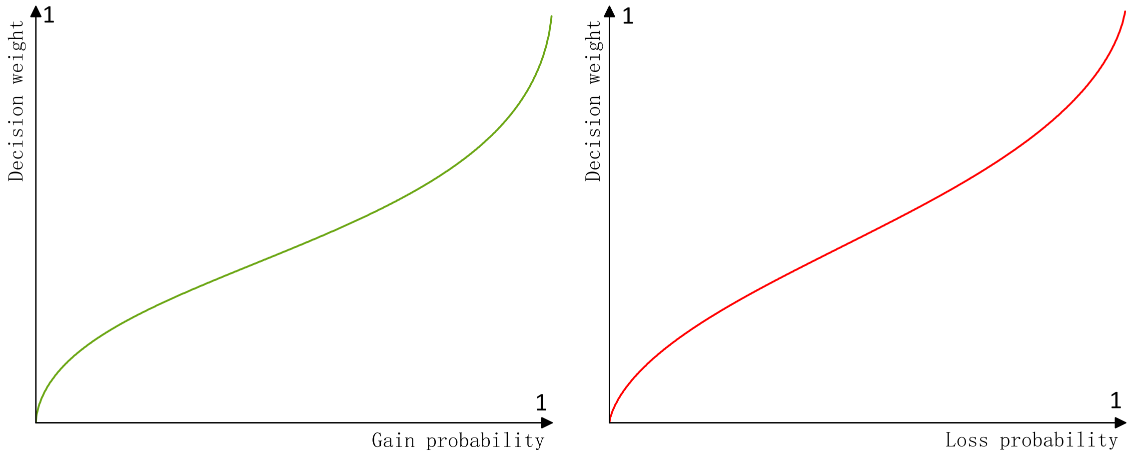

Figure 2.6: Probability weight function.

Probability distortion replaces objective probabilities with decision weights derived from w^+ and w^- applied to cumulative probabilities. Empirically, these weighting functions are typically inverse-S shaped: small probabilities tend to be overweighted and moderate-to-large probabilities underweighted (with domain asymmetries allowed). This feature is central to cumulative prospect theory and can generate a preference for positively skewed ("lottery-like") payoffs and simultaneous demand for downside protection, depending on where mass lies relative to reference point.

Despite the empirical support for nonlinear probability transformations, existing results do not provide conclusive evidence that behavioral portfolio selection and mean-variance models can be applied interchangeably in practice. A primary limitation of many prior studies lies in their reliance on strong assumptions, particularly the omission of certain foundational aspects of behavioral portfolio selection frameworks.

For example, Das et al. [71] integrate both mental accounting and the safety-first principle into their modeling approach. However, they often neglect the full behavioral process wherein decision-makers apply subjective weights to objective probabilities—a key behavior in prospect theory.

Furthermore, the assumption of normal distributions for assets returns has been widely critiqued as being unrealistic [72]. To date, the only study that performs a comparative analysis without imposing any prior distributional assumptions is that of Hens and Mayor [18]. Their research demonstrates that, under cumulative prospect theory, asset allocations diverge notably from those predicted by mean-variance analysis when returns are non-normally distributed.

While Hens and Mayor's empirical setup benefits from avoiding the normality assumption, its applicability is constrained by the limited size of the dataset—just 8 assets and 15 return realizations. This limited scope restricts diversification and weakens the generalizability of the results. Additionally, similar to Levy and Levy [73] and Levy et al. [74], their framework does not fully reflect the complete structure of behavioral retail investor portfolio selection. Specifically, although behavioral biases are accounted for, the safety-first principle—central to retail investor behavior—is omitted.

These observations highlight the need for a more comprehensive integration of both behavioral and structural components—such as safety-first, mental accounting, and probability distortion—when modeling portfolio selection behavior for retail investors.

2.2.2 Advances in Prospect Theory and Retail Investor Portfolios

In this section, I will survey the most significant advances in prospect theory and retail investor portfolios, including reference dependence, prospect theory for attribute outcomes and retail investor asset pricing model.

Reference dependence

Although substantial progress has been made in recent years, the majority of existing research continues to rely on the expected utility theory, which presumes that investors act rationally to optimize their expected wealth. However, this assumption frequently fails to reflect actual investor behavior in real-world scenarios. Since the 1980s, behavioral finance has emphasized that cognitive biases significantly influence the decision-making processes of investors [62].

Prospect theory, a cornerstone of behavioral finance, utilizes cognitive psychology to explain how irrational tendencies affect economic choices [75].

Building on these foundations, a growing body of research has emerged that integrates prospect theory into portfolio selection. For instance, Wang et al. [76] present a fuzzy portfolio selection approach that allows investors to delay their decisions. Zhou et al. [77] introduce a decision-making strategy aiding managers in identifying optimal portfolios based on multiple expert opinions. These contributions have substantially advanced the literature in both prospect theory and portfolio optimization.

Ferro et al. [78] propose a parameterized quantum theory model that incorporates both rank-dependent theory and prospect theory to capture risky decision-making behaviors, validated through lottery choice data. Gao et al. [79] develop a multi-attribute decision-making framework using prospect theory to model travel-related behaviors, while Grant et al. [80] examine decision-making processes involved in cashing out bets within the prospect theory paradigm.

Given the demonstrated capability of prospect theory in capturing decision-making behavior under risk, numerous studies have explored its potential in portfolio selection, particularly under market conditions marked by uncertainty and volatility. For example, Fulga [81] proposes a selection method grounded in cumulative prospect theory. Similarly, Tian et al. [82] integrate cumulative prospect theory within a fuzzy environment for portfolio selection, and subsequent work extends this approach by incorporating multi-criteria decision-making techniques [83].

Despite the pivotal role of reference dependence in prospect theory, the mechanism through which reference points are determined remains underexplored. Baillon et al. [84] introduce a comprehensive reference-dependent framework that includes prospect theory and enables differentiation of the reference point rule from other behavioral components. This framework facilitates empirical investigation into how reference points influence decisions under risk.

Substantial efforts have been devoted to modeling subjective emotions within decision-making processes, particularly through cognitive dissonance frameworks [85]. Disappointment theory, for instance, posits that the intensity of dissatisfaction with uncertain outcomes grows proportionally with the gap between expectations and actual realizations [86, 87]. Building on this foundation, later research introduces the optimal belief framework, which assumes that individuals internally believe in the potential for future positive outcomes, contributing to their ex-ante well-being [88]. In a more refined form, this framework models the trade-off between anticipated satisfaction and subsequent disappointment [89].

Best and Frauer [90] examine the practical implementation of prospect theory portfolios within real-world asset allocation scenarios, incorporating factors such as risk-free borrowing and lending, margin constraints, and prohibitions on short-selling risky assets. The portfolio selection model under prospect theory and kinked linear utility is formulated as follows:

$$\max_{x_t} \begin{cases} \sum_s \pi_{ts}(1 + r_{pts}(\mathbb{X}_t)) & \text{if } (1 + r_{pts}(\mathbb{X}_t)) > \hat{\omega} \\ \sum_s \pi_{ts} l(1 + r_{pts}(\mathbb{X}_t)) & \text{if } (1 + r_{pts}(\mathbb{X}_t)) \leq \hat{\omega} \end{cases} \tag{2.21}$$

subject to:

$$\begin{aligned} & x_{i,t} \geq 0, \quad \forall i, \quad x_{Lt} \geq 0, \quad x_{Bt} \leq 0, \\ & \sum_i x_{i,t} + x_{Lt} + x_{Bt} = 1, \\ & \sum_i m_{it} x_{it} \leq 1. \end{aligned} \tag{2.22}$$

where $\mathbb{X}_t = (x_{1,t}, \cdots, x_{n,t}, x_{Lt}, x_{Bt})'$, and $x_{i,t}, x_{Lt}, x_{Bt}$ represent investment proportions, lending, and borrowing in security i at time t, respectively. π_{ts} is the state probability, and $r_{pts}(\mathbb{X}_t)$ denotes the ex-ante return. $\hat{\omega}$ is the reference point, l is the loss-aversion slope, and m_{it} represents the initial margin requirement for asset i.

He and Strub [91] investigate how alternative mechanisms for partially endogenous reference–point formation shape optimal portfolio choices in the presence of loss aversion. Given a predefined reference level B_0, the investor's problem is formalized as follows:

$$\begin{aligned} \max_{X} \quad & V_A(X|B_0) \\ \text{s.t.} \quad & \mathbb{E}[\rho X] \leq x_0, \quad X \geq 0. \end{aligned} \tag{2.23}$$

Disappointment theory [92] provides a psychological framework for understanding when outcomes worser than expectations, investors' reactions and how such reactions influence future behavior. Disappointment arises when actual results fall below expectations or an internal benchmark, leading to emotions such as regret, anger, or frustration, which in turn can alter future decisions.

More specifically, when an individual is faced with an outcome m_i, disappointment is experienced if the outcome is worse than other possible outcomes. Suppose the set of outcomes is $\{m_1, \cdots, m_n\}$ with corresponding probabilities $\{p_1, \cdots, p_n\}$, the disappointment function is computed using the following index:

$$D(A) = \sum_{i=1}^{n} \sum_{m_j \geq m_i} p_i p_j H(m_i - m_j). \tag{2.24}$$

Here, $H(\cdot)$ is a dispersion function that is non-negative on an interval, reflects sensitivity to variation. Following [93], this study adopts $H(z) = z$ as a reasonable choice for portfolio applications.

F is the cumulative distribution function over continuous outcomes, the disappointment index is calculated by:

$$D(A) = \int_{-\infty}^{+\infty} \int_{-\infty}^{A} H(A - x)\, dF(x) = \int_{-\infty}^{+\infty} \int_{-\infty}^{A} H(y - x)\, dF(x)\, dF(y). \tag{2.25}$$

Prospect theory for attribute outcomes

Although prospect theory has been widely accepted, recent studies have pointed out certain limitations [94, 95].

Researchers such as Fishburn [96] and Miyamoto and Wakker [97] have investigated multi-attribute utility within non-expected utility theory but limited their focus to same-sign outcomes. Zank [98] and Bleichrodt and Miyamoto [99] extended this to the context of prospect theory, although their modeling strategies differ from this paper's approach.

A key question in multi-attribute prospect theory is determining when a specific attribute leads to a perceived gain or loss. Zank [98], and later Bleichrodt and Miyamoto [99], illustrate this issue with an example: Suppose a research associate is contemplating switching jobs and must assess several job-related attributes such as salary, commute time, living costs, and available research time. To judge whether a job offer constitutes a gain or a loss, each component of the offer is evaluated against a personal reference point—typically the candidate's current position. One method is to judge whether the overall package is better or worse than her current job, and then analyze which components contribute positively or negatively relative to other alternatives.

Retail investor asset pricing model

Shefrin and Statman [3] developed a behavioral asset pricing framework that accounts for the influence of noise traders on market pricing efficiency. They explored how these irrational traders affect asset pricing, market volatility, return anomalies, and the persistence of inefficiencies. Investor psychology, emotional biases, and irrational behaviors frequently play significant roles in financial markets, contributing to anomalies in asset pricing.

The retail investor asset pricing model suggests that investors value assets not only for their utilitarian benefits—such as low risk and high returns—but also for expressive and emotional rewards. For instance, an asset may be perceived as desirable because it provides social recognition, patriotic satisfaction, or emotional excitement derived from trading [4].

2.2.3 Research Gaps in Prospect Theory and Retail Investor Portfolios

The integration of prospect theory and retail investor portfolio selection has significantly enhanced understanding of investor behavior under uncertainty, offering a more realistic alternative to traditional finance models. By accounting for psychological biases such as loss aversion, probability distortion, and reference point dependency, these theories provide valuable insights into how investors perceive risk and make decisions. However, as financial markets evolve and new challenges emerge, several gaps remain in the practical application and theoretical development of prospect theory and retail investor portfolio models. These gaps present promising opportunities for future research aimed at improving model robustness, adaptability, and real-world applicability. In the following section, several key directions for advancing the field will be outlined, focusing on dynamic modeling, alternative risk measures, and real-world validations of retail investor portfolio models. These future directions are expected to further bridge the gap between theory and practice, ultimately contributing to more effective and behaviorally sound investment strategies.

Incompleteness of prospect theory

Although loss aversion is a central element of prospect theory, it accounts for only one facet of the psychological forces shaping investor behavior. In practice, decisions are influenced by a suite of biases—such as overconfidence, regret aversion, and mental accounting—that materially affect how risk is perceived and how choices are made under uncertainty.

Focusing solely on loss aversion may oversimplify complex decision-making processes and limit the model's explanatory power. Incorporating a broader set of behavioral biases can provide a more comprehensive understanding of investor behavior, better capturing the nuances of real-world investment scenarios. Doing so will enhance the predictive accuracy of retail investor portfolio models and improve their applicability across different market conditions. Moreover, this approach can help financial institutions design more effective investment strategies and personalized financial products that account for diverse investor preferences and biases.

So in summary, retail investor portfolio models could developed by incorporating a broader range of biases to better capture investor behavior and study the interaction of multiple biases and their impact on portfolio performance.

Absence of combinations of traditional finance and behavioral insights

Traditional finance models, rooted in rational decision-making and efficient markets, often fail to fully explain real-world investor behavior, particularly during periods of market volatility or economic uncertainty. Behavioral finance addresses these limitations by incorporating psychological biases and cognitive distortions into financial models. However, behavioral models alone can sometimes lack the rigorous mathematical structure and predictive reliability of traditional models.

Developing hybrid models that combine traditional finance theories with behavioral insights is crucial to bridge this gap. Such models can retain the analytical precision and consistency of traditional approaches while capturing human behavior's complexities, like loss aversion, overconfidence, and regret aversion. These hybrid frameworks are better equipped to explain anomalies in financial markets, improve risk assessment, and enhance portfolio optimization strategies. By acknowledging both rational and irrational investor behaviors, hybrid models provide more realistic and actionable insights for financial practitioners, policymakers, and researchers, making them highly relevant in both academic and practical contexts.

Therefore, building upon contemporary advancements in prospect theory, establishing a comprehensive theoretical framework that systematically incorporates decision-makers' behavioral patterns across diverse environmental contexts constitutes a critical research imperative. Such a framework holds significant potential to enhance predictive accuracy regarding retail investor behavior in markets characterized by inherent uncertainty, while concurrently providing actionable investment guidance. In this study, a theory-centric strategy through enhancements to prospect theory is proposed to systematically incorporates retail investors' behavior patterns across diverse environmental contexts. The detailed descriptions of this prospect theory framework will be introduced in Chapter 4.

The convergence of contemporary portfolio-selection theory and retail investor portfolio has yielded models that embed intricate mathematical formulations and high-dimensional decision spaces. Such richness, while indispensable for capturing investors' psychological biases and market frictions, renders many problems intractable to exact solvers and off-the-shelf optimization software. Moreover, practical portfolio management demands solutions within tight time frames, especially when market conditions evolve rapidly. PSO, a population-based meta-heuristic renowned for its simplicity and computational efficiency, has therefore become a popular surrogate for exhaustive search in this context. Nevertheless, the canonical PSO algorithm was originally conceived for low- to moderate-dimensional landscapes with relatively smooth topologies; when confronted with the non-convex, discontinuous, and high-dimensional structures typical of modern behavioral portfolio models, it is prone to premature convergence and sub-optimal exploration. Bridging this gap motivates ongoing research into enhanced PSO variants—incorporating, for example, adaptive parameters, hybrid learning strategies, or cooperative swarm decompositions—to bolster global search capability and deliver reliable, high-quality solutions under realistic computational budgets.

2.3 Particle Swarm Optimization

This section reviews the theoretical foundations, algorithmic advancements, and practical applications of PSO, a metaheuristic algorithm pivotal for solving high-dimensional, non-convex optimization problems inherent to retail investor portfolio selection. Structured into five subsections, it systematically bridges PSO's evolution with its role in addressing computational challenges identified in Sections 2.1 and 2.2. Section 2.3.1 traces PSO's origin and biological inspiration, establishing its core mechanics and relevance to portfolio optimization. Section 2.3.2 details algorithmic innovations—multi-subpopulation strategies, diversity preservation, and hybrid techniques—that mitigate premature convergence and enhance scalability. Section 2.3.3 explores PSO's empirical success across domains such as feature selection, wireless communications, and image processing, validating its adaptability to complex, real-world problems. Section 2.3.4 evaluates PSO's performance through benchmark fitness functions, emphasizing its robustness in navigating multimodal and non-separable landscapes. Finally, Section 2.3.5 identifies critical unresolved challenges—including theoretical convergence guarantees, parameter sensitivity, and scalability in discrete spaces—while proposing novel enhancements such as adaptive swarm decomposition and co-evolutionary strategies. These contributions not only align with the dissertation's second objective (algorithmic innovation) but also advance PSO's applicability to retail investor portfolio models. Collectively, the subsections progress from foundational principles to cutting-edge developments, framing PSO as both a versatile computational tool and a focal point for interdisciplinary innovation in optimization research.

2.3.1 Origin and Background Information of Particle Swarm Optimization

The concept and design of PSO are inspired by collective behaviors observed in bird flocking and fish schooling. In natural environments, bird flocks tend to follow the individual closest to a food source. This phenomenon of social coordination is abstracted into algorithmic logic within PSO, where each particle is modeled as a bird in the swarm and also a feasible solution to the problem. These particles explore the solution space collaboratively to discover the best feasible solution.

Several characteristics make PSO a favorable choice for optimization:

a. It is relatively straightforward to program and deploy;

b. Three hyper-parameters only involved: inertia weight, cognitive and social components. Minor changes in any of these can lead to significant differences in convergence behavior, as demonstrated in [100, 101];

c. The algorithm is highly adaptable and can be effectively combined with other optimization techniques.

PSO achieves effective search performance by coordinating particle movements across the search domain and utilizing shared information within the swarm to guide convergence.

The optimization objective is assumed to acquire the minimum of a S-dimensional fitness function $\mathcal{F}(\cdot)$. N particles constitute the swarm to execute the search process. Each particle's position could be represented as:

$$\mathbb{P}_n = (\mathbb{P}_{n,1}, \mathbb{P}_{n,2}, \cdots, \mathbb{P}_{n,s}, \cdots, \mathbb{P}_{n,S}), \quad 1 \leq n \leq N,\ 1 \leq s \leq S. \tag{2.26}$$

During the iteration process, each particle updates its velocity and position $\mathbb{T}$ times, $\mathbb{T}$ is a sufficiently large integer.

$$\begin{aligned} &\nu_{n,s} \leftarrow \tau * \nu_{n,s} + l_1 * \mathrm{random}(0,1) * (\mathbb{P}best_{n,s} - \mathbb{P}_{n,s}) + l_2 * \mathrm{random}(0,1) * (\mathcal{G}best_s - \mathbb{P}_{n,s}), \\ &\mathbb{P}_{n,s} \leftarrow \mathbb{P}_{n,s} + \nu_{n,s}, \end{aligned} \tag{2.27}$$

where τ denotes the inertia coefficient, l_1 and l_2 are the cognitive and social components respectively. $\mathbb{P}best_n$ refers to the historically best-known position of particle n with the associated fitness value $\mathbb{P}value_n$, and $Gbest$ signifies the best-known solution among all feasible solutions, with corresponding fitness $Gvalue$.

2.3.2 Advances in Particle Swarm Optimization

There exists a diverse array of strategies aimed at enhancing the PSO structure, which can be categorized as follows.

Adopting multi-sub-populations

Sugantham first introduced the concept of incorporating genetic algorithm subpopulations into the PSO framework in 2001 [102], including a reproduction mechanism. A dynamic multi-swarm PSO structure is proposed in [103], in which the main swarm was partitioned into several smaller swarms. The dynamic structures was frequently reconfigured to facilitate inter-swarm information exchange.

A symbiotic version of PSO is designed to optimize neural fuzzy systems [104]. Chang later introduced an improved PSO variant tailored to multi-modal function optimization tasks [105]. The original swarm is split into multiple sub-swarms according to particle indices. Its velocity update rule consults each sub-swarm's top performing particle, replacing the traditional global best particle from the complete population.

Improving the selection strategy

Al-kazemi and Mohan proposed a phased PSO method [106], wherein particles were organized according to temporary objectives across multiple stages. These temporary goals directed particles to explore either toward or away from their personal or global best locations.

Departing from the standard PSO strategy, an alternative approach guides particles to avoid their worst-known positions instead of pursuing the best. Yang and Simon [107] introduced a technique that focuses on tracking the worst positions rather than the best ones, enabling particles to escape from suboptimal areas.

Leontitsis et al. [108] developed a new mechanism called the repel operator. This operator leverages knowledge of both personal and global best and worst positions. The idea is to direct particles away from their worst-known locations and instead guide them toward optimal solutions, improving convergence speed.

Modifying particle's update formula

Numerous studies have proposed techniques to enhance PSO performance. These include modifying the velocity update rule, adjusting swarm size and termination conditions, and tuning PSO parameters and neighborhood topologies.

Velocity clamping is one such strategy that helps prevent uncontrolled velocity growth and divergence. It restricts particle movement within predefined velocity limits. For instance, the maximum allowable velocity is defined as a linear mapping from its searching space boundary difference [26], which has demonstrated effectiveness.

Swarm particle number also known as population size, plays a pivotal role in convergence. Research by [109] explored this issue, while [110] found that smaller swarms often lead to local optima due to limited search diversity. Conversely, overly large populations can enhance solution quality but significantly increase computational load. The characteristic of the objective function decides the optimal population size, and it is generally advised to use between 20 and 50 particles in PSO applications [111, 112].

Common termination criteria for PSO runs include limiting the number of iterations, a method frequently adopted in the literature [113], and setting a cap on the number of fitness evaluations [114, 115].

Typically, three control parameters are used in PSO: inertia weight, cognitive and social components. These parameters significantly affect the algorithm's behavior, and numerous works have sought to enhance PSO by fine-tuning them.

Inertia weight was introduced in [116] as a stochastic value to accommodate dynamic environments, eliminating the need to preset large or small weights. Cognitive and social coefficients (also known as acceleration coefficients) govern how particles balance exploration and exploitation. According to [11], a high cognitive-to-social coefficient ratio may lead particles to disperse widely across the search space. In [117], a hierarchical structure with a time-varying acceleration strategy was proposed. At the beginning of optimization, a high cognitive and low social coefficient is used to encourage broad exploration. Later in the process, this balance is reversed to intensify exploitation around promising regions.

Finally, particles in PSO interact through specific structures known as neighborhood topologies. These structures govern the communication and information sharing among particles. Various neighborhood frameworks have been evaluated and verified to enhance performance across different applications.

Combining PSO with other search techniques

The PSO algorithm is typically enhanced for two core objectives: the first is to increase population diversity and mitigate premature convergence, while the second focuses on enhancing its local exploitation capability. To address the former, a wide range of models have been developed [118]. Many of these models adopt hybrid techniques by incorporating genetic operators into PSO. For instance, methods involving selection [119, 120, 121], crossover operations [120, 122], mutation strategies [123], and Cauchy mutation [124] have been explored to improve diversity and enable the algorithm to better escape local optima.

In addition, Meng et al. [125] put forward a novel hybrid strategy termed crisscross search PSO, which diverges from traditional PSO and its variants by encoding each particle explicitly through its personal best position, $pbest$.

Improvements for multi-modal problems

This approach is tailored for addressing multi-modal optimization tasks, aiming to discover multiple high-quality optima. To achieve this, Parsopoulos and Vrahatis [126] implemented techniques such as deflection, stretching, and repulsion to explore numerous local minima by preventing particles from revisiting previously discovered optima. However, this strategy tends to generate new local optima near the boundaries of previously identified ones, potentially causing the algorithm to converge prematurely. To overcome this issue, Jin et al. [127] introduced a novel function transformation mechanism designed to circumvent such drawbacks.

An additional variant is the niche-based PSO introduced by Brits et al. [128], which employs several subpopulations concurrently to identify and monitor multiple optimal solutions. In a subsequent study, Brits et al. [129] proposed an alternative approach to locate multiple optima simultaneously by modifying the method of computing fitness values. Schoeman and Engelbrecht [130] further enhanced this process by implementing vector dot product operations in parallel, thereby improving optimization performance.

Keeping diversity of the population

Maintaining population diversity is essential for strengthening the global exploration ability of PSO. A widely used safeguard is to reinitialize a subset of particles—or, when necessary, the entire swarm—once diversity drops below a specified threshold. Lovbjerg and Krink [131] embedded self-organized criticality into the PSO mechanism to quantify inter-particle proximity and, based on this diversity metric, decide when particle positions should be reset.

Clerc [132] put forward a deterministic approach named Re-Hope. This method was employed when the search space was relatively limited and no solutions had been located (termed as No-Hope), prompting a reset of the swarm. To preserve diversity and strike a balance between global and local searches, Fang et al. [133] introduced a decentralized variant of quantum-inspired PSO incorporating cellular structures.

The cellular structured quantum-inspired PSO-*lbest* was assessed on a set of 42 benchmark functions that span a variety of characteristics, and its performance was benchmarked against several PSO variants featuring diverse topologies and other swarm intelligence algorithms.

2.3.3 Applications of Particle Swarm Optimization

Due to its simplicity and strong performance, PSO has been extensively adopted as a practical optimization technique for addressing a broad spectrum of real-world problems, including but not limited to feature selection, wireless communication systems, image analysis, and electric power optimization.

Feature selection

Feature selection is the task of choosing a subset y of features from a total of x original ones ($y \leq x$), aiming to optimize a specific evaluation metric [134, 135]. This process is critical in data mining and machine learning, as it helps eliminate irrelevant or redundant features [136].

PSO has been recognized as an effective method for feature selection in diverse problem domains. For instance, the work in [137] proposed an enhanced binary PSO (BPSO) model that integrates Lévy flight for local search, and inertia weight for global exploration, along with mutation to maintain population diversity. In [138], a binary PSO approach was adopted for selecting input features in intelligent joint moment prediction. Further, a cooperative binary PSO with a strategy of varying multiple inertia weights was developed in [139]. The binary PSO was also combined with differential evolution in [140] to address feature selection challenges in electromyography (EMG) signal classification.

Wireless communications

PSO has been widely utilized for optimizing various wireless communication tasks, such as those involving wireless sensor networks [141], cognitive radio networks [142], intelligent reflecting surface systems [143], edge computing [144], ad hoc networks [145], signal processing [146], and antenna optimization [147]. It has proven useful for addressing key challenges in wireless sensor networks, including node localization, deployment optimization, and clustering. A thorough overview of PSO applications in wireless sensor networks is provided in [148]. In cognitive radio networks, which face non-convex optimization challenges, PSO is leveraged to improve energy usage, spectral efficiency, and sensing latency.

The study in [149] applied standard PSO to primary-user detection, and simulation results indicated reductions exceeding 80% in both energy consumption and sensing time.

To further enhance efficiency, improved PSO versions were explored. For example, [150] proposed a hybrid model integrating PSO and gravitational search algorithms to optimize energy consumption in 5G cognitive radio contexts.

Image processing

PSO has also demonstrated effectiveness in solving a range of image processing optimization issues, such as image enhancement [151], image compression [152], and watermarking [153]. One particularly noteworthy application is in multilevel image thresholding segmentation.

2.3.4 Benchmark Fitness Functions

Benchmark fitness functions are indispensable for evaluating and contrasting the performance of optimization algorithms. Despite the extensive catalog of benchmarks proposed in the literature, no universally accepted standard suite has been established. To ensure fair evaluation, these functions should ideally encompass diverse characteristics [154].

Assessing the reliability, efficiency, and effectiveness of optimization algorithms is typically done using a predefined suite of standard test functions or benchmarks. Literature reveals that the number of benchmark functions employed varies greatly across studies, ranging from a few to several dozen. Although no universally accepted collection of test functions exists, an effective set should be comprehensive and impartial. For any novel optimization algorithm, it is essential to validate its efficacy against a wide set of functions and benchmark its results against existing methods. A common methodology involves comparing multiple algorithms across a broad test suite, particularly in function optimization studies [155, 156]. However, one must be cautious, as an algorithm's superiority can be misrepresented if the test problems lack diversity or are overly tailored. Hence, to meaningfully compare algorithms, it is critical to recognize the problem types each algorithm performs well on. This classification helps define where an algorithm is most appropriate. An effective benchmark suite should include a wide range of problems, covering characteristics such as unimodality, multimodality, regularity, irregularity, separability, non-separability, and various dimensionalities.

Unconstrained optimization problems are commonly categorized into artificial test functions and real-world applications. Artificial functions are synthetic scenarios designed to test an algorithm's capability under diverse and often complex conditions. These can involve one or more global optima, local minima, long valleys, flat regions, null spaces, or steep ridges. They are modifiable and widely used to simulate varied difficulties in testing algorithms. In contrast, real-world problems stem from domains like physics, chemistry, engineering, and mathematics. These problems are typically more complex, involving real data and intricate algebraic or differential formulations, making them less manipulable.

The primary goal in global optimization is to determine the optimal solution χ^* from a domain Ξ under a collective of objective functions $\mathbb{G} = \{g_1, g_2, \cdots, g_n\}$. Specifically, single-objective optimization could be modeled by a mapping $Ss \subset \mathcal{R}^d \to \mathcal{R}$, the searching space is defined by additional constraints. The problem typically seeks to either maximize or minimize f, but minimization is most common and maximization is often achieved by minimizing $-f$. A standard optimization formulation is:

$$\min_x f(x) \tag{2.28}$$

The true optimum could be a single solution or a set of all equally optimal points in D, possibly infinite. Thus, a competent global optimization method should strive for either globally optimal or near-optimal results. Benchmark functions often reflect various structural properties such as continuity, convexity, linearity, modality, and separability [157].

1. Modality.A function's modality is characterized by the count of peaks present in its landscape. Multiple local optima increase the risk of premature convergence, as optimization algorithms may become trapped in sub-optimal solutions.

2. Basins. A basin is a region with steep descent around an optimum. Algorithms are naturally drawn to such areas, potentially impairing their global search capacity. According to [158], a basin for maximization is analogous to a plateau. Problems may contain multiple such regions.

3. Valleys. Valleys occur when regions of minimal variation are flanked by steep descents [158]. Like basins, they attract optimizers, slowing convergence as the algorithm explores the flat region.

4. Separability. This refers to how independently the variables in a function can be optimized. Separable functions allow each variable to be treated independently, simplifying the optimization process. A separable function could be expressed as a sum of functions with single variables [159]. Conversely, if variables are dependent, the function is non-separable. In separable functions, objective functions can be written as:

$$f(x_1, \cdots, x_m) = \sum_{i=1}^{m} f_i(x_i) \tag{2.29}$$

5. Dimensionality. As noted in [157] and [160], increasing the number of dimensions generally complicates the optimization task from the searching space's exponential growth. For non-linear problems, this poses a challenge for most optimization techniques.

2.3.5 Research Limitations in Particle Swarm Optimization

As a comparatively new methodology, PSO has garnered considerable attention in recent years. Its merits can be summarized as follows: (1) strong robustness and ready adaptability to diverse application domains, requiring only minimal modifications. (2) Owing to its nature as a swarm evolutionary algorithm, it inherently supports distributed processing, making parallel computation straightforward. (3) It exhibits rapid convergence toward optimal solutions. (4) The algorithm is highly compatible with other algorithms, facilitating hybrid approaches to enhance performance.

Although the PSO algorithm has seen significant advancements in terms of speed, quality, and robustness through years of development, several open challenges remain unresolved.

These include, but are not limited to:

1. **Random convergence analysis.** Despite PSO's demonstrated effectiveness in practical problems and some initial theoretical findings, formal mathematical convergence proofs and convergence rate estimates are still lacking.

2. **Parameter determination.** The parameters of PSO are usually set based on specific problem contexts, empirical knowledge, and extensive testing, which undermines its generalizability. Identifying efficient and convenient parameter-setting methods remains an important area of research.

3. **Discrete/binary PSO algorithm.** Most of the literature reviewed concentrates on continuous-variable formulations, whereas comparatively few studies address extensions of PSO to discrete (combinatorial) optimization, a setting that introduces additional methodological challenges.

4. **Customized algorithm design.** Tailoring PSO to match the characteristics of various problem types is a valuable research direction. For particular applications, it is crucial to deepen the understanding of PSO and broaden its applicability. Additionally, emphasis should be placed on high-efficiency PSO variants, such as PSO integrated with rule-based systems, neural networks, fuzzy logic, evolutionary techniques, simulated annealing, tabu search, bio-inspired intelligence, and chaos theory, to overcome local optima entrapment.

5. **Inadequate update mechanisms among particles.** Further investigation should prioritize the design of efficient update mechanisms and foundational update equations that achieve a principled trade-off between global exploration and local exploitation in PSO variants.

6. **Expanding PSO applications.** In current practice, PSO is applied predominantly to problem classes with continuous decision variables, a single optimization objective,

no explicit constraints, and deterministic (non-stochastic) settings. There is a need to emphasize applications in discrete, multi-objective, constrained, stochastic, and dynamic optimization problems to expand PSO's application domains.

Despite PSO's extensive application in optimization tasks due to its flexibility and simplicity, it still faces two key challenges when applied to urban optimization problems involving a large number of variables [161]. The primary difficulty lies in the substantial computational burden encountered when tackling large-scale instances. Wang et al. [162] proposed a new technique leveraging escape velocity and particle reinitialization to improve iteration efficiency and reduce computation time. A second limitation is the degradation of PSO performance as the dimensionality of the search space increases. A commonly adopted remedy partitions the original task into smaller sub-problems and addresses them via cooperative, co-evolutionary procedures that exchange information among sub-components [163].

Although PSO has matured in terms of algorithmic performance and practical implementation, most current research emphasizes its application and refinement, while theoretical studies remain underdeveloped. To address this gap, this research introduces an innovative PSO algorithm that incorporates swarm cooperation and a novel evolving mechanism. This variant aims to balance global search capabilities with local exploitation efficiency.

Additionally, building upon the proposed cooperative swarm PSO, another PSO algorithm featuring adaptive learning rates is introduced. This adaptive PSO targets the second challenge mentioned earlier—parameter tuning—by employing reinforcement learning strategies. Detailed discussions of these two proposed PSO variants are provided in Chapter 6.

Chapter 3

DEVELOPMENT OF MULTI-OBJECTIVE MODEL INTEGRATING MULTIPLE BEHAVIORAL DECISION THEORIES

In Section 2.1, I conducted a systematic and comprehensive review of portfolio selection frameworks, revealing that both traditional models and existing behavioral-based approaches predominantly focus on isolated behavioral tendencies among investors—such as loss aversion or return chasing—while neglecting their dynamic interplay. This narrow focus undermines the ability of such models to achieve an optimal balance between risk and return, particularly in complex market environments characterized by uncertainty and behavioral heterogeneity. This critical limitation aligns with the first research gap identified in Section 1.2, where oversimplified behavioral assumptions hinder the practical applicability of portfolio models to real-world decision-making scenarios. To address this gap, the current chapter adopts a model-driven methodological framework that synthesizes multiple behavioral dimensions (e.g., reference dependency, probability distortion, and adaptive risk preferences) into a unified portfolio optimization structure. By integrating cross-behavioral dynamics and multi-objective constraints, this approach aims to reconcile theoretical rigor with empirical validity, thereby enhancing the robustness and adaptability of behavioral portfolio models in achieving investor-specific risk-return equilibrial.

By jointly integrating prospect theory with disappointment theory, the proposed conceptual framework explicitly incorporates emotional influences while delivering a comprehensive characterization of individuals' decision processes under uncertainty. Building on this foundation, the portfolio selection scheme targets a balanced return–risk trade-off by concurrently maximizing expected utility and total utility. The practical effectiveness of the model is substantiated through Case Studies 1 and 2. This original multi-objective portfolio selection model and the findings have been complied in an international journal paper [164] by **X. Wang**, Y. Ouyang, Y. Li, S. Liu, L. Teng and B. Wang. Multi-objective portfolio selection considering expected and total utility. *Finance Research Letters*, 104552, 2023.

3.1 Introduction of the Multi-objective Portfolio Selection Model

Although prospect theory has greatly enriched our understanding of decision-making under risk, it is not free of shortcomings. Empirical evidence sometimes contradicts its predictions, and when the theory is applied to practical portfolio selection, noticeable gaps often remain between theoretical outcomes and realized results. These discrepancies may stem, for example, from the fact that actual wealth fluctuations do not align with the trading choices forecast by prospect theory. Consequently, any real-world application must recognize these limitations and treat prospect-theoretic predictions with caution.

To deepen insight into human decision-making, [92] introduced *disappointment theory.*

This framework extends prospect theory by examining how people respond to outcomes that fall short of their expectations. Whereas prospect theory offers a broad lens on choice under uncertainty, disappointment theory highlights the emotional impact of unmet expectations and thereby enriches the behavioral narrative.

Acknowledging that investment risk is shaped both by market volatility and by investors' emotional responses, this section develops a portfolio selection framework that jointly integrates expected utility theory, prospect theory, and disappointment theory. A central feature borrowed from prospect theory is its reference dependence, which emphasizes that investors appraise outcomes and choose among risky alternatives relative to one or more context-specific benchmarks or reference points.

The key contribution of the proposed framework is its joint use of prospect theory and disappointment theory to capture emotional considerations more fully. By accommodating these psychological factors, the model offers a more comprehensive account of actual decision behavior and clarifies several empirical deviations from classical economic predictions.

3.2 Multi-Objective Portfolio Selection Model Integrating Multiple Decision Theories

This section sets out the mathematical formulation of the multi-objective portfolio selection model.

Zadeh [165] proposed fuzzy set theory and then developed by Dubois and Prade [166]. In fuzzy set theory, fuzzy variables are connected with possibility distributions just like how random variables are connected with probability distributions in probability theory. A convex, normal fuzzy set could often model a fuzzy variable, and its membership function could often produce a possibility distribution.

For the subsequent discussion, let $\pi_{\vec{\varsigma}}(t)$ denote the possibility distribution function of the fuzzy variable $\vec{\varsigma}$ and let $f_{\Xi}(t)$ be the membership function of a fuzzy set Ξ. The fuzzy variable $\vec{\varsigma}$ is called normal if there exists $l \in \mathbf{R}$ such that $\pi_{\vec{\varsigma}}(q) = 1$. Throughout this work, fuzzy variables are assumed to be normal and are marked with a tilde. The possibility and necessity measures of the event $\vec{\varsigma} \in \Xi$ are defined by

$$\Pi_{\vec{\varsigma}}(\Xi) = \sup_t \min\{\pi_{\vec{\varsigma}}(t), f_\Xi(t)\}, \tag{3.1}$$

$$N_{\vec{\varsigma}}(\Xi) = \inf_t \max\{1 - \pi_{\vec{\varsigma}}(t), f_\Xi(t)\}, \tag{3.2}$$

where $\Pi_{\vec{\varsigma}}(\Xi)$ quantifies how possible it is that $\vec{\varsigma}$ lies in Ξ, while $N_{\vec{\varsigma}}(\Xi)$ quantifies how certain it is that $\vec{\varsigma}$ belongs to Ξ. When Ξ is a crisp set, these reduce to

$$\Pi_{\vec{\varsigma}}(\Omega) = \sup_{t \in \Omega} \pi_{\vec{\varsigma}}(t) \tag{3.3}$$

$$N_{\vec{\varsigma}}(\Xi) = \inf_{t \notin \Xi} [1 - \pi_{\vec{\varsigma}}(t)] \tag{3.4}$$

Let $q \in \mathbb{R}$. Define the possibility and necessity that $\vec{\varsigma}$ exceeds q as

$$\mathbf{Pos}(\vec{\varsigma} \geq q) = \Pi_\Xi([q, +\infty)]) = \sup_t \{\pi_\Xi(t) | t \geq q\} \tag{3.5}$$

and

$$\mathbf{Nec}(\vec{\varsigma} \geq q) = N_\Xi([q, +\infty)]) = 1 - \sup_t \{\pi_\Xi(t) | t < q\}. \tag{3.6}$$

$\mathbf{Pos}(\vec{\varsigma} \leq q)$ and $\mathbf{Nec}(\vec{\varsigma} \leq q)$ can be similarly deduced. then it is easy to obtain the following (see Figure 3.1):

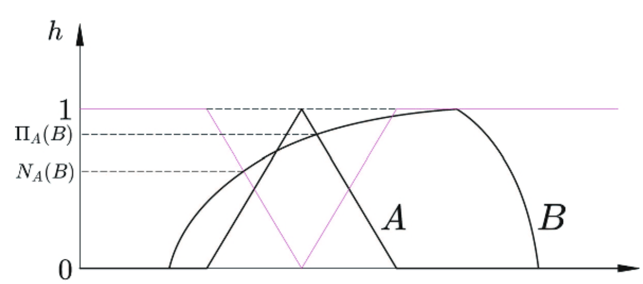

Figure 3.1: Possibility and necessity measures.

Based on above definitions, the chance of the event $\{\vec{\varsigma} \leq q\}$ could be quantified by

$$\mathbf{Cr}\{\vec{\varsigma} \leq q\} = \frac{1 + \sup\limits_{\vec{\varsigma} \leq q} f_{\Xi}(t) - \sup\limits_{\vec{\varsigma} > q} f_{\Xi}(t)}{2} \tag{3.7}$$

As a self-dual measurement, i.e., $\mathrm{Cr}\{\vec{\varsigma} > q\} = 1 - \mathrm{Cr}\{\vec{\varsigma} \leq q\}$, the expected value of $\vec{\varsigma}$ could be derived as follows

$$\mathbf{E}[\vec{\varsigma}] = \int_0^{+\infty} \mathbf{Cr}\{\vec{\varsigma} \geq q\} dq - \int_{-\infty}^{0} \mathbf{Cr}\{\vec{\varsigma} \leq q\} dq. \tag{3.8}$$

Consider an investor who allocates capital to a set of candidate securities $(a_1, \ldots, a_n)$ over a given period. For security a_i, let fuzzy variable $\tilde{p}_i$ represents the predicted price and p_i is the current price. Suppose a_i pays a dividend d_i during the period. The (fuzzy) return rate of a_i over the period is represented by $\vec{\varsigma_i}$, defined as

$$\vec{\varsigma_i} = \frac{\vec{p_i} - p_i + r_i}{p_i} \tag{3.9}$$

Its expected return rate is expressed via the expectation of $\vec{\varsigma_i}$ using 3.8:

$$\mathbf{E}[\vec{\varsigma_i}] = \int_0^{+\infty} \mathbf{Cr}\{\vec{\varsigma_i} \geq l\} dl - \int_{-\infty}^{0} \mathbf{Cr}\{\vec{\varsigma_i} \leq l\} dl. \tag{3.10}$$

Let the portfolio contain securities $(a_1, \ldots, a_n)$ with corresponding investment proportions $(x_1, \ldots, x_n)$. Suppose fuzzy variable $\vec{\Lambda}$ predicts the portfolio's future return rate. $\vec{\Lambda}$ is a linear summation of the securities' return rates.

$$\vec{\Lambda} = x_1 * \vec{\varsigma_1} + \ldots + x_n * \vec{\varsigma_n}. \tag{3.11}$$

In the presumption of expected utility, the rational investor always maximizes the portfolio's utility, i.e., the expectation of the portfolio return:

$$\max \mathbf{E}[\vec{\Lambda}] = \max(\int_{0}^{+\infty} \mathbf{Cr}\{\vec{\Lambda} \geq q\}dq - \int_{-\infty}^{0} \mathbf{Cr}\{\vec{\Lambda} \leq q\}dq). \tag{3.12}$$

In line with Equation 2.17 and the reference point is assigned as the status quo, then the prospect-theoretic valuation of the portfolio can be computed as

$$\mathbf{PT}_r[\vec{\Lambda}] = \int_{\vec{\Lambda} \leq r} \mathbf{U}(\vec{\Lambda})d\mathbf{w}(\vec{\Lambda}) + \int_{\vec{\Lambda} \geq r} \mathbf{U}(\vec{\Lambda})d\mathbf{w}(1 - \vec{\Lambda}), \tag{3.13}$$

According to Equation 2.25, the portfolio's disappointment index is

$$\mathbf{D}(\vec{\Lambda}) = \int_{-\infty}^{+\infty} \int_{-\infty}^{\vec{\Lambda}} \mathbf{H}(y - x)d\mathbf{F}(x)d\mathbf{F}(y). \tag{3.14}$$

The portfolio's total utility is defined as the difference between the prospect and the disappointment [167]

$$\mathbf{TU}(\vec{\Lambda}) = \mathbf{PT}_r(\vec{\Lambda}) - \mathbf{D}(\vec{\Lambda}). \tag{3.15}$$

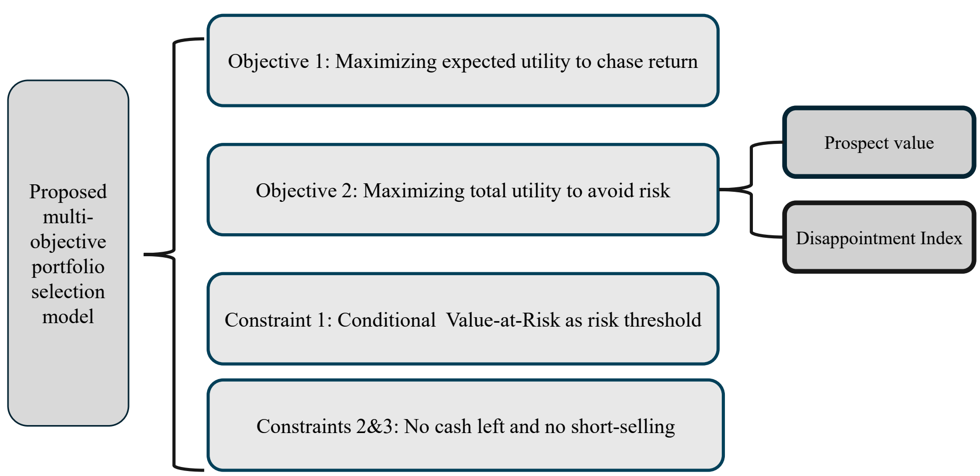

Figure 3.2: Illustration of the multi-objective portfolio selection model.

Furthermore, the proposed multi-objective framework is illustrated intuitively by Figure 3.2. The framework integrates three factors, expected, prospect and disappointment. The model maximizes the expected and total utility simultaneously. The risk metric is assigned as CVaR. The resulting optimization formulation, denoted **(E&TU)**, is presented as follows:

$$\begin{cases} \max\ \mathbf{E}[\vec{\Lambda}] = \max(\int_0^{+\infty} \mathbf{Cr}\{\vec{\Lambda} \geq q\}dq - \int_{-\infty}^{0} \mathbf{Cr}\{\vec{\Lambda} < q\}dq), \\ \max\ \mathbf{TU}(\vec{\Lambda}) = \max[\int_{\vec{\Lambda} \leq r_0} \mathbf{U}(\vec{\Lambda})d\mathbf{w}(\vec{\Lambda}) + \int_{\vec{\Lambda} > r_0} \mathbf{U}(\vec{\Lambda})d\mathbf{w}(1-\vec{\Lambda}) \\ -\int_{-\infty}^{+\infty}\int_{-\infty}^{\vec{\Lambda}} \mathbf{H}(y-x)d\mathbf{F}(x)d\mathbf{F}(y)], \\ \text{s.t.} \\ \mathbf{CVaR}_{1-\gamma}(\vec{\mathbb{L}}) < \Upsilon, \\ x_1 + x_2 + \cdots + x_n = 1,\ x_1, x_2, \cdots, x_n \geq 0. \end{cases} \tag{3.16}$$

In this model, the portfolio's return rate and prospective loss are denoted by $\vec{\Lambda}$ and $\vec{\mathbb{L}}$, respectively. By symmetry of gains and losses, it follows directly that $\vec{\Lambda} = -\vec{\mathbb{L}}$. γ is the prescribed confidence level and Υ is the risk threshold in CVaR. The last constraint enforces no short selling and no cash left.

3.3 Numerical Examples: Validation of the Multi-objective Portfolio Selection Model

In this section, the effectiveness of the proposed multi-objective framework in balancing return and risk is validated by two cases followed by.

3.3.1 Comparison Methods to the Multi-objective Portfolio Selection Model

In this section, three benchmark models are introduced as comparative baselines, in order to assess the prospective effectiveness of the proposed multi-objective framework.

a. Buy&Hold Portfolio Selection (**B&H**)

B&H investment strategy is a fundamental and widely studied approach in portfolio management and financial economics. It involves purchasing a diversified set of assets and holding them over a long-term horizon, irrespective of short-term market fluctuations. The core principle of this strategy is that financial markets tend to grow over time, and attempting to time the market through frequent trading can lead to suboptimal performance due to transaction costs and behavioral biases.

B&H is grounded in the efficient market hypothesis, which holds that asset prices incorporate all available information; consequently, sustained outperformance through active trading is unlikely to be achieved. Moreover, under the assumption of risk aversion in classical portfolio theory, long-term investors with well-diversified portfolios can achieve optimal returns by minimizing trading costs and capitalizing on compounding effects.

In behavioral finance, the **B&H** strategy is also supported by prospect theory and loss aversion, as frequent trading can lead to excessive reaction to short-term losses, reducing long-term gains. Empirical studies have shown that long-term investors often outperform active traders due to reduced exposure to market timing risks and lower tax liabilities associated with capital gains.

Within this framework, the investor maintains the initial portfolio weights throughout the entire holding period; no re-balancing is performed once the positions are established. By treating every asset as equally important, it is assumed that the allocation to each security is identical. Owing to its simplicity, the **B&H** strategy is frequently adopted as a baseline for benchmarking alternative models. Its formal expression is given by:

$$
\begin{cases}
\max \mathbf{E}[x_1 * \vec{\varsigma_1} + \ldots + x_n * \vec{\varsigma_n}], \\
\text{s.t.} \\
x_1 = x_2 = \ldots = x_n = \dfrac{1}{n}
\end{cases}
\tag{3.17}
$$

in which the constraint enforces that the asset is equally distribution.

The **B&H** model remains a cornerstone of passive investment strategies, aligning with long-term wealth accumulation objectives. While it offers simplicity and efficiency, its effectiveness depends on market conditions and investor risk preferences. In modern portfolio management, hybrid strategies that incorporate periodic rebalancing or dynamic asset allocation may enhance traditional buy-and-hold approaches.

b. Expected Utility-CVaR Portfolio Selection (**EU-C**)

Traditional portfolio selection models typically pursue the maximization of investment return under a prescribed risk level. In this study, I adopt a benchmark in which the expected value is the sole optimization objective, while CVaR serves as the risk constraint. This baseline is chosen because it is a single-objective counterpart that also employs CVaR as the risk measure, making it directly comparable to the **E&TU** formulation. The **EU-C** model integrates expected utility maximization with a CVaR constraint, offering a rigorous framework for decision-making under uncertainty that balances return objectives with tail-risk management.

The **EU-C** model addresses scenarios where the retail investor seeks to maximize the expected utility of outcomes while restricting exposure to extreme losses. Formally, it combines: 1) Objective: Maximize the expected utility , where expected utility is a concave utility function reflecting risk preferences. 2) Constraint: Enforce CVaR less than a predefined maximum acceptable risk level, where CVaR quantifies the expected loss beyond the quantile.

Consequently, this comparison enables us to examine how introducing multiple objectives changes portfolio selection behavior. The mathematical program for **EU-C** is given by:

$$\begin{cases} \max \mathbf{E}[x_1 * \vec{\varsigma}_1 + \ldots + x_n * \vec{\varsigma}_n], \\ \text{s.t.} \\ \mathbf{CVaR}_{1-\gamma}(-x_1 * \vec{\varsigma}_1 - \ldots - x_n * \vec{\varsigma}_n) < \Upsilon, \\ x_1 + x_2 + \ldots + x_n = 1, x_1, x_2, \cdots x_n \geq 0, \end{cases} \tag{3.18}$$

The **EU-C** model provides a theoretically sound and practical approach for optimizing decisions under uncertainty. By harmonizing expected utility maximization with CVaR constraints, it is particularly suited for risk-averse agents in finance, insurance, and resource management.

c. Multi-Objective Portfolio Selection with VaR (**MO-V**)

Sharpe ratio and VaR ratio were assigned as two parallel objectives of this model [162]. Adopting this model as a comparison benchmark because, like the **E&TU** framework, it is inherently multi-objective. Unlike single-objective baselines, the **MO-V** formulation treats VaR together with the expected value as optimization targets. Using **MO-V** as a comparator helps reveal how adding behavioral components (e.g., prospect and disappointment considerations) may alter portfolio selection outcomes.

$$\begin{cases} \max \ \mathrm{SR}\big[x_1\tilde{\varsigma}_1 + \cdots + x_n\tilde{\varsigma}_n\big], \\ \max \ \mathrm{VR}\big[x_1\tilde{\varsigma}_1 + \cdots + x_n\tilde{\varsigma}_n\big], \\ \text{s.t.} \quad x_1 + x_2 + \ldots + x_n = 1, x_1, x_2, \cdots x_n \geq 0 \end{cases} \tag{3.19}$$

where SR and VR denote the Sharpe ratio and the VaR ratio, respectively. Note that the VaR ratio is computed as

$$\mathrm{VR}\big[x_1\tilde{\varsigma}_1 + \cdots + x_n\tilde{\varsigma}_n\big] = \frac{\mathbf{E}\big[x_1\tilde{\varsigma}_1 + \cdots + x_n\tilde{\varsigma}_n\big] - r_0}{\mathrm{VaR}_{1-\gamma}\big[x_1\tilde{\varsigma}_1 + \cdots + x_n\tilde{\varsigma}_n\big]}, \tag{3.20}$$

where r_0 is the reference return rate.

3.3.2 Case Study 1: SSE 50 Index Real Market Case

This section presents a real market case study for benchmarking investment performance against several comparison methods. This study examines whether the proposed multi-objective framework attains an effective trade-off between return and risk. For the empirical assessment, ten stocks were randomly sampled from the Shanghai Securities 50 Index, as summarized in Table 3.1.

Table 3.1: Sampled stocks in Case Study 1.

Stock No.	Code	Stock No.	Code
1	600010	2	600028
3	600196	4	600276
5	600406	6	600436
7	603260	8	603288
9	603501	10	603986

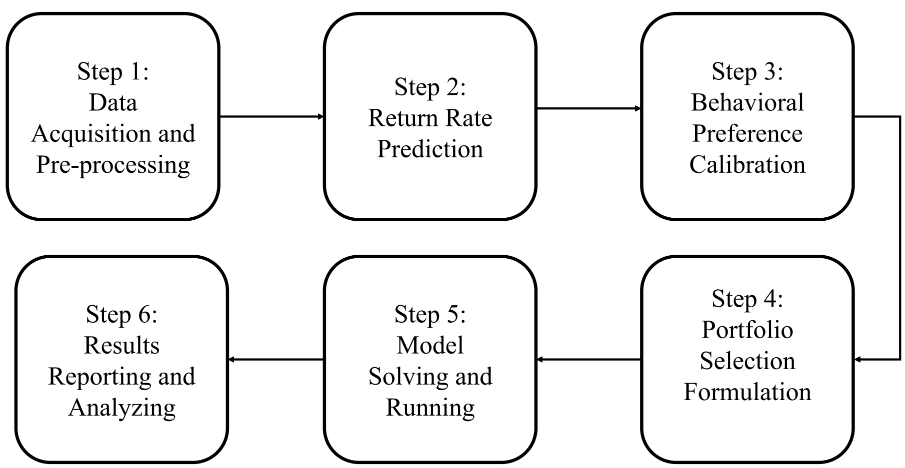

Figure 3.3: Flowchart of portfolio selection models.

Figure 3.3 lists the detailed procedures of the proposed multi-objective framework, which is the same to the multiple reference points portfolio selection model that will be introduced in Chapter 4. Step 1. Data acquisition and pre-processing. Collecting historical data for the selected stocks over the past 12 months, filtering outliers, handling missing data. Step 2. Return rate prediction. Experts were invited to predict expected returns for the given period in the form of fuzzy variable. Then aggregating all expert assessments into a fuzzy variable ς_i for each stock. Step 3. Behavioral preference calibration. Behavioral assumptions will be linked to real inputs and assigned. Step 4. Portfolio selection model formulation. The mathematical form of the proposed framework and comparison models could be formulated. Step 5. Model solving and running. The return prediction for each stock serves as input variables to the proposed portfolio models, with the optimization-derived investment schemes constituting the output solutions. The current chapter employs the improved cooperative PSO (ICPSO) algorithm integrated with fuzzy simulation as the solution methodology, while Chapter 4 utilizes the adaptive cooperative PSO (ACPSO) algorithm coupled with fuzzy simulation. Detailed technical specifications of these solution algorithms are systematically presented in Chapter 5. Conducting empirical validation of the optimized investment strategies under live market conditions. Step 6. Systematically collect and statistically analyze the performance metrics of the implemented strategies within authentic trading environments.

The case study spans from 1 Jan. 2023 to 31 Mar. 2023, covering 90 calendar days, of which 59 are trading sessions. Guided by domain expertise and observations from publicly available financial reports, predictive returns for each candidate stock are encoded as fuzzy variables and reported in Table 3.2. In that table, (a, b), (a, b, c) and (a, b, c, d) respectively represent a Gaussian variable, a triangular variable and a trapezoidal variable in fuzzy set.

Several parameters are specified prior to optimization, including the risk threshold Υ, the confidence level $1 - \gamma$, and the reference point r_0 in Equation 3.16. Following the recommendation in [162], $\Upsilon = 0.1$ and $\gamma = 0.1$. The reference point r_0 as 1.003, representing the risk-free rate.

Each model's performance is determined by its stock holdings, as shown in Figure 3.4

Table 3.2: Return predictions for sampled stocks in Case Study 1.

Stock No.	Return	Stock No.	Return
1	(0.95, 0.51)	2	(1.02, 0.77)
3	(0.88, 1.01)	4	(1.08, 1.07)
5	(0.83, 1.05, 1.22)	6	(0.88, 0.93, 1.10)
7	(0.87, 1.02, 1.42)	8	(0.83, 0,94, 1.03, 1.2)
9	(0.88, 1.01, 1.11, 1.41)	10	(0.83, 0.99, 1.03, 1.33)

and Table 3.3. **EU-C** places the entire allocation into just two securities — elevating risk but potentially increasing return but elevating risk, whereas **B&H** displays excessive diversification. In contrast to the concentration of **EU-C** and the broad spread of **B&H**, the intermediate allocation from **MO-V** holds six stocks, consistent with its dual objective of boosting expected payoff (via the Sharpe ratio) while containing risk (via VaR). The proposed multi-objective framework **E&TU** selects four constituents, namely No. 3, 4, 9, and 10.

Table 3.3: Stock position in Case Study 1.

Model \ Stock	1	2	3	4	5	6	7	8	9	10
E&TU	0	0	0.301	0.203	0	0	0	0	0.224	0.272
B&H	0.1	0.1	0.1	0.1	0.1	0.1	0.1	0.1	0.1	0.1
EU-C	0	0	0	0.654	0.346	0	0	0	0	0
MO-V	0	0	0.178	0.174	0.124	0	0	0.251	0.166	0.107

The investment performance of the four portfolio selection models is assessed using six criteria listed in Table 3.4. These six measures are computed at the end of the investment horizon by Equation 3.21- 3.26.

$$\mathbf{CW} = \sum_{i=1}^{n} x_i' * p_i', \tag{3.21}$$

where x_i' and p_i' are the security investment proportion and the terminal price of i-th term.

$$\mathbf{AY} = \mathbf{CW}^{n/252} - 1, \tag{3.22}$$

Figure 3.4: Stock position in Case Study 1.

Table 3.4: Summary of selected criteria

Type	Criterion	Abbreviation	Description
return	wealth accumulation	CW	total wealth at horizon.
return	annual percentage yield	AY	average annualized return.
risk	maximum drawdown	MD	Largest peak-to-trough loss.
Risk	volatility	Vol	Return dispersion (std. dev.).
Risk-adjusted return	Sharpe index	SR	Excess return per volatility.
Risk-adjusted return	Calmar index	CR	Annual return / max drawdown.

A trading year is assumed to contain 252 days.

$$\mathbf{MD} = \max_{1 \leq i \leq n} \frac{\mathrm{M}_i - \mathbf{CW}_i}{\mathrm{M}_i}, \tag{3.23}$$

where M_i denotes the running peak up to day i, and $\mathbf{CW}_i$ is the wealth accumulation on the i-th day.

$$\mathbf{Vol} = \sqrt{252} * \Sigma, \tag{3.24}$$

with Σ being the standard deviation of the portfolio's returns.

$$\mathbf{SR} = \frac{\mathbf{AY} - r_0}{\Sigma}, \tag{3.25}$$

where x_0 is the chosen reference (benchmark) return rate.

$$\mathbf{CR} = \frac{\mathbf{AY}}{\mathbf{MD}}. \tag{3.26}$$

The computed metric values for the four aforementioned models are reported in Table 3.5, with the best-performing figures highlighted in bold for clarity.

Table 3.5: Performance under selected criteria at the end of the given period in Case Study 1.

Criterion / Model	**CW**	**AY**	**MD**	**Vol**	**SR**	**CR**
E&TU	1.197	0.801	0.127	0.313	**2.56**	**6.307**
B&H	1.037	0.147	**0.072**	**0.087**	1.69	2.042
EU-C	**1.238**	**0.973**	0.167	0.479	2.03	5.826
MO-V	1.151	0.613	0.134	0.351	1.75	4.575

Furthermore, to provide an intuitive visualization of the hierarchical performance relationships among the four models across the six aforementioned metrics, a corresponding radar chart has been systematically constructed and is presented in Figure 3.5. The radar chart analysis demonstrates a systematic positive correlation between radial distance from the origin and model performance superiority across all evaluated metrics, with outermost positional coordinates indicating optimal behavioral alignment under respective measurement dimensions.

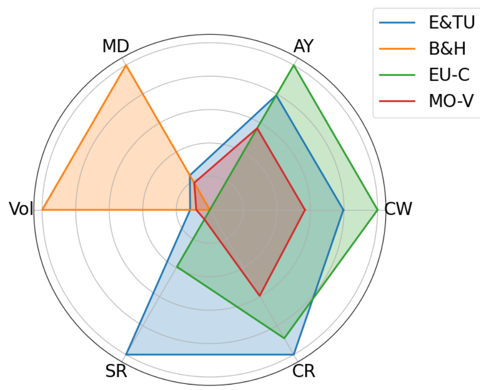

Figure 3.5: Performance under selected metrics in Case Study 1 (Radar Chart).

Table 3.5 and Figure 3.5 reveal that every model produces greater cumulative wealth at the end of the investment horizon than at its outset, reflecting the upward movement of most of the ten constituent stocks during the period. Because **B&H** adopts a highly diversified stance, it delivers the lowest return but also the lowest risk. At the opposite extreme, **EU-C** concentrates the portfolio, yielding the highest return and the highest risk. Positioned between these two, **MO-V** and **E&TU** occupy an intermediate region on both the return and risk axes, illustrating the ability to balance the two dimensions.

As expected utility and total utility are two parallel objectives of the proposed **E&TU** model. Pursuing expected utility induces a return-seeking orientation, whereas maximizing total utility—which embeds loss aversion from prospect theory and disappointment aversion from disappointment theory—encourages risk-mitigating decisions. Consequently, **E&TU** outperforms **B&H** and **MO-V** in return-seeking capability while surpassing **EU-C** and **MO-V** in risk avoidance. When evaluated on a risk-adjusted basis, **E&TU** exhibits the most favorable trade-off between reward and risk.

Taken together, the results indicate that **E&TU** generates steadier and more reliable profit streams than the alternative portfolio selection baselines considered.

3.3.3 Case Study 2: NYSE Real Market Data Case

In portfolio-selection research, variations across markets and time periods can exert a pronounced influence on model robustness. To further assess the effectiveness of the proposed multi-objective framework in settings with multiple risky assets, an auxiliary illustrative case study—adapted from prior literature [162] is provided. Wang et al. [162] selected 10 stocks from New York Stock Exchange and provided return rate predictions to these stocks for future four months, from Dec. 30, 2011, as listed in Table 3.6.

Table 3.6: Return rate predictions for stocks in Case Study 2.

Security No.	Ticker*	Return	Expected Value**
1	STV	(-0.129, 0.091, 0.259)	0.078
2	CNEP	(-0.280, 0.254, 0.689)	0.231
3	CNTF	(-0.306, 0.161, 0.461)	0.119
4	CBEH	(-0.462, 0.487, 0.872)	0.346
5	CHL	(-0.071, 0.083, 0.148)	0.061
6	ACH	(-0.109, 0.164, 0.267)	0.122
7	CAST	(-0.263, -0.077, 0.085)	-0.006
8	DANG	FG(0.199, 0.099)	0.199
9	CNAM	FG(0.250, 0.124)	0.250
10	CBAK	FG(0.032, 0.015)	0.032

* : short alphanumeric code that uniquely identifies a publicly traded stock.
** : calculated by Equation 3.8.

Similarly to Case Study 1, ICPSO was also adopted as the solution algorithm in this case to obtain the optimal stock position, as tabulated in Figure 3.6. Then Table 3.7 lists the results of the criterion of the four portfolio selection frameworks. Table 3.4 was listed for easy reference.

To provide an intuitive visualization of the hierarchical performance relationships among the four models across the six aforementioned metrics, a corresponding radar chart has

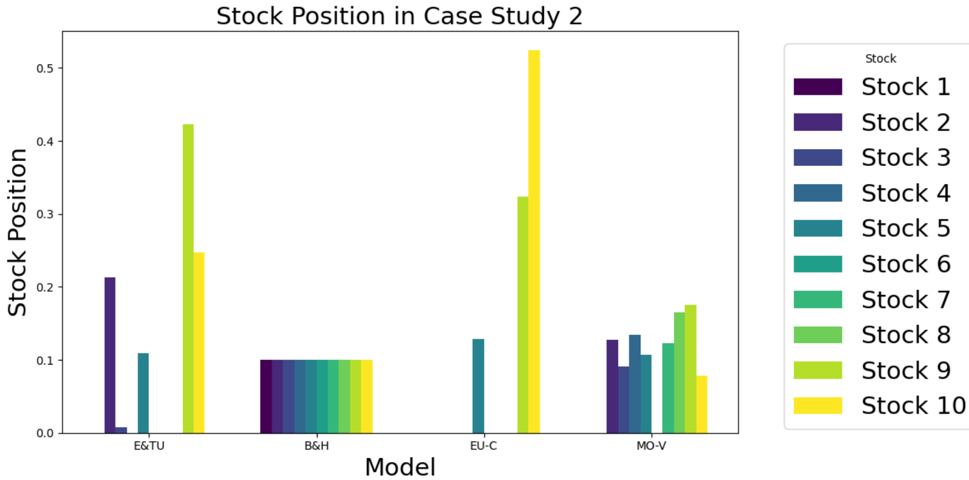

Figure 3.6: Stock position in Case Study 2.

Table 3.7: Performance under selected criteria at the end of the given period in Case Study 2.

Criterion / Model	**CW**	**AY**	**MD**	**Vol**	**SR**	**CR**
E&TU	**1.442**	**1.326**	0.211	0.359	**3.694**	**6.2844**
B&H	1.159	0.477	0.204	0.278	1.716	2.338
EU-C	1.238	0.973	**0.176**	**0.257**	3.786	5.528
MO-V	1.151	0.613	0.216	0.313	1,959	2.838

Table 3.4: Summary of selected criteria.

Type	**Criterion**	**Abbr.**	**Description**
Return	wealth accumulation	**CW**	Total wealth at horizon.
Return	annual percentage yield	**AY**	Average annualized return.
Risk	maximum drawdown	**MD**	Largest peak-to-trough loss.
Risk	volatility	**Vol**	Return dispersion (std. dev.).
Risk-adjusted return	Sharpe index	**SR**	Excess return per volatility.
Risk-adjusted return	Calmar index	**CR**	Annual return / max drawdown.

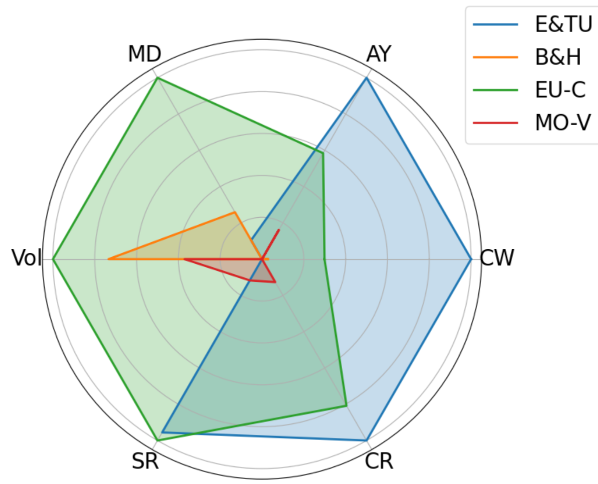

Figure 3.7: Performance under selected criteria in Case Study 2 (Radar Chart).

been systematically constructed and is presented in Figure 3.7. From the data presented in Figure 3.7 and Table 3.7, it is clear that, relative to the over–diversified allocation of **B&H**, **EU-C** concentrates its holdings in stocks No. 5, No. 9, and No. 10. **EU-C** delivers not only higher returns but also stronger results on risk criteria, indicating that the stock selections are supported by reliable return forecasts in this case. **E&TU** achieves top-tier investment returns and simultaneously attains the best risk-adjusted performance, demonstrating the framework's capability to pursue gains while containing risk. Hence, **E&TU** can be regarded as an effective portfolio selection approach.

This chapter presents a new multi-objective portfolio selection model that integrates expected-utility theory, prospect theory, and disappointment theory. Maximizing expected utility guides the allocation toward return seeking, whereas maximizing total utility (comprising prospect value and a disappointment index) steers the allocation toward risk control. Two empirical studies using real market data are conducted to assess effectiveness, with the proposed model compared against three alternative portfolio methods. Across return, risk, and risk-adjusted-return criteria, the proposed model consistently produces more stable profits than the comparators.

To fill in the first research gap, incompleteness and narrowness of behavioral-based portfolio selection models, this chapter adopts a model-driven approach to propose a multi-objective portfolio selection model that integrates multiple behavioral decision theories. Complementing it, the following chapter will adopt a theory-centric approach to propose an enhanced prospect theory that encompasses diverse decision biases, and a portfolio selection model that targets the same gap. Taken together, the two proposed portfolio selection models try to fill in the first research gap from distinct perspectives, and a comprehensive exposition of the latter will be provided in Chapter 4.

Chapter 4

ENHANCEMENT OF PROSPECT THEORY ENCOMPASSING DIVERSE DECISION BIASES

In Chapter 3, I adopted a model-driven approach to propose a multi-objective portfolio selection framework aimed at addressing the first research gap. In contrast, the current chapter employs a theoretically innovative methodology to resolve the same gap. As articulated previously, Chapters 3 and 4 represent complementary approaches toward achieving the overall objective of this study: developing a unified framework to comprehensively characterize investor behavior. While Chapter 3 focuses on structural refinements to portfolio models through behavioral multi-objective optimization, this chapter advances theoretical enhancements to prospect theory, integrating adaptive reference points and dynamic risk constraints. Together, these parallel strategies synergistically address the limitations of existing behavioral portfolio models, ensuring both methodological diversity and conceptual coherence in achieving the overarching goal of bridging behavioral realism with computational tractability in portfolio optimization.

To comprehensively depict investor behavior patterns and to provide investment guidance in highly uncertain and volatile markets, this study introduces a multiple reference point model for representing prospect theory and based on this, develops a portfolio selection optimization framework. The effectiveness of this model is validated through Case Studies 3 and 4. This multiple reference point framework and the findings have been complied in an international journal paper: [168] by **X. Wang**, B. Wang, T. Long and Y. Wu. Prospect theory-based portfolio selection using multiple fuzzy reference intervals. *IEEE Transactions on Systems, Men and Cybernetics: Systems*, 55(10): 7100-7114, 2025.

4.1 Introduction of the Prospect Theory Encompassing Diverse Decision Biases

Although prior studies have developed portfolio models grounded in advances in prospect theory, the related works could be further extended considering the following three aspects: First, the key property of prospect theory is reference dependable. Investors perceive gains and losses with respect to a reference point (e.g. the risk-free rate). In this regard, an outcome with continuous distribution can be split into two separate domain, gain and loss [77]. Although prospect theory is widely accepted, some studies [169] question its accuracy in fitting investors' investment paradigms in complex real-world decision-making environments. For instance, Chapman et al. [170] observed that while investors indeed exhibit loss aversion, some choose high-risk investment targets when faced with opportunities for high returns, a phenomenon that prospect theory cannot explain. Beyond the status quo, numerous studies advocate introducing alternative reference points; moreover, observed choice patterns have been explained by specifying value functions that incorporate multiple reference points [171]. Comparing with classical prospect theory, the use of multiple reference points divides the prospect value function into more specific domains, e.g. the domain of return rate lower than a minimum requirement, the domain of return rate higher than a goal and the domain of return rate between the minimum requirement and goal [172]. In this way, the multiple reference points-based prospect theory is able to address investors' psychological mechanisms in a more detailed manner, thus providing more comprehensive decision support for investors especially those who are more sensitive to risk-taking and goal-seeking.

Second, most of the existing studies assumed that the numerical value of reference point is exactly known. This is reasonable since investors have their specific target returns towards an investment, or they can directly set the value according to the risk-free rate. However, for some investors, the reference point could be ambiguous and hard to determine due to the variation of psychological processes and the complicated nature of financial market. In this regard, the uncertainty of reference points could be considered in the prospect theory-based portfolio selection. More importantly, for a given distribution of security return, the setting of different reference points can certainty has an impact on the portfolio selection. Therefore, it is of interest to co-optimize the reference point values with portfolio selection, so that not only the exact reference point can be determined, but also an optimal investment decision can be made.

Finally, prospect theory - widely regarded as the most influential framework for characterizing human decision behavior - has been extensively employed to account for the effects of psychological factors on the choices of decision makers. Although prospect theory shows certain strong aspects than expected utility theory in portfolio selection, the latter is still widely adopted by a number of investors. Moreover, as noted in [173], although the prospect optimal portfolio often lies on the mean–variance frontier (i.e., the locus representative of expected utility choices), it implies an exceptionally low level of risk aversion. Consequently, investors modeled under expected utility with conventional degrees of risk aversion would not select the prospect optimal allocation. Therefore, it could be meaningful to incorporate the merits of expected utility into the prospect theory based fuzzy portfolio selection, so that providing expected utility investors with trusted decision support.

Based on the above analysis, this study introduces an enhanced prospect theory that encompasses diverse decision biases and a portfolio selection model based on the enhanced prospect theory could be formulated. First, for each forecasted membership function of security returns, two reference points i.e., the minimum requirement and goal are used to divide the prospect value function into three domains, the curvature parameters and related coefficients of which are set differently. Second, the uncertainty of reference points is addressed in the proposed model, and I try to find effective portfolio by optimizing the numerical values of the minimum requirement and goal together with capital allocations. Third, the model is established to incorporate expected utility into prospect theory based fuzzy portfolio selection. Especially, mean-absolute deviation is converted to a constraint of the proposed model, thus avoiding the assignment of extreme reference points.

4.2 Prospect Theory Encompassing Diverse Decision Biases

In this section, I provide a comprehensive exposition of the enhanced prospect theory that encompasses diverse decision biases to fill in the first research gap, incompleteness and narrowness in behavioral-based portfolio selection. Specifically, this section focuses on the theoretical rationale and computational methodology for developing an enhanced prospect theory framework that incorporates multiple dynamic reference points, alongside its application to portfolio selection modeling.

4.2.1 Using of Two Reference Points

With respect to a single reference point, the prospect value in classical prospect theory can be divided into a gain domain and a loss domain, as shown in Figure 4.1-(a), in which the reference point is set as 0.05. However, researchers have doubted that the using of one reference point may not sufficiently describe investors' psychological mechanisms [172], especially for those investors who are sensitive to both risk-taking and goal-seeking. More specifically, according to the discussion in [174], investors' psychological mechanisms can be rank ordered as failure ($r_i < \texttt{MR}$, $\texttt{MR}$ is the value of the minimum requirement), success ($r_i > \texttt{G}$, $\texttt{G}$ is the value of the goal) and status quo ($\texttt{MR} \leq r_i \leq \texttt{G}$). Figure 4.1 illustrates the motivations for using two reference points, involving reference point uncertainties and incorporating expected utility theory into prospect theory-based fuzzy portfolio selection. Therefore, in this study, I consider the minimum requirement and goal as the two reference points which divide the prospect value function into three domains, as shown in Figure 4.1-(b). Accordingly, the classical prospect value function is revised to Equation 4.1 for investors who are sensitive to both risk-taking and goal-seeking.

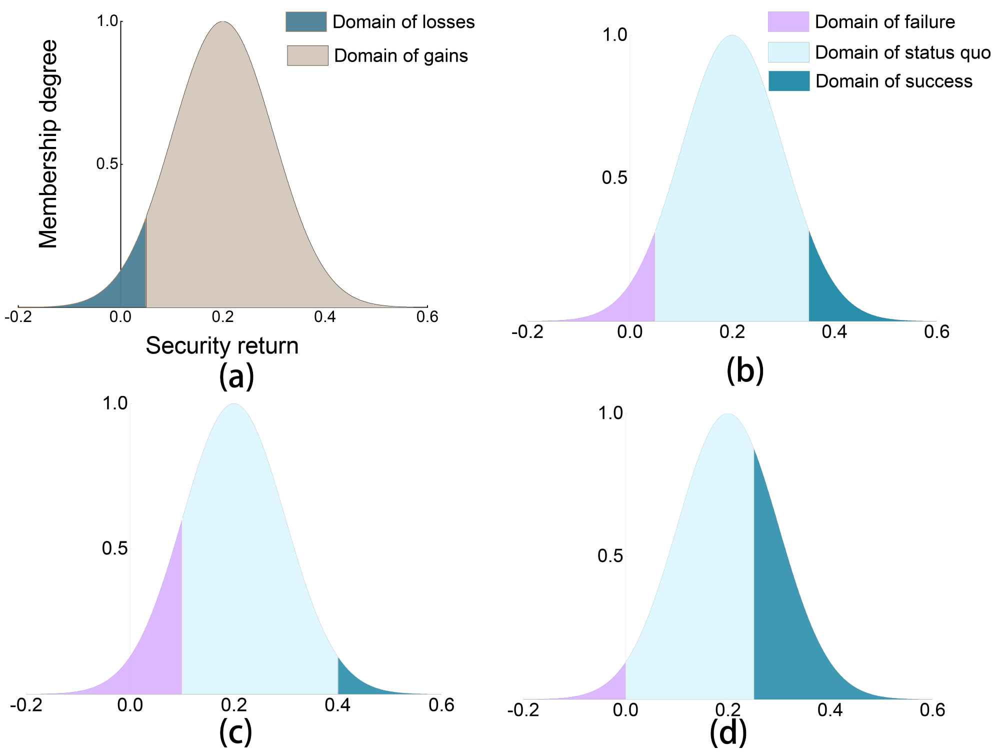

Figure 4.1: Motivations of using two reference points.

$$v(r_i) = \begin{cases} (r_i - \texttt{MR})^{\alpha} + \eta(r_i - \texttt{G})^{\gamma}, & r_i > \texttt{G}, \\ (r_i - \texttt{MR})^{\alpha}, & \texttt{MR} \leq r_i \leq \texttt{G}, \\ -\lambda(\texttt{MR} - r_i)^{\beta}, & r_i < \texttt{MR}, \end{cases} \tag{4.1}$$

where r_i is any realization of ξ_i. α, β and γ represent the curvature parameters for status quo, failure and success respectively. λ and η are the loss aversion ratio and seeking pride ratio, and it is assumed that $\lambda \geq \eta \geq 1$ which follows the rank order mentioned above. Moreover, the prospect value of the success domain includes two parts: $(r_i - \mathtt{MR})^{\beta}$ indicates the prospect value of reaching the minimum requirement, while $\eta(r_i - \mathtt{G})^{\alpha}$ reflects additional satisfaction of achieving the goal. Generally, Equation 4.1 can be changed without difficulty to accommodate investors with different rank orders.

Figure 4.2 shows how expected utility theory, classical prospect theory and prospect theory with two reference points used in this study quantitatively describe the relationship between investment returns and their utility to the investor. As can be seen from the figure, expected utility theory is a linear map which considers the effects produced by gains and losses to be equal in magnitude. In this demonstration figure, setting $\alpha = \beta = 0.88$, $\lambda = 2.25$ which follows the findings in [66]. The reference point is set as 0. Prospect theory considers the effects by losses to be more significant than expected utility theory. The differences between prospect theory and expected theory when the return is negative is significantly smaller than the difference when the return exceeds the reference point. In this demonstration figure, the minimum requirement is 0, the same as the value of the reference point, and the goal is 0.12.

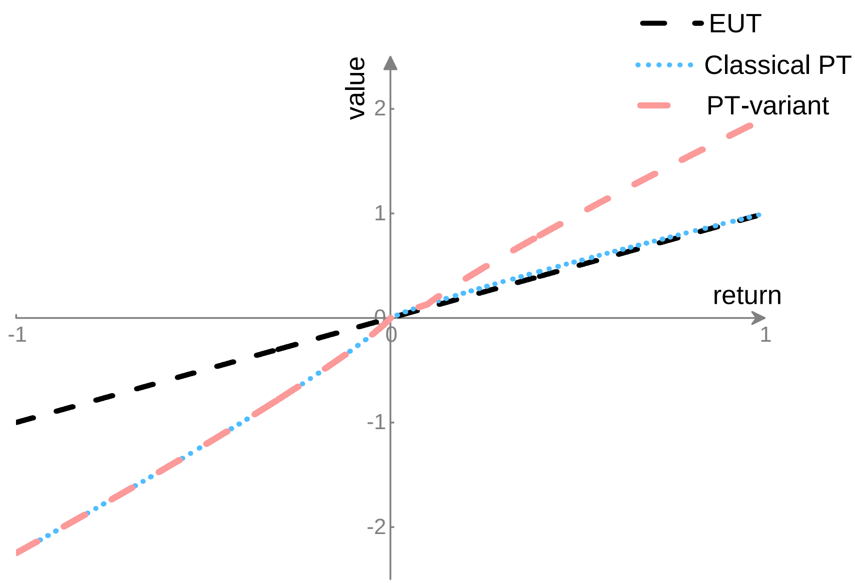

Figure 4.2: Utility functions of expected utility theory, classical prospect theory and prospect theory with two uncertain reference points.

The prospect theory-variant used in this study assumes that the impact produced is the same as prospect theory until the investment return reaches the goal. However, after the return exceeds the goal, the return will have a more significant impact on the investor due to the return chasing behavior of the investor.

4.2.2 Consideration of Reference Points Uncertainties

In this research, the minimum requirement and goal are taken as imprecise values for two reasons. First, due to the variation of psychological process and the complicated nature of financial market, it could be difficult for some investors to assign exact minimum requirement and goal. For example, these values might be expressed with ambiguity such as the minimum requirement is about 8% or the goal is within [20%, 25%]. Therefore, it is reasonable to consider the ambiguity of reference points. Second, for a given membership distribution of security return, the assignment of varied the minimum requirement and the goal leads to different prospect values. For example, if Equation 4.1 is taken as the prospect value function, then the prospect value of condition that the minimum requirement is 0.05 and the goal is 0.35 is larger than that of the minimum requirement is 0.1 and the goal is 0.4, as shown in Figure. 4.1-(b) and Figure 4.1-(c). Therefore, the prospect value is sensitive to reference points, and investors with varied minimum requirement and goal could have totally different evaluations upon the same distribution of security return, which certainty affects the result of portfolio optimization. In view of this, it is also meaningful to investigate the impact of varied reference points on portfolio selection.

4.2.3 Incorporation of Expected Utility Theory

Finally, the motivation of incorporating expected utility into prospect theory based fuzzy portfolio selection is explained. In some cases, an investor may set small values to both minimum requirement and goal, e.g. Figure. 4.1-(d) depicts the membership degree when the minimum requirement and goal are 0 and 0.25. According to Equation 4.1, it can be found that the overall prospect value of Figure 4.1-(d) is obviously larger than that of Figure 4.1-(b) and Figure. 4.1-(c). Essentially, for a given distribution of security return, the smaller minimum requirement and goal are, the larger the prospect value will be, and vice versa. Nevertheless, the behavior of obtaining large prospect values via setting small reference points is unacceptable for rational investors, especially those expected utility investors who aim to maximize the possibility of obtaining high expected wealth because the distribution of security return is fixed and does not change with reference points. Generally, it is an important concern for typical expected utility investors to give such a confidence interval, so that the chance of obtaining high expected wealth can be maximized.

Therefore, aims at improving the practical significant of prospect theory, this study incorporates the merits of expected utility into prospect theory based fuzzy portfolio selection by using mean-absolute deviation. Specifically, the cumulative return and absolute deviation of the portfolio is combined to the following inequality, which will be applied as a constraint of the proposed model.

$$\mathbf{E}\left[\sum_{i=1}^{n} x_i \vec{\xi_i}\right] - \rho \mathbf{A}\left[\sum_{i=1}^{n} x_i \vec{\xi_i}\right] \geq L, \tag{4.2}$$

where $\vec{\xi_i}$ in constraint 4.2 represents the return rate variable of security i, $\mathbf{E}[\cdot]$ and $\mathbf{A}[\cdot]$ indicate the cumulative return and absolute deviation of the portfolio, ρ is a non-negative risk coefficient and L is an adjusted return level set by an investor. As discussed later in Section 4.2.4, constraint represented by Equation 4.2 could avoid the setting of extreme minimum requirement and goal, thus improving the prospect theory portfolio selection.

Let e be the expected value of fuzzy variable . Then the absolute deviation of $\vec{\xi}$ is defined as:

$$\mathbf{A}[\vec{\xi}] = \mathbf{E}[|\vec{\xi} - e|]. \tag{4.3}$$

And for a portfolio decision including n securities, its absolute deviation can be calculated as :

$$\mathbf{A}\left[\sum_{i=1}^{n} x_i \vec{\xi_i}\right] = \mathbf{E}\left[\left|\sum_{i=1}^{n} x_i \vec{\xi_i} - \mathbf{E}\left[\sum_{i=1}^{n} x_i \vec{\xi_i}\right]\right|\right], \tag{4.4}$$

where $\vec{\xi_i}$ represents the fuzzy return of security i and x_i is the proportion of total fund invested in security i.

As mentioned before, mean-absolute deviation generates similar portfolio to that of mean-variance within a fraction of time required to solve. Therefore, in this thesis, mean-absolute deviation is used to incorporate excepted utility into prospect theory based fuzzy portfolio selection.

4.2.4 Mathematical Modeling of the Proposed Prospect Theory Framework

In this section, the mathematical formulation of the prospect theory based fuzzy portfolio selection model proposed in this study and is presented and discussed its impact. This model aims to maximize the overall prospect value subjects to a given mean-absolute deviation level, as shown in Equation 4.5.

$$\begin{cases} \max \sum_{i=1}^{n} v(\vec{\xi_i}) = \sum_{i=1}^{n} x_i \left[v(\vec{\xi}_{i,f}) + v(\vec{\xi}_{i,sq}) + v(\vec{\xi}_{i,s}) \right], \\ \text{s.t. } \mathbf{E}\left[\sum_{i=1}^{n} x_i \vec{\xi_i} \right] - \rho \mathbf{E}\left[\sum_{i=1}^{n} x_i \vec{\xi_i} \right] \geq L_1, \\ \qquad \rho \geq 0, \\ \qquad x_1 + x_2 + \cdots x_n = 1, x_1, x_2, \cdots x_n \geq 0. \end{cases} \tag{4.5}$$

$$\begin{cases} \max \mathbf{E}\left[\sum_{i=1}^{n} x_i \vec{\xi_i} \right] - \rho \mathbf{E}\left[\sum_{i=1}^{n} x_i \vec{\xi_i} \right], \\ \text{s.t.} \sum_{i=1}^{n} v(\vec{\xi_i}) = \sum_{i=1}^{n} x_i \left[v(\vec{\xi}_{i,f}) + v(\vec{\xi}_{i,sq}) + v(\vec{\xi}_{i,s}) \right] \geq L_2, \\ \qquad \rho \geq 0, \\ \qquad x_1 + x_2 + \cdots x_n = 1, x_1, x_2, \cdots x_n \geq 0. \end{cases} \tag{4.6}$$

In Equation 4.5, $v(\vec{\xi}_{i,f})$, $v(\vec{\xi}_{i,sq})$ and $v(\vec{\xi}_{i,s})$ represent the prospect values of the failure, status quo and success domains of each security respectively, which can be calculated by Equation 4.7. The last constraint means that short sale is not allowed and no cash left. Meanwhile, the structure of Equation 4.5 can be changed easily to maximize $\mathbf{E}[\cdot] - \rho\mathbf{A}[\cdot]$ subjects to a predefined level of prospect value, as shown in Equation 4.6.

$$\begin{cases} v(\vec{\xi}_{i,f}) = \displaystyle\int_{-\infty}^{\texttt{MR}} -\lambda(\texttt{MR} - r_i)^{\gamma} \mu_{\vec{\xi}_i}(r_i)\mathrm{d}r_i. \\ v(\vec{\xi}_{i,sq}) = \displaystyle\int_{\texttt{MR}}^{\texttt{G}} (r_i - \texttt{MR})^{\beta} \mu_{\vec{\xi}_i}(r_i)\mathrm{d}r_i. \\ v(\vec{\xi}_{i,s}) = \displaystyle\int_{\texttt{G}}^{+\infty} \left[(r_i - \texttt{MR})^{\beta} + \eta(r_i - \texttt{G})^{\alpha}\right] \mu_{\vec{\xi}_{i,s}}(r_i)\mathrm{d}r_i. \end{cases} \tag{4.7}$$

Before giving the solution algorithm, some properties of the two reference points are briefly discussed. Table 4.1 lists the impact from the fluctuations of the minimum requirement (when the goal is fixed) and the goal (when the minimum requirement is fixed) on the prospect value as well as the cumulative return and absolute deviation, where '↑' and '↓' express the increasing and decreasing of the corresponding values. '-' means that the change of reference points has no influence on the values.

Table 4.1: Impact from fluctuations of the minimum requirement and goal.

	MR ↓	MR ↑	G ↓	G ↑
$V(\vec{\xi}_{i,f})$	↑	↓	-	-
$v(\vec{\xi}_{i,sq})$	↑	↓	↓	↑
$v(\vec{\xi}_{i,s})$	↑	↓	↑	↓
$v(\vec{\xi}_i)$	↑	↓	↑	↓
$\mathbf{E}\left[\sum_{i=1}^{n} x_i\vec{\xi}_i\right]$	↑	↓	↓	↑
$\mathbf{A}[\sum_{i=1}^{n} x_i\vec{\xi}_i]$	↑	↓	↓	↑

Table 4.1 illustrates that, as a non-negative value, the decreasing of minimum requirement improves the overall prospect value ($v(\vec{\xi}_i)$) and the cumulative return ($\mathbf{E}[\cdot]$), but increases the investment risk taken since the absolute deviation ($\mathbf{A}[\cdot]$) has been increased. By contrast, the rising of minimum requirement reduces the absolute deviation, which however leads to a lower prospect value and cumulative return. On the goal side, the decreasing of the goal improves the overall prospect value and absolute deviation, but reduces the cumulative return. By comparison, the increasing of the goal produces a higher cumulative return, which however deteriorates the prospect value as well as the absolute deviation.

Based on the above analysis, the following preliminary conclusions can be arrived at: firstly, the decreasing of both minimum requirement and goal results in a higher overall prospect value; secondly, the decreasing of the minimum requirement and the increasing of the goal produces a higher cumulative return; finally, the increasing of the minimum requirement and the decreasing of the goal leads to a lower absolute deviation. Therefore, in view of the above contradictions, it is meaningful to co-optimize the reference points with capital allocations.

In Equation 4.5, the mean-absolute deviation function incorporates investment return and risk indexes simultaneously. The effects of this function before introducing the solution algorithm are briefly discussed. To streamline the discussion, supposing the investment scheme was made from two independent security. Security's return rates are denoted by two symmetric triangular fuzzy variable $\vec{\xi_1} = (a_1, b_1, c_1)$ and $\vec{\xi_2} = (a_2, b_2, c_2)$. Assuming that the expected return and risks of $\vec{\xi_2}$ are higher than those of $\vec{\xi_1}$. which means $a_2 < a_1 < 0 < b_1 < b_2 < c_1 < c_2$. Suppose the investment proportion for $\vec{\xi_1}$ is x_1, and for $\vec{\xi_2}$ is x_2, $x_1 = 1 - x_2$.

Since $\vec{\xi_1}$ and $\vec{\xi_2}$ are symmetric, then the expected return of $\vec{\xi_1}$ and $\vec{\xi_2}$ are b_1 and b_2. Assuming the expected return of the investment scheme is b_0. Since $\vec{\xi_1}$ and $\vec{\xi_2}$ are independent, then $b_0 = \mathbf{E}\left[\sum_{i=1}^{n} x_i\vec{\xi_i}\right] = x_1\vec{\xi_1} + x_2\vec{\xi_2}$. It is obvious $b_1 \leq b_0 \leq b_2$. The absolute deviation of the portfolio could be calculated as :

$$\mathbf{A}[\sum_{i=1}^{2} x_i\vec{\xi_i}] = \mathbf{E}[\sum_{i=1}^{2} x_i \mid \vec{\xi_i} - b_0 \mid] = \sum_{i=1}^{2} x_i\mathbf{E}[\mid \vec{\xi_i} - b_0 \mid] \tag{4.8}$$

In order to calculate the expected value of $\mid \vec{\xi_i} - b_0 \mid$, the membership function $\mu_1(t)$ of $\vec{\xi_1}$ was divided into two parts $\mu_{1L}(t)$ and $\mu_{1R}(t)$ by b_0. Similar to this, $\mu_2(t)$ was divided into $\mu_{2L}(t)$ and $\mu_{2R}(t)$.

$$\mu_{1L}(t) = \begin{cases} \frac{c_1-b_1}{t+c_1-b_0}, & 0 \leq t \leq b_0 - b_1, \\ \frac{b_1-a_1}{b_0-a_1-t}, & b_0 - b_1 < t \leq b_0 - a_1. \end{cases} \tag{4.9}$$

$$\mu_{1R}(t) = \frac{c_1 - b_1}{c_1 - b_0 - t}, \; 0 < t \leq c_1 - b_1. \tag{4.10}$$

$$\mu_{2L}(t) = \frac{b_2 - a_2}{b_0 - a_2 - t},\ 0 \le t \le b_0 - a_2. \tag{4.11}$$

$$\mu_{2R}(t) = \begin{cases} \dfrac{b_2 - a_2}{t + b_0 - a_2}, 0 \le t \le b_2 - b_0, \\ \dfrac{c_2 - b_2}{c_2 - b_0 - t}, b_2 - b_0 < t \le c_2 - b_0. \end{cases} \tag{4.12}$$

Based on the definitions of credibility measurement and expected value to fuzzy variables, it is easy to derive the $POS(\cdot)$, $NEC(\cdot)$ and $Cr(\cdot)$ of event $\mid \xi_1 - b_0 \mid \le r$ and $\mid \xi_2 - b_0 \mid \le r$, as presented in Equations 4.13 $\sim$ 4.24:

$$POS_{1L} = \begin{cases} \dfrac{r + c_1 - b_0}{c_1 - b_1}, 0 \le r \le b_0 - b_1, \\ 1, b_0 - b_1 < r \le b_0 - a_1. \end{cases} \tag{4.13}$$

$$POS_{1R} = \frac{c_1 - b_0}{c_1 - b_1},\ 0 < t \le c_1 - b_1. \tag{4.14}$$

$$NEC_{1L} = \begin{cases} 0, r \le b_0 - b_1, \\ \dfrac{r + b_1 - a_0}{b_1 - a_1}, b_0 - b_1 < t \le b_0 - a_1. \end{cases} \tag{4.15}$$

$$NEC_{1R} = \frac{r + b_0 - b_1}{c_1 - b_1}. \tag{4.16}$$

$$Cr_{1L} = \begin{cases} \dfrac{1}{2}\dfrac{r + c + 1 - b_0}{c_1 - b_1}, 0 \le r \le b_0 - b_1, \\ \dfrac{1}{2} + \dfrac{1}{2}\dfrac{r + b_1 - b_0}{b_1 - a_1}, b_0 - b_1 < r \le b_0 - a_1. \end{cases} \tag{4.17}$$

$$Cr_{1R} = \begin{cases} \dfrac{1}{2}\dfrac{c_1 - b_1 + r}{c_1 - b_1}, 0 < r \le c_1 - b_0, \\ \dfrac{1}{2} + \dfrac{1}{2}\dfrac{c_1 - b_0}{c_1 - b_1}, c_1 - b_0 < r \le c_1 - b_1. \end{cases} \tag{4.18}$$

$$POS_{2L} = \frac{b_0 - a_2}{b_2 - a_2},\ 0 \le r \le b_0 - a_2. \tag{4.19}$$

$$NEC_{2L} = \frac{b_2 - b_0 + r}{b_2 - a_2},\ 0 \le r \le b_0 - a_2. \tag{4.20}$$

$$POS_{2R} = \begin{cases} \dfrac{r + b_0 - a_2}{b_2 - a_2}, \; 0 \le r \le b_2 - b_0, \\ 1, b_2 - b_0 < r \le c_2 - b_0. \end{cases} \tag{4.21}$$

$$NEC_{2R} = \begin{cases} 0, \;\; 0 < r \le b_2 - b_0, \\ \dfrac{r + c_2 - b_2}{c_2 - b_2}, \; b_2 - b_0 < r \le c_2 - b_0 \end{cases} \tag{4.22}$$

$$Cr_{2L} = \frac{1}{2} + \frac{1}{2}\frac{r}{b_2 - a_2}, \;\; 0 \le r \le b_0 - a_2. \tag{4.23}$$

$$Cr_{2R} = \begin{cases} \dfrac{1}{2}\dfrac{r + b_0 - a_2}{b_2 - a_2}, \; 0 \le r \le b_2 - b_0, \\ 1 - \dfrac{1}{2}\dfrac{c_2 - b_0 - r}{c_2 - b_2}, \; b_2 - b_0 < r \le c_2 - b_0. \end{cases} \tag{4.24}$$

Then the expected value of $\mid \vec{\xi_1} - b_0 \mid$ and $\mid \vec{\xi_2} - b_0 \mid$ could be calculated since the credibility function is self-dual.

$$\begin{aligned} \mathbf{E}[|\vec{\xi_1} - b_0|] =& (b_0 - b_1) + \frac{(b_0 - b_1)^2}{2(c_1 - b_1)} + \frac{1}{4}(b_1 - a_1) \\ &+ \frac{1}{2}(c_1 - b_0) - \frac{(c_1 - b_0)^2}{4(c_1 - b_1)}, \end{aligned} \tag{4.25}$$

$$\mathbf{E}[|\vec{\xi_2} - b_0|] = \frac{1}{4}(2b_0 - a_2 - 2b_2 + c_2). \tag{4.26}$$

Assuming a special condition $b_1 = b_2$ which means these two security holds the same expected return. Then it's obvious $b_0 = b_1 = b_2$. Since $\vec{\xi_1}$ and $\vec{\xi_2}$ are symmetric, assuming $c_1 - b_1 = b_1 - a_1 = \Delta_1$, $c_2 - b_2 = b_2 - a_2 = \Delta_2$, $\Delta_2 \ge \Delta_1$. Then the absolute deviation of the portfolio could be denoted as follow:

$$\mathbf{A}[\sum_{i=1}^{2} \vec{\xi_i}] = \frac{1}{2}(x_1\Delta_1 + x_2\Delta_2). \tag{4.27}$$

Then the mean-absolute deviation of this portfolio could be denoted as follow:

$$\mathbf{E}[\sum_{i=1}^{2} \vec{\xi_i}] - \rho\mathbf{A}[\sum_{i=1}^{2} \vec{\xi_i}] = b_0 - \frac{1}{2}\rho(x_1\Delta_1 + x_2\Delta_2). \tag{4.28}$$

Since ρ is a predefined constant, b_0 is also a constant in this example, and $\Delta_2 \geq \Delta_1$. Obviously this function will maximize x_1 while minimize x_2, which means increase the investment proportion of the first security while decrease the other. The first security is more conservative than the second one, and it may yield lower potential returns ($c_1 \leq c_2$) and involve less risk ($a_1 \geq a_2$) compared to the second one. Thus it is easy to draw the conclusion that the mean-absolute deviation function is a risk-sensitive function, which will drive the model to be conservative

4.3 Numerical Examples: Validation of the Prospect Theory-based Portfolio Selection Model

In this section, the proposed portfolio selection model's effectiveness in balancing investment return and risk is validated through two case studies that use real market data. The portfolio selection itself is built on enhanced prospect theory framework that encompasses diverse behavioral biases.

4.3.1 Case Study 3: SSE 50 Index Real Market Case

Problem description: This case discusses impacts of the following settings on portfolio selection: the impact of setting two reference points compared to setting one reference point, the impact of uncertain intervals compared to fixed values for the reference points, and the impact of different values of the parameter ρ, L_1 and L_2 in Equation 4.5 and Equation 4.6. In this case, considering a portfolio selection problem includes 10 stocks randomly selected from Shanghai Securities 50 Index. Experts carefully examined the public financial reports of these companies, along with historical stock prices and other relevant economic data, to provide price predictions for these stocks over the next three months in the future, i.e. from Oct. 1, 2022 to Dec. 31, 2022.

Supposing the closing price of security i at Sept. 30, 2022 is p_{ci}, the predicted price during the selected time window is represented as fuzzy variable p_i, the dividend is d_i. So the return rate of security i from Oct. 1, 2022 to Dec. 31, 2022 is modeled as fuzzy variable $\xi_i = \frac{p_i+d_i}{p_{ci}}$. Table 4.2 lists the selected stocks and their corresponding predicted return rates. (a, b, c) represents a triangular fuzzy variable.

Table 4.2: Return rate predictions of selected stocks in Case Study 3.

Stock No.	Code	Return Rate
1	600000	(0.85, 1.03, 1.15)
2	600048	(0.83, 1.02, 1.22)
3	600050	(0.77, 1.22, 1.75)
4	600276	(0.72, 1.02, 1.13)
5	600309	(0.89, 1.07, 1.29)
6	600703	(0.91, 1.07, 1.17)
7	600809	(0.87, 1.12, 1.31)
8	601012	(0.84, 1.02, 1.14)
9	601668	(0.91, 1.02, 1.09)
10	603986	(0.87, 1.05, 1.21)

In order to discover the impact of setting two reference points compared to setting one reference point, a one reference point fuzzy portfolio selection model is proposed, shown in Equation 4.29, as the comparison model to the mathematical model described in Equation 4.5. Also the one reference point fuzzy portfolio selection model shown in Equation 4.30 is the comparison model to the model described in Equation 4.6. The prospect values in Equations 4.29 and 4.30 are calculated by Equation 2.19. Moreover, there are some parameter values needed to be specified in advance, which are listed in Table 4.3, before running the real-market case study.

$$\begin{cases} \max \sum_{i=1}^{n} x_i v(\xi_i) \\ s.t. \mathbf{E}\left[\sum_{i=1}^{n} x_i \xi\right] - \rho \mathbf{A}\left[\sum_{i=1}^{n} x_i \xi_i\right] \geq L_1 \\ \qquad \rho, x_i \geq 0, i = 0, 1, ..., n \\ \qquad \sum_{i=1}^{n} x_i = 1, i = 0, 1, ..., n. \end{cases} \tag{4.29}$$

$$
\begin{cases}
\max \mathbf{E}\left[\sum_{i=1}^{n} x_i\xi_i\right] - \rho\mathbf{A}\left[\sum_{i=1}^{n} x_i\xi_i\right] \\
s.t. \sum_{i=1}^{n} x_i v(\xi_i) \geq L_2 \\
\qquad \rho, x_i \geq 0, i = 0, 1, ..., n \\
\qquad \sum_{i=1}^{n} x_i = 1, i = 0, 1, ..., n.
\end{cases}
\tag{4.30}
$$

Table 4.3: Parameter settings for Case Study 3.

Parameter	Description	Value
α	Curvature parameter for status quo	0.88
β	Curvature parameter for fail	0.88
γ	Curvature parameter for success	0.88
λ	Loss aversion ratio	2.25
η	Seeking pride ratio	2.25
ρ	Coefficient in Equations 4.5, 4.6, 4.29 and 4.30	0.5
L_1	Constraint in Equations 4.5 and 4.29	1.1
L_2	Constraint in Equations 4.6 and 4.30	1.1

Specifying $\alpha = 0.88$, $\beta = 0.88$ and $\lambda = 2.25$ according to Tversky and Kahneman's [66] findings. Setting $\gamma = 0.88$ and $\eta = 2.25$ is done in order to maintain consistency between the psychological mechanism of investors under two reference points and classical prospect theory, and to maximize the alignment with real investor decision-making scenarios. Setting the value of ρ to be 0.5, L_1 and L_2 to be 1.1 is done in order to ensure feasible solutions for the various investment portfolio models involved in this case.

In order to discover the impact of uncertain intervals compared to fixed values for the reference points, uncertainty reference points and fixed reference points to fuzzy portfolio selection models in this study are introduced. Therefore, there are 8 fuzzy portfolio selection models will be discussed in this case, as illustrated by Figure 4.3, which are two uncertainty reference points model in Equation 4.5 named as TUP, two uncertainty reference points model in Equation 4.6 named as TUE, two fixed reference points model in Equation 4.5 named as TFP, two fixed reference points model in Equation 4.6 named as TFE, one un-

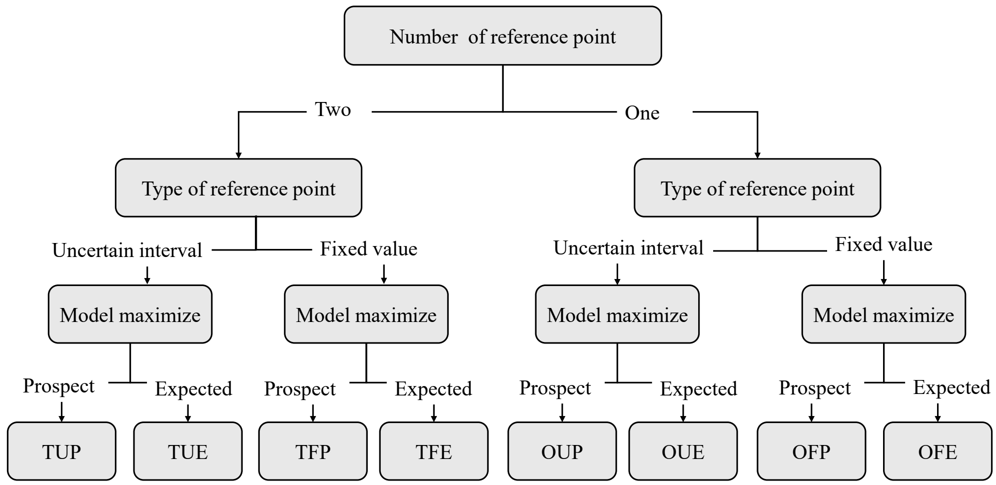

Figure 4.3: 8 portfolio selection models in Case Study 3.

certainty reference points model in Equation 4.29 named as OUP, one uncertainty reference points model in Equation 4.30 named as OUE, one fixed reference points model in Equation 4.29 named as OFP, one fixed reference point model in Equation 4.30 named as OFE.

The assignment of reference points should comply with the real investment paradigm, therefore setting minimum requirement as non-loss and the goal as the average return of the selected stocks within the investment period. Therefore the uncertain interval for minimum requirement is specified as a fuzzy triangular variable $(0.985, 1.001, 1.017)$, the fixed value for minimum requirement is specified as 1.000, the uncertain interval for the goal is specified as a fuzzy triangular variable $(1.015, 1.021, 1.032)$ and the fixed value for the goal is specified as 1.021.

The optimal solutions for each model were obtained using ACPSO, which represents the stock position results of each model within the investment period, as listed in Figure 4.4.

It can be seen from Figure 4.4 that when using two reference points, using the prospect values as the objective function results in a relatively concentrated stock distribution in the investment portfolio. It can also be observed that using two reference points leads to a more

Figure 4.4: Stock position in Case Study 3.

Table 4.4: Stock position in Case Study 3.

	1	2	3	4	5	6	7	8	9	10
TUP	0	0	0.767	0	0	0	0.233	0	0	0
TUE	0	0	0.154	0	0.234	0.357	0.255	0	0	0
TFP	0	0	0.645	0	0	0	0.355	0	0	0
TFE	0	0	0.132	0	0.257	0.418	0.193	0	0	0
OUP	0	0	0.133	0	0	0	0.867	0	0	0
OUE	0	0	0	0	0	0	1	0	0	0
OFP	0	0	0.127	0	0	0	0.873	0	0	0
OFE	0	0	0	0	0	0	1	0	0	0

diversified investment portfolio compared to using one reference point. Additionally, having uncertain intervals or fixed values for reference points may cause fluctuations in the specific allocations of selected stocks in the investment portfolio. All these stock position results were tested in the real market to obtain their corresponding investment performances. Their performances were assessed by six widely adopted metrics whose definitions and descriptions were listed in Table 3.4. The metric values of these fuzzy portfolio selection models are listed in Table 4.5). Within Table 4.5, the best performances are highlighted in boldface for better illustration.

Table 3.4: Summary of selected criteria.

Type	**Criterion**	**Abbr.**	**Description**
Return	wealth accumulation	**CW**	Total wealth at horizon.
Return	annual percentage yield	**AY**	Average annualized return.
Risk	maximum drawdown	**MD**	Largest peak-to-trough loss.
Risk	volatility	**Vol**	Return dispersion (std. dev.).
Risk-adjusted return	Sharpe index	**SR**	Excess return per volatility.
Risk-adjusted return	Calmar index	**CR**	Annual return / max drawdown.

Table 4.5: Performance under selected criteria at the end of the given period in Case Study 3.

Metric	Return		Risk		Risk-adjusted return	
	CW	AY	MD	Vol	SR	CR
TUP	**1.311**	**1.245**	0.106	0.243	**5.123**	**11.745**
TUE	1.108	0.434	0.158	**0.148**	2.932	2.747
TFP	1.258	1.032	**0.089**	0.227	4.546	11.596
TFE	1.088	0.352	0.156	0.131	2.687	2.256
OUP	1.241	0.963	0.220	0.321	3.010	4.377
OUE	1.226	0.904	0.251	0.410	2.205	3.602
OFP	1.240	0.960	0.219	0.330	2.909	4.384
OFE	1.226	0.904	0.251	0.410	2.205	3.602

To provide an intuitive visualization of the hierarchical performance relationships among the eight models across the six aforementioned metrics, a corresponding radar chart has been systematically constructed and is presented in Figure 4.5. From Table 4.5 and Figure 4.5, it can be observed that all models experienced growth during the selected investment period.

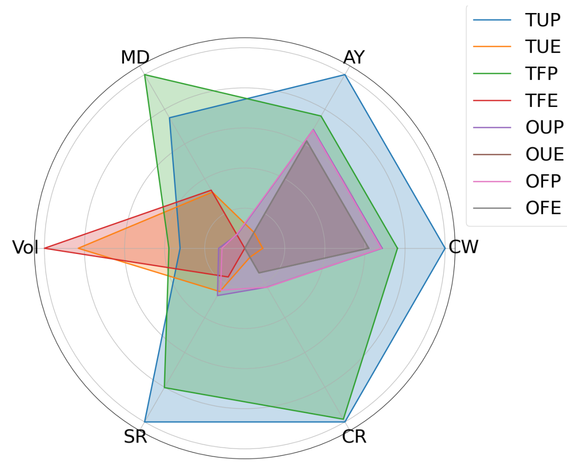

Figure 4.5: Performance under selected criteria in Case Study 3 (Radar Chart).

This is because the four stocks being invested in also experienced growth, which demonstrates the effectiveness of stock return prediction in Table 4.2.

From the risk metrics, MD and Vol, in Table 4.5, it can be concluded that the risk associated with using a single reference point in portfolio selection is greater than that of using two reference points. This suggests that incorporating two reference points in portfolio selection can effectively reduce investment risk. In Section 4.2.4, the objective function in Equation 4.6 have been demonstrated that drives the portfolio selection model to be risk-sensitive , which also results in model TUE performing exceptionally well under the risk metric Vol.

Introducing reference point goal into portfolio selection enhances the model's inclination toward pursuing higher returns. Therefore, it can be observed that models incorporating two reference points exhibit stronger performance in both the CW and AY return metrics. Lastly, utilizing reference points within uncertain intervals, as opposed to fixed values, not only aligns the model more closely with investors' decision-making behaviors in uncertain markets but also bolsters the model's performance under the SR and CR risk-adjusted return metrics. Consequently, the performance of the model TUP is optimal under these two metrics.

Hence, it is easy to conclude from this case study that the introduction of two reference points in the portfolio selection model based on prospect theory enhances the model's capacity to pursue higher returns, thereby encouraging investments in stocks with the potential for future high yields. Simultaneously, when the reference points encompass uncertain alongside fixed values, the model exhibits heightened resilience against risk. These findings underscore the ability of the portfolio selection model incorporating two uncertain reference points to achieve more robust returns. Consequently, it is easy to assert that the fuzzy portfolio selection model based on prospect theory proposed in this study is indeed effective.

4.3.2 Case Study 4: NYSE and NASDAQ Real Market Case

Problem description: This section includes a comparison study based on real market data, validating the effectiveness of balancing investment return and risk of the portfolio selection model based on enhanced prospect theory that encompasses diverse behavioral biases in the real market through comparison with three portfolio selection models. In this case, 31 stocks were selected from NYSE and NASDAQ, and the return rates of these stocks from the period Jan. 4, 2016 to Oct. 7, 2016 (40 weeks) expressed in fuzzy variables can be obtained from [57], as listed in Table 4.6.

Comparison models: Buy & Hold (B&H) model is often chosen as a benchmark model due to its ability to intuitively display the average return performance of the stock-pool. Expected utility-CVaR (EU-C). The objective of this model is to maximize the expected return of the portfolio selection scheme while adopts the Conditional Value-at-Risk (CVaR) as the risk constraint. Prospect theory-based mean-variance (PT-MV). Srivastava et al. [175] propose a prospect theory-based portfolio selection model within the framework of mean-variance under uncertainty with ambiguity.

Based on experts' knowledge, the uncertain interval of the reference point minimum requirement was assigned as a triangular variable $(0.992, 1.000, 1.007)$ which is a reflection of the risk-free rate and the average return rate of NYSE and NASDAQ in the past three months. And the uncertain interval of the reference point goal was assigned as a triangular

Table 4.6: Return rate predictions for stocks in Case Study 4.

Stock No.	Ticker	Fuzzy return rates	Stock No.	Ticker	Fuzzy return rates
1	AAPL	[0.04 1.86 2.16 11.95]	2	AIG	[0.02 1.84 2.18 8.52]
3	BA	[0.14 1.57 1.93 9.14]	4	BAC	[0.19 2.58 3.06 9.10]
5	BRK-B	[0.03 1.17 1.44 3.73]	6	C	[0.05 2.06 3.28 10.26]
7	CSCO	[0.03 1.81 2.20 10.96]	8	CVS	[0.06 1.24 1.40 5.17]
9	CVX	[0.03 1.00 1.46 8.27]	10	D	[0.01 1.10 1.43 5.36]
11	DIS	[0.04 1.35 1.62 8.50]	12	F	[0.01 1.20 1.43 5.36]
13	FB	[0.23 1.50 1.69 13.60]	14	GE	[0.03 1.32 1.62 6.87]
15	GM	[0.23 2.12 2.50 11.72]	16	GOOGL	[0.12 1.79 1.90 8.75]
17	HD	[0.04 1.35 1.62 8.50]	18	JNJ	[0.01 1.20 1.43 5.36]
19	JPM	[0.01 1.50 1.66 7.87]	20	KMI	[0.14 1.94 2.54 16.49]
21	KO	[0.06 1.38 1.42 4.76]	22	MMM	[0.03 1.05 0.95 8.68]
23	MSFT	[0.05 1.88 2.10 8.60]	24	ORCL	[0.12 1.51 1.66 6.61]
25	PFE	[0.06 1.27 1.62 8.61]	26	PG	[0.03 1.19 1.59 5.82]
27	SLB	[0.01 1.91 2.12 10.10]	28	UTX	[0.01 1.53 1.93 5.93]
29	WFC	[0.08 1.76 2.33 6.65]	30	WMT	[0.00 1.41 1.54 7.71]
31	XOM	[0.05 1.14 1.34 5.56]			

variable $(1.013, 1.051, 1.072)$ which is based on the return rate prediction of the stocks in the pool. Other parameters were adopted the similar assignments in Table 4.3. Similar to the ablation study, ICPSO was adopted to find the optimal solution of the aforementioned portfolio selection models, and these solutions are the stock position of each model which will be tested by real market data. And these models were evaluated by six metrics whose definitions and definitions were listed in Table 3.4.

The metric values of these fuzzy portfolio selection models were listed in Table 4.7, the best performances are highlighted in boldface for better illustration.

Table 3.4: Summary of selected criteria.

Type	**Criterion**	**Abbr.**	**Description**
Return	wealth accumulation	**CW**	Total wealth at horizon.
Return	annual percentage yield	**AY**	Average annualized return.
Risk	maximum drawdown	**MD**	Largest peak-to-trough loss.
Risk	volatility	**Vol**	Return dispersion (std. dev.).
Risk-adjusted return	Sharpe index	**SR**	Excess return per volatility.
Risk-adjusted return	Calmar index	**CR**	Annual return / max drawdown.

To provide an intuitive visualization of the hierarchical performance relationships among

Table 4.7: Performance under selected criteria at the end of the given period in Case Study 4.

Criterion	Return		Risk		Risk-adjusted return	
	CW	**AY**	**MD**	**Vol**	**SR**	**CR**
TUP	**1.127**	**0.165**	0.116	0.123	**1.279**	**1.422**
B&H	1.018	0.023	**0.073**	**0.074**	0.311	0.311
EU-C	1.101	0.131	0.105	0.173	0.757	1.248
PT-MV	1.077	0.103	0.084	0.122	0.844	1.226

the four models across the six aforementioned metrics, a corresponding radar chart has been systematically constructed and is presented in Figure 4.5. Under the metrics of cumulative wealth and annual yield, B&H model performs the worst, indicating its inferior ability to generate investment returns. This is due to B&H model's strategy of evenly distributing liquid cash across all invest-able stocks without any selection, which only reflects the average return of the stock pool. Therefore, this model is widely chosen as a benchmark in the field of portfolio research. However, due to its overly diversified investment strategy, it performs exceptionally well in terms of volatility. PT-MV model employs prospect theory in characterizing investor behavior paradigms within the mean-variance framework. Mean-variance has been well-observed of risk-concentration, as discussed previously.

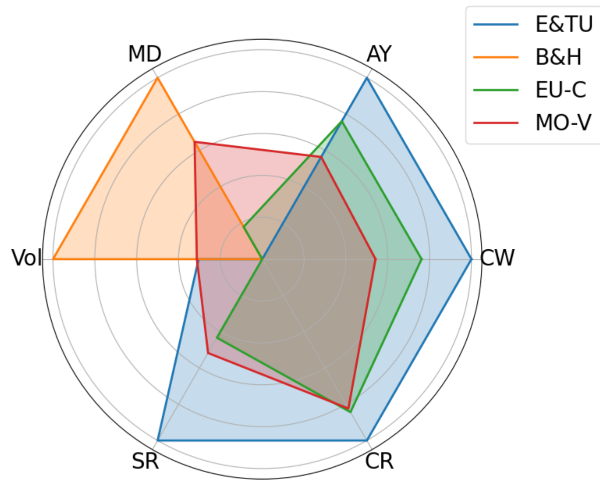

Figure 4.6: Performance under selected criteria in Case Study 4 (Radar Chart).

The fuzzy portfolio selection model proposed in this study, based on prospect theory with two uncertain interval reference points, takes into account not only the loss aversion effect but also the pursuit of returns by investors, thus exhibiting optimal performance under the metrics of cumulative wealth and annual yield. This demonstrates that the use of a variant of prospect theory with two reference points can effectively enhance the model's ability to generate returns, which is the goal of many investors. In terms of volatility, this model outperforms the PT-MV model, proving that the introduction of prospect theory in portfolio research can effectively reduce investment volatility. Finally, on the Sharpe ratio metric, this model performs optimally. Therefore, it easy to conclude that while achieving optimal investment returns, this model's ability to control risk has not deteriorated. It effectively balances the achievement of portfolio returns and risk aversion.

Chapter 5

DEVELOPMENT OF PARTICLE SWARM OPTIMIZATION ITERATIVE STRATEGY

In Chapter 4, I propose an enhanced prospect theory that encompasses diverse behavioral biases. Then a multiple reference point portfolio selection model based on this enhanced prospect theory is proposed. The intricate mathematical structure of the proposed portfolio selection model defies direct solutions by existing optimization software. Real-world portfolio selection problems are also typically high-dimensional, further complicating the search for feasible solutions. When PSO - the popular heuristic algorithm applied in portfolio selection and related engineering optimization - confronts these challenges, it often traps in local minima or premature convergence. These shortcomings constitute the second research gap in this study.

To address this gap, the current chapter employs a methodological approach centered on optimizing PSO's iterative strategies, including adaptive parameter tuning, cooperative swarm mechanisms, and hybrid metaheuristic integration. By refining the algorithm's exploration-exploitation balance and enhancing its capacity to navigate high-dimensional solution spaces, this framework aims to overcome the computational bottlenecks inherent in traditional PSO implementations. These advancements not only align with the dissertation's second research objective, optimizing PSO iterative strategy, but also establish a robust computational foundation for solving behaviorally complex portfolio optimization problems with improved accuracy and scalability.

In this chapter, fuzzy simulation will be introduced first, an approximation method to estimate the objective functions and chance constraints. Two original heuristic algorithms will be proposed then, improved cooperative particle swarm optimization algorithm (ICPSO) which serves as the solution algorithm, seeking the optimal solutions - namely, the best investment scheme - for both the portfolio selection model proposed in Chapter 3 and its comparison counterparts. And adaptive cooperative particle swarm optimization (ACPSO) serves as the solution algorithm, seeking the optimal solutions for both the portfolio selection model proposed in Chapter 4 and its comparison counterparts.

The novelty and contributions of ICPSO stem from an original designed iterative scheme built on swarm-decomposition techniques. The stability parameter range of this scheme will be identified through sensitivity analysis, and its capacity to obtain optimal solutions will be validated in Computational Study 1. Building on ICPSO, I further incorporate an original learning rates mechanism, yielding ACPSO. The performances improvements delivered by ACPSO by ICPSO will be demonstrated in Computational Study 2. These two solution algorithms have been complied in the following two international journal papers: [168] by **X. Wang**, B. Wang, T. Long and Y. Wu. Prospect theory-based portfolio selection using multiple fuzzy reference intervals. *IEEE Transactions on Systems, Men and Cybernetics: Systems*, 55(10): 7100-7114, 2025. and [176] by **X. Wang**, B. Wang, T. Li, H. Li, and J. Watada. Multi-criteria fuzzy portfolio selection based on three-way decisions and cumulative prospect theory. *Applied Soft Computing*, 134: 110033, 2023.

5.1 Introduction of Particle Swarm Optimization Iterative Strategy

In recent years, research in the field of portfolio selection has endowed its analytical models with more exquisite mathematical structures. These structures have significantly advanced the integration of portfolio selection research with academia and industry, yielding impactful results. Whilst these structures have, to some extent, made it challenging to quickly obtain exact numerical solutions for these portfolio selection problems. For instance, when the objective functions or the chance constraints are non-convex or non-smooth, approximation methods are often required for solving them.

PSO, along with other swarm algorithms, such as ant colony optimization, as well as other, meta-heuristic algorithms including genetic algorithm and differential evolution, has been successfully applied in many academia and industry research fields, such as portfolio selection, power systems and signal processing to solve their field-related optimization problems. Despite these success, PSO still plagued by two problems which has been discussed in Section 2.3. And in this research, proposing two PSO algorithms to tackle the aforementioned issues.

5.2 Fuzzy Simulation

In previous sections, I delineate the foundational concerning the expected value, prospect value, disappointment index and mean absolute deviation of a fuzzy variable, elucidating the methodologies employed for their calculation when applied to individual fuzzy variables. But it is imperative to acknowledge that, given the inter-dependencies among securities within portfolio, the conventional methods outlined above cease to be applicable. To resolve this inherent challenge, Liu and Iwamura [177], as well as Liu and Liu [178] proffer a discretization technique termed "fuzzy simulation". In this study, employing the fuzzy simulation approach to approximate the expected value, prospect value and absolute deviation, effectively circumventing the constraints posed by correlated securities within the portfolio scheme.

Assuming γ_{ψ_m}, γ_{φ_m} and γ_{ϕ_m} are membership functions to fuzzy variables ψ_m, φ_m and ϕ_m, respectively. For brevity, take $\psi = \{\psi_1, \psi_2, \cdots \psi_M, \varphi_1, \varphi_2, \cdots \varphi_N, \phi_1, \phi_2, \cdots \phi_N\}$. Use $\vee$ and $\wedge$ to denote the max and min operators, respectively. If $f(\psi)$ is a function of ψ, then by extension theorem from Zadeh [165], the membership function of $f(\psi)$ can be induced from ψ_m, φ_m and ϕ_m as :

$$\psi(t) = \sup_{t=(t_1,t_2,\ldots,t_{M+2N})} \Big(\min_{1\leq m\leq M} \gamma_{\psi_m}(t_m)\Big) \ \wedge \ \Big(\min_{1\leq n\leq N} \gamma_{\varphi_n}(t_{M+n}) \wedge \gamma_{\phi_n}(t_{M+N+n})\Big). \tag{5.1}$$

The following fuzzy-simulation routine [179] can be adopted to calculate $\mathbf{Cr}\{f(\psi) \leq r\}$, $r \in \mathbb{R}$:

Simulation for $\mathbf{Cr}[f(\psi) \leq r]$

[Step 1]. Randomly generate vectors $\vec{a}_k^m = (t_{k,1}, t_{k,2}, \ldots, t_{k,M+2N})$ so that $\gamma_{\psi_n}(t_{k,n}) \geq \epsilon$, $\gamma_{\varphi_n}(t_{k,M+n}) \geq \epsilon$, and $\gamma_{\phi_n}(t_{k,M+N+n}) \geq \epsilon$, for $m = 1, \ldots, M$, $n = 1, \ldots, N$, and $k = 1, \ldots, K$. Here ϵ is a sufficiently small constant and K is a sufficiently large integer.

[Step 2]. For each k, compute

$$\lambda_k = \min\Big\{ \{\gamma_{\psi_m}(t_{k,m})\}_{m=1}^{M} \ \cup \ \{\gamma_{\varphi_n}(t_{k,M+n})\}_{n=1}^{N} \ \cup \ \{\gamma_{\phi_n}(t_{k,M+N+n})\}_{n=1}^{N} \Big\} \tag{5.2}$$

[Step 3]. Return

$$L(r) = \frac{1}{2}\bigg(\max_{1\leq k\leq K} \{\lambda_k \mid g(\vec{a}_k^m) \leq r\}\bigg) + 1 - \bigg(\max_{1\leq k\leq K} \{\lambda_k \mid g(\vec{a}_k^m) > r\}\bigg) \tag{5.3}$$

The quantity $\mathbf{Cr}\{f(\psi) \leq r\}$ is then estimated by $L(r)$. To obtain $\min\{\hat{r} \mid \mathbf{Cr}\{f(\psi) \leq \hat{r}\} \geq$

$\beta\}$, the smallest r can be found by bisection, such that $L(r) \geq \beta$; this r serves as the desired estimate.

Since $f(\psi) \geq 0$, one has $E[f(\psi)] = \int_0^{+\infty} \mathbf{Cr}\{f(\psi) \geq r\}\, dr$. A fuzzy-simulation estimator proceeds as follows [179].

Simulation for $E[f(\psi)]$

[Step 1]. Initialize $e \leftarrow 0$.

[Step 2]. Independently sample real vectors $\vec{b}_i = (b_{i,1}, b_{i,2}, \ldots, b_{i,M+2N})$, $i = 1, \ldots, I$, such that $\gamma_{\psi_m}(b_{i,m}) \geq \zeta$, $\gamma_{\varphi_n}(b_{i,M+n}) \geq \zeta$, and $\gamma_{\phi_n}(b_{i,M+N+n}) \geq \zeta$ for all $m = 1, \ldots, M$ and $n = 1, \ldots, N$. Here ζ is small and N is a sufficiently large integer.

[Step 3]. Set $w = f(\vec{b}_1) \wedge f(\vec{b}_2) \wedge \cdots \wedge f(\vec{b}_I)$ and $v = f(\vec{b}_1) \vee f(\vec{b}_2) \vee \cdots \vee f(\vec{b}_I)$.

[Step 4]. Draw r uniformly from $[w, v]$ and update $e \leftarrow e + L(r)$.

[Step 5]. Repeat Step 4 a total of I times.

[Step 6]. Return $w + e \cdot (v - w)/I$ as the estimator of $E[f(\xi)]$.

Through the preceding steps, the expected value of a fuzzy set whose components are mutually dependent fuzzy variables can be derived. Therefore, once the predicted fuzzy returns, i.e., $[\xi_1 + \xi_2 + \ldots + \xi_n]$, and stock positions, i.e., $[x_1 + x_2 + \ldots + x_n]$, for the selected stocks have been determined, the investment expected return, i.e., $\mathbf{E}[x_1 \cdot \xi_1 + x_2 \cdot \xi_2 + \ldots + x_n \cdot \xi_n]$, can be computed using steps outlined above. Likewise, similar steps allow us to approximate the portfolio scheme's prospect value, disappointment index and mean-absolute deviation.

5.3 Improved Cooperative Particle Swarm Optimization Algorithm

In order to mitigate premature convergence and entrapment in local optima, ICPSO is introduced. Its design strengthens the particles' exploratory capacity across the whole decision space. Relative to standard PSO variants, ICPSO contains two distinctive features, as listed below and marked within the highlight box in the solution process.

1. The entire swarm is partitioned into several sub-swarms, after which every coordinate of every particle inside its respective sub-swarm is updated. Existing high-dimensional PSO extensions generally follow one of two routes: (i) partition the decision space itself and restrict particles to updating the coordinates that belong to the sub-space in which they reside [180]; (ii) divide the swarm into sub-swarms but update only a subset of particles in each group [181]. ICPSO adopts neither extreme; instead, each sub-swarm updates all of its members in all dimensions.

2. A bespoke location-update rule is applied to the current sub-swarm best particle so as to curb premature stagnation.

The solution process of ICPSO can be summarized as below, and the pseudocode of ICPSO algorithm will be provided in Appendix Algorithm 1:

[Step 1]. Particle initialization: Positions of N particles were initialized, the position of the i_{th} particle is represented by a $K \times 1$ real-valued matrix

$$\mathcal{P}_i = [x_{i,1}, x_{i,2}, ..., x_{i,K}]^{\mathrm{T}}, \tag{5.4}$$

$x_{i,k}$ is the k-dimensional coordinates of the i_{th} particle in the K-dimension search space.

[Step 2]. Swarm decomposing: Randomly split the full swarm of N particles into M sub–swarms, where $1 \leq M \leq N$ and $M \in \mathbb{Z}$. If M divides N, each sub–swarm contains N/M particles. Otherwise, let $r = N\%M$ be the remainder under the modulo operation. Assign $(N-r)/(M-1)$ particles to each of the first $(M-1)$ sub–swarms, and place the remaining r particles in the last sub–swarm.

[Step 3]. Fitness calculation: Calculating the value of the fitness function for each particle. Then initializing personal best fitness value $\mathcal{P}value$, personal best location $\mathcal{P}best$, sub-swarm best fitness value $\mathcal{S}value$, sub-swarm best location $\mathcal{S}best$, global best fitness value $\mathcal{G}value$, global best location $\mathcal{G}best$, where $\mathcal{S}value$ and $\mathcal{S}best$ represent the best fitness value and its corresponding location in each sub-swarm.

[Step 4]. Using the personal best $\mathcal{P}best$, the sub–swarm best $\mathcal{S}best$, and the global best $\mathcal{G}best$ obtained in **Step 3**, each particle is updated according to the procedures given below.

If the i_{th} particle is not the one corresponding to the $\mathcal{S}best$, its velocity and location can be updated as:

$$
\begin{aligned}
&v_{i,k} \leftarrow \tau \cdot v_{i,k} + C_1 \cdot r(0,1) \cdot (\mathcal{P}best_{i,k} - x_{i,k}) + C_2 \cdot r(0,1) \cdot (\mathcal{S}best_{i,k} - x_{i,k}), \\
&x_{i,k} \leftarrow x_{i,k} + v_{i,k},
\end{aligned}
\tag{5.5}
$$

where τ is the inertia weight, C_1 and C_2 are the learning weights and $\mathcal{S}best_{i,k}$ is the k-dimensional coordinates of the best sub-swarm location $\mathcal{S}best$ of which sub-swarm the i_{th} particle is in. Otherwise if the i_{th} particle is the one corresponding to the $\mathcal{S}best$, its velocity and location can be updated as:

$$
\begin{aligned}
v_{i,k} &\leftarrow \tau \cdot v_{i,k} + \mathcal{G}best_k, \\
x_{i,k} &\leftarrow v_{i,k} + x_{i,k}.
\end{aligned}
\tag{5.6}
$$

[Step 5]. Each newly created particle is examined against the constraints of the optimization task. Any infeasible particle is regenerated by reapplying the procedures in **Step 4**.

[Step 6]. .Repeat **Step 3 $\sim$ 5** for a predetermined number of iterations. After the final cycle, assign $\mathcal{G}value$ as the problem's optimal objective value, and take the corresponding location $\mathcal{G}best$ as the final solution.

From the above workflow it follows that ICPSO employs two distinct velocity and position update mechanisms: (i) an *intra–sub-swarm* rule and (ii) an *inter–sub-swarm* rule. The intra–sub-swarm update (Eq. 5.5), which is closely related to the standard PSO rule (Eq. 2.27), enables particles to extensively explore the subspace that hosts the corresponding sub-swarm. Such thorough exploration is particularly important for nonconvex problems, a situation frequently encountered in practice. The inter–sub-swarm update (Eq. 5.6) drives the particle $\mathcal{S}best_m$ toward $\mathcal{G}best$, thereby accelerating convergence, mitigating premature stagnation, and lowering computational cost. Empirical studies will subsequently be conducted to verify the effectiveness of ICPSO.

5.4 Adaptive Cooperative Particle Swarm Optimization Algorithm

To deal with the issue "curse of dimensionality" of PSO while facing large-scale optimization problems, a novel PSO algorithm is proposed by combining time-varying acceleration coefficient strategy and cooperative strategy. Specifically, the time-varying acceleration coefficient strategy refers to adopting deep deterministic policy gradient (DDPG) [182] to determine the optimal serial values of C_1 and C_2 in the iteration process.

Deterministic policy–gradient reinforcement learning belongs to the policy–based family of RL methods. Its aim is to learn a mapping $\pi : \mathcal{S} \rightarrow \mathcal{A}$ from environmental states to actions that maximizes the expected long–term return. The learning problem is typically modeled as a Markov decision process. As illustrated in Figure 5.1, the agent and environment operate in a closed loop: at each discrete time step t, the agent observes the current state s_t, selects an action a_t according to its policy, executes that action, receives a scalar reward r_t from the environment, and transitions to the next state s_{t+1}.

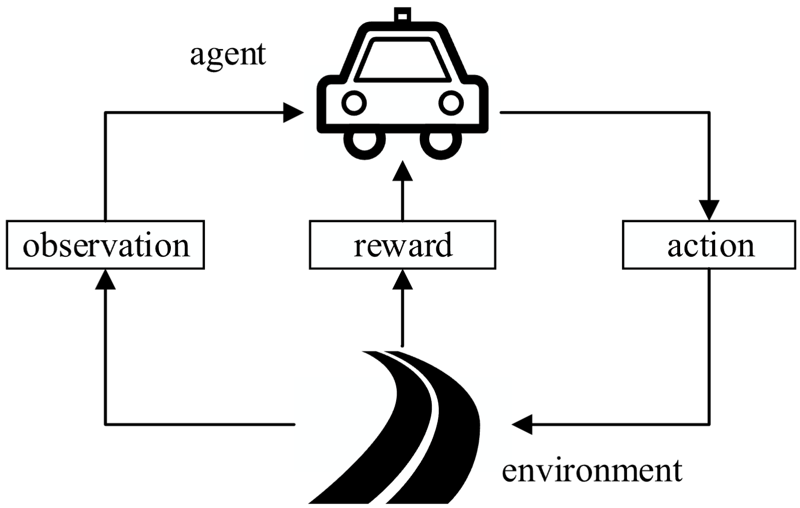

Figure 5.1: Interaction between the agent and the environment.

Conventional RL methods, hindered by limited representational capacity, cope well only with problems whose state and action spaces are of low dimension. Real-world scenarios, however, often involve high-dimensional states and continuous control, sharply restricting the reach of such classical techniques [183].

Breakthroughs in image recognition [184], natural-language understanding, and other areas have demonstrated that deep learning can extract hierarchical features from high-dimensional inputs [185]. Furthermore, deep neural networks are recognized as universal function approximators [186], capable of estimating value functions and policies in complex domains. Consequently, deep reinforcement learning—which couples RL with deep networks—has attracted considerable research interest in recent years.

Policy–based approaches constitute a fundamental branch of RL that directly optimizes the decision policy, and they are particularly efficient for problems involving high–dimensional state spaces and continuous action spaces. These advantages are exactly what this research requires: 1. The searching space corresponding to the serial value C_1 and C_2 can sometimes be high-dimensional (over 500), 2. Serial value C_1 and C_2 are continuous.

Many policies in the literature are specified as probability distributions or densities and are therefore stochastic: for any state, multiple actions can be sampled with nonzero probability. By contrast, in numerous tasks the policy is deterministic, mapping each state to a single action $a = \mu(s)$. Silver et al. [187] established the deterministic policy–gradient theorem,

$$\bigtriangledown_\theta J(\theta) = E[\bigtriangledown_a Q_{mu}(s,a) \bigtriangledown_\theta \mu(s)|_{a=\mu_\theta(s)}] \tag{5.7}$$

and introduced both on-policy and off-policy deterministic actor–critic methods by embedding this result into the broader policy–gradient framework. Building on these ideas, the DDPG algorithm learns deterministic policies within an actor–critic architecture and extends them to continuous action spaces. As sketched in Figure 5.2, DDPG estimates the Q-function using off-policy data and the Bellman equation, then exploits the learned Q-function to improve the policy. This procedure mirrors the logic of Q-learning, where the optimal action in each state is obtained from the optimal action–value function [188]:

$$a^*(s) = \arg\max_a Q^*(s,a) \tag{5.8}$$

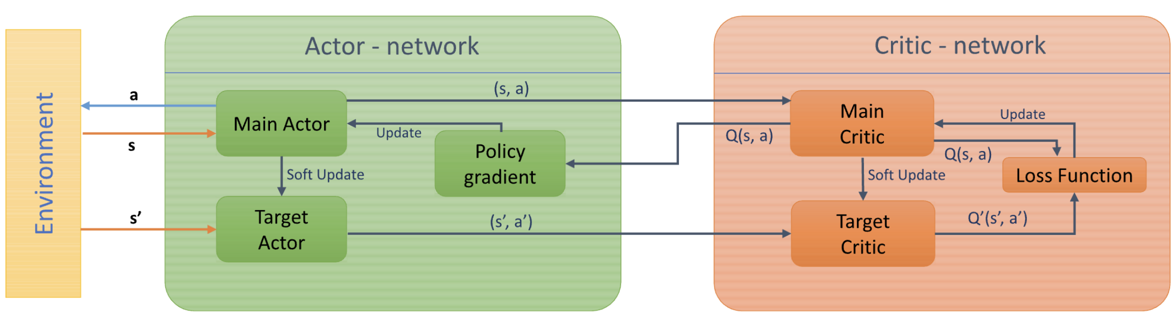

Figure 5.2: DDPG algorithm structure.

What's more, two techniques of deep Q-network, experience replay and the target network were applied to DDPG.

a. Experience Replay: Because deterministic policy–gradient methods permit off-policy learning, DDPG maintains a replay buffer of past transitions and samples random mini-batches to train the critic, thereby improving data efficiency and breaking deleterious temporal correlations.

b. Target Network: To curb value overestimation and enhance training stability, DDPG maintains slow-moving target networks. Unlike the hard copy used in vanilla DQN, DDPG applies a soft update each iteration so that the targets track the main networks gradually:

$$\begin{aligned} \omega^{'} &\leftarrow \tau\omega + (1-\tau)\omega^{'} \\ \theta^{'} &\leftarrow \tau\theta + (1-\tau)\theta^{'} \end{aligned} \tag{5.9}$$

here, θ and θ' denote the parameters of the primary actor network and its target counterpart, while ω and ω' correspond to the parameters of the main critic network and the target critic network, respectively; the coefficient $\tau \ll 1$ controls the soft-update rate. To encourage exploration in continuous-action settings, DDPG typically injects Ornstein–Uhlenbeck noise into the policy outputs [189]. To mitigate the overestimation bias of the critic, Fujimoto et al. [190] introduced Twin Delayed Deep Deterministic (TD3), which augments DDPG with three principal components:

(a) Clipped Double Q-learning—two independent critics are trained and the smaller of their estimates is used as the target.

(b) Delayed policy and target updates—the actor (and target networks) are updated less frequently than the critic to mitigate error accumulation.

(c) Target policy smoothing—the target action is perturbed by small noise before evaluating the target, regularizing the estimate and reducing overfitting in Q-value approximation.

DDPG has demonstrated its capacity to acquire competitive policies for all tasks in this repertoire, leveraging low-dimensional observations while maintaining uniform hyper-parameters and network architecture across the board. Notably, across several instances, DDPG has consistently exhibited its ability to acquire proficient policies for various tasks while upholding constancy in hyper-parameter settings and network structure [182]. The cooperative strategy refers to dividing the raw particle swarm into several sub-swarms. Each sub-swarm iterates independent and identically while information exchanging still exists among sub-swarms.

Suppose that the objective of the ACPSO algorithm is to find the minimum of a fitness function denoted by $\mathcal{F}(\cdot)$. The swarm comprises N particles and is partitioned into M sub-swarms, with each sub-swarm containing N/M particles. It should be noted that if $N\%M \neq 0$ (% represents the modulo operation), then the first through $(N-1)_{th}$ sub-swarm will contain $(N - N\%M)/(M-1)$ particles, while the last sub-swarm will contain $N\%M$ particles.

ACPSO stores the best position ever achieved by each sub-swarm, denoted as $Sbest_m = (sb_{m,1}, sb_{m,1}, \cdots, sb_{m,D})$ and its fitness value is $Svalue_m$, where $m = 1, 2\cdots, M$. This position corresponds to the minimum fitness value among all the particles that have been a part of the m_{th} sub-swarm.

Assume that ACPSO executes T iterations to search for the optimum. During the t-th iteration, if the i-th particle within the m-th sub-swarm is not the sub-swarm best $Sbest_m$, then its velocity and position are updated as follows:

$$\begin{aligned} &v_{i,k} \leftarrow \omega \cdot v_{i,k} + C_1^{(t)} \cdot (pb_{i,k} - p_{i,k}) + C_2^{(t)} \cdot (sb_k - p_{i,k}), \\ &p_{i,k} \leftarrow p_{i,k} + v_{i,k}. \end{aligned} \tag{5.10}$$

And if particle i is same with $Sbest_m$, its velocity and position can be updated as follows:

$$\begin{aligned} v_{i,k} &\leftarrow \tau \cdot v_{i,k} + g_k \\ p_{i,k} &\leftarrow v_{i,k} + p_{i,k} \end{aligned} \tag{5.11}$$

It should be noted that the values of C_1 and C_2 in ACPSO are determined by DDPG and form a list whose length equals to the iteration times T. C_1^t and C_2^t are the learning rates in the t_{th} iteration. The procedures of adopting DDPG to determine the optimal serial of C_1 and C_2 are listed below, and the pseudocode of adopting DDPG to search for the optimal serial values of C_1^t and C_2^t will be provided in Appendix Algorithm 2.

[**Step 1**].Initialization

[*Step 1.1*]. Randomly initialize actor and critic network $\mu(s|\theta^\mu)$, $Q(s,a|\theta^Q)$ with weights θ^μ, θ^Q.

[*Step 1.2*]. Initialize target network μ' and Q' with weights $\theta^{\mu'} \leftarrow \theta^\mu, \theta^{Q'} \leftarrow \theta^Q$

[*Step 1.3*]. Initialize replay buffer D_b

[*Step 1.4*].Initialize the Ornstein-Uhlenbeck (OU) noise process $\mathcal{M}$.

[**Step 2**]. Outer loop (Episodes). For each episode, $i = 1$ to N_b:

[*Step 2.1*]. Randomly generate position P_i and velocity V_i of N_b particles.

[*Step 2.2*]. Evaluate each particle's position using the fitness function $F_b(P_i)$, storing,

$$Pvalue_i \leftarrow F(P_i), \qquad Pbest_i \leftarrow P_i$$

[*Step 2.3*]. Determine the global best:

$$Gvalue \leftarrow \min\{Pvalue_i\}, \qquad Gbest \leftarrow \underset{Pbest_i}{\operatorname{argmin}}\{F_b(Pbest_i)\}, i = 1, 2, \cdots, N_b$$

[**Step 3**]. Action execution (time steps). For $t = 1$ to T_b:

[*Step 3.1*]. Set the state s_t as the global best:

$$s_t \leftarrow Gbest$$

[*Step 3.2*]. Compute the action: $a_t \leftarrow \mu(s_t|\theta^\mu) + \mathcal{M}_t$ where $\mathcal{M}_t$ is the exploration noise.

[*Step 3.3*]. Update particle velocities $V_{j,k}$ and positions $P_{j,k}$ by rules in Equation 5.12

$$\begin{aligned} v_{j,k} &= \omega \cdot v_{j,k} + C_1 \cdot (pb_{j,k} - p_{j,k}) + C_2 \cdot (g_k - p_{j,k}), \\ p_{j,k} &= p_{j,k} + v_{j,k}. \end{aligned} \tag{5.12}$$

[*Step 3.4*]. If $F_b(P_j) < Pvalue_j$, then $Pbest_j = P_j$ and $Pvalue_j = F_b(P_j)$.

[**Step 4**]. Rewards and Replay Buffer.

[*Step 4.1*]. Compute the reward r_t:

$$r_t = -\Delta(Gvalue + \frac{1}{N}\sum_{i=1}^{N_b} Pvalue_i)$$

and scale r to $[-0.1, 0.1]$.

[*Step 4.2*]. Store experience (s_t, a_t, r_t, s_{t+1}) into D_b.

[**Step 5**.] Actor-critic updates:

[*Step 5.1*]. Randomly sample a minibatch of n experiences (s_i, a_i, r_i, s_{i+1}) from D_b.

[*Step 5.2*]. Compute target values. $y_i = r_i + \gamma Q'(s_{i+1}, \mu'(s_{i+1}|\theta^{\mu'})|\theta^{Q'})$

[*Step 5.3*]. Update the critic network by minimizing the loss:

$$L = \frac{1}{n}\sum_i (y_i - Q(s_i, ai|\theta^Q))^2 \tag{5.13}$$

[*Step 5.4*]. Update the actor network using the sampled policy gradient:

$$\nabla_{\theta^\mu} J \approx \frac{1}{N_b} \sum_i^{N_b} \nabla_a Q(s, a|\theta^Q)|_{s=s_i, a=\mu(s_i)} \nabla_{\theta^\mu} \mu(s|\theta^\mu)|_{s_i} \tag{5.14}$$

[**Step 6**]. Target network update: Update the target networks using a soft update rule:

$$\begin{aligned} \theta^{Q'} &\leftarrow \tau\theta^Q + (1-\tau)\theta^{Q'} \\ \theta^{\mu'} &\leftarrow \tau\theta^\mu + (1-\tau)\theta^{\mu'} \end{aligned} \tag{5.15}$$

[**Step 7**]. End of episode: Output the best action a_t at $t = 0$.

The motivation behind adopting DDPG to determine the learning rates C_1 and C_2 over time is to balance the exploration and exploitation abilities of PSO based on the current iteration status. The input parameter for Algorithm 2 include a benchmark fitness value function $F_b(\cdot)$, searching space dimension D_b, particle number N_b and iteration time T_b. The optimal serial of values for C_1 and C_2 are stored in the output variable a_t.

The input parameter for ACPSO includes the objective fitness value function $F_o(\cdot)$, searing space dimension D_o, particle number N_o, sub-swarm number M, acceleration coefficient in Equation 5.11, optimal serial of values for C_1 and C_2 determined by the optimal serial values searched by DDPG, iteration time T_o and constraints. The optimal fitness value *Gvalue* and position *Gbest* are stored in the output variable which is the optimal solution to the objective fitness value function. The solution process of ACPSO can be summarized as below, and the pseudocode of ACPSO will be provided in Appendix Algorithm 3:

[**Step 1**]. Particle initialization: Positions of N particles were initialized, the position of the i_{th} particle is represented by a $K \times 1$ real-valued matrix

$$\mathcal{P}_i = [x_{i,1}, x_{i,2}, ..., x_{i,K}]^{\mathrm{T}}, \tag{5.16}$$

, $x_{i,k}$ is the k-dimensional coordinates of the i_{th} particle in the K-dimension search space.

[Step 2]. Swarm decomposing: Randomly split the full swarm of N particles into M sub–swarms, where $1 \leq M \leq N$ and $M \in \mathbb{Z}$. If M divides N, each sub–swarm contains N/M particles. Otherwise, let $r = N\%M$ be the remainder under the modulo operation. Assign $(N - r)/(M - 1)$ particles to each of the first $(M - 1)$ sub–swarms, and place the remaining r particles in the last sub–swarm.

[Step 3]. Fitness calculation: Calculating the value of the fitness function for each particle. Then initializing personal best fitness value $\mathcal{P}value$, personal best location $\mathcal{P}best$, sub-swarm best fitness value $\mathcal{S}value$, sub-swarm best location $\mathcal{S}best$, global best fitness value $\mathcal{G}value$, global best location $\mathcal{G}best$, where $\mathcal{S}value$ and $\mathcal{S}best$ represent the best fitness value and its corresponding location in each sub-swarm.

[Step 4]. Particle update: Using the personal best $\mathcal{P}best$, the sub–swarm best $\mathcal{S}best$, and the global best $\mathcal{G}best$ obtained in **Step 3**, each particle is updated according to the procedures given below.

For $t = 1$ to T_o, for the i_{th} particle is not the one corresponding to the $\mathcal{S}best$, its velocity and location can be updated as Equation 5.10. Otherwise if the i_{th} particle is the one corresponding to the $\mathcal{S}best$, its velocity and location can be updated as Equation 5.11.

[Step 5]. Feasibility check: Every newly generated particle is checked to see if the constraints in the optimization problem have been met and regenerate invalid ones using the above procedures in **Step 4**.

[Step 6]. Swarm iteration: Iterating **Step 3 $\sim$ 5** for a predefined number of times.

After the last iteration, $\mathcal{G}value$ is taken as the optimal result of the optimization problem, and its corresponding location $\mathcal{G}best$ is the final answer of the problem.

5.5 Sensitivity Analysis: Verification of the Proposed Solution Algorithms

In this section, I will carry out a sensitivity-analysis study to verify that the proposed algorithm can obtain credible solutions to the optimization problem. The experiment will also examine how problem characteristics—namely, structure, dimensionality, and searching space—affect algorithmic performance, as well as how key algorithm parameters, including inertia weight and learning rates, influence the results. All experiments in this thesis were implemented with Python on a Dell U8S9M95 3.5 Ghz personal computer.

5.5.1 Experimental Settings

The sensitivity analysis experiment is designed to systematically assess how various problem characteristics and algorithm parameters influence the performance of the proposed optimization algorithm. In this experiment, eight distinct scenarios are devised to assess ICPSO's capacity to obtain the optimal solutions of benchmark fitness functions, each scenario employs a different mix of problem characteristics and algorithm parameters. Table 5.1 outlines the experiment settings used in this analysis.

Two types of test fitness functions are employed: $f_1(x) = \sum_1^n x_i^2$, a simple and widely used convex function, and $f_2(x) = \sum_1^n |x_i| + \prod_i^n |x_i|$, which is more complex due to the inclusion of both additive and multiplicative terms.

To examine the effect of problem dimensionality, scenarios are constructed with varying values of n (e.g., 50, 100, 1,000, and 10,000). The searching space Ss, representing the bounds of each decision variable x_i, is also varied (e.g., [10,10], [50,50], and [100, 100]) to explore how the searching range impacts convergence and solution quality.

This experimental setup allows us to isolate the influence of structural complexity, dimensional scale, and variable bounds on optimization outcomes. Additionally, the experiment will investigate how algorithmic parameters—specifically, inertia weight and learning rates—affect the performance across these scenarios. The combination of diverse test functions and controlled variations in problem attributes provides a comprehensive basis for evaluating robustness and adaptability of the algorithm under different conditions.

Table 5.1: Sensitivity analysis experiment settings

Scenario No.	Function	n	Ss
1	$f_1(x) = \sum_{i=1}^{n} x_i^2$	1 000	[10,10]
2		10 000	[10,10]
3		1 000	[100,100]
4		10 000	[100,100]
5	$f_2(x) = \sum_{i}^{n} \lvert x_i \rvert + \prod_{i}^{n} \lvert x_i \rvert$	100	[10,10]
6		50	[10,10]
7		50	[50,50]
8		100	[50,50]

5.5.2 Results of Sensitivity Analysis

This experiment evaluates how inertia weight τ and learning rates C_1, C_2 affect algorithmic performance under diverse experimental scenarios, while also aiming to identify stable ranges for both parameters. Inertia weight τ is a critical factor in ICPSO's velocity-update rule: as Equations 5.5 and 5.6 indicates, every particle's speed—whether or not it is the best in its sub-swarm—is influenced by this weight. Therefore, analyzing the impact of inertia weight on overall performance is indispensable. Equations 5.3 and 5.4 were listed below for easy reference.

$$\text{Equation} \quad 5.3 : v_{i,k} \leftarrow \tau \cdot v_{i,k} + C_1 \cdot rand(0,1) \cdot (\mathcal{P}best_{i,k} - x_{i,k}) + C_2 \cdot rand(0,1) \cdot (\mathcal{S}best_{i,k} - x_{i,k})$$

$$\text{Equation} \quad 5.4 : v_{i,k} \leftarrow \tau \cdot v_{i,k} + \mathcal{G}best_k$$

This experiment assesses ICPSO's optimization performance across eight scenarios while varying the inertia weight from 0.1 to 1.0 in increments of 0.1. The results are reported in Table 5.2. Scenarios 1–4 employ the relatively simple first test fitness function, whereas Scenarios 5–8 use the more complex second test fitness function. Holding all other settings constant, the solutions produced in Scenarios 5–8 are noticeably poorer than those in Scenarios 1–4, demonstrating that a more intricate objective-function landscape degrades ICPSO's effectiveness. This challenge is not unique to ICPSO but plagues PSO-based algorithms in general. It is likewise evident that increasing the dimensionality of the test fitness functions and enlarging the search space both impair ICPSO's ability to reach the global optimum; however, these factors lie outside this experiment's primary focus and are therefore not discussed further.

Table 5.2: Effects and stability range of inertia weight.

IW* \ No.**	1	2	3	4	5	6	7	8
0.1	8.56×10^{-245}	7.40×10^{-196}	3.08×10^{-149}	3.52×10^{-248}	3.15×10^{-85}	1.24×10^{-113}	2.20×10^{-127}	1.50×10^{-114}
0.2	2.03×10^{-205}	6.36×10^{-202}	2.79×10^{-177}	1.69×10^{-203}	6.04×10^{-92}	2.79×10^{-80}	2.97×10^{-110}	5.50×10^{-110}
0.3	7.30×10^{-172}	2.25×10^{-163}	8.53×10^{-165}	5.97×10^{-172}	6.50×10^{-70}	1.28×10^{-95}	5.61×10^{-83}	3.92×10^{-72}
0.4	9.24×10^{-103}	5.95×10^{-136}	3.43×10^{-96}	4.06×10^{-101}	1.59×10^{-62}	4.63×10^{-56}	1.37×10^{-64}	6.30×10^{-55}
0.5	6.87×10^{-66}	1.65×10^{-72}	6.60×10^{-74}	3.05×10^{-80}	3.03×10^{-36}	3.51×10^{-34}	4.26×10^{-33}	2.20×10^{-39}
0.6	4.39×10^{-29}	9.84×10^{-23}	2.41×10^{-22}	1.16×10^{-33}	5.16×10^{-16}	7.02×10^{-20}	2.75×10^{-11}	1.03×10^{-18}
0.7	1.98×10^{-1}	1.86×10^{-2}	3.56×10^{2}	4.00	2.34	2.20×10^{-6}	1.38×10^{-1}	1.24×10^{1}
8	2.71×10^{4}	1.86×10^{4}	2.30×10^{6}	2.58×10^{7}	1.49×10^{2}	6.22×10^{1}	2.31×10^{26}	1.43×10^{2}
0.9	7.18×10^{3}	4.37×10^{3}	3.06×10^{7}	1.06×10^{8}	1.58×10^{2}	8.39×10^{8}	6.13×10^{41}	5.43×10^{116}
1	1.03×10^{4}	2.14×10^{4}	2.43×10^{7}	1.68×10^{8}	7.02×10^{13}	6.42×10^{6}	6.04×10^{36}	1.33×10^{114}

* : IW stands for inertia weight τ.
** : No. stands for the scenario number.

An examination of how inertia weight affects ICPSO's search ability shows that all solutions remain acceptable (defined as $< 10^{-5}$) when $\tau \leq 0.6$. In contrast, once $\tau \geq 0.8$ the algorithm produces uniformly unacceptable results, straying far from the theoretical optimum of 0. Step-by-step logs across the eight test scenarios reveal that at $\tau \geq 0.8$ ICPSO fails to evolve at all—the final solution is simply the algorithm's initial random position. At $\tau = 0.7$, an acceptable solution emerges only in Scenario 6; the other seven scenarios do not meet the threshold. These observations suggest that $\tau \approx 0.7$ marks the stability boundary for ICPSO, a limit shaped both by problem characteristic and other algorithm parameters, as well as by the algorithm's intrinsic randomness. When τ is set within the interval $[0.1, 0.4]$, ICPSO consistently generates very high-quality solutions; any performance variation is attributable mainly to random initialization and the algorithm's inherent stochasticity, yet overall results remain highly satisfactory. With $\tau = 0.5$ or 0.6, solution quality drops slightly but is still acceptable. These findings indicate that choosing a relatively small τ effectively strengthens ICPSO's ability to reach the optimal solution.

As Equation 5.3 makes clear, learning rates C_1 and C_2 heavily influence particle-velocity updates, so assessing their effects on algorithmic performance is indispensable. Two additional considerations underpin this inquiry. First, learning rates are pivotal hyper-parameters in PSO research; identifying their effective range here will furnish a valuable benchmark for future studies. Second—and more critically—ACPSO improves upon ICPSO by embedding adaptive learning-rate serials. Defining a stable baseline range will spare time and effort when searching for optimal serials, while our experimental results will also help validate learning-rate serials produced by the DDPG approach.

Table 5.3: Effects and stability range of learning rates.

LR* \ No.**	1	2	3	4	5	6	7	8
0.5	5.01×10^{-138}	7.79×10^{-129}	1.75×10^{-139}	4.99×10^{-138}	2.87×10^{-66}	2.06×10^{-69}	1.30×10^{-65}	1.45×10^{-68}
1	5.30×10^{-181}	1.60×10^{-175}	1.05×10^{-175}	2.57×10^{-181}	5.80×10^{-92}	5.39×10^{-89}	7.63×10^{-87}	2.32×10^{-92}
1.5	2.97×10^{-142}	2.74×10^{-164}	1.09×10^{-145}	2.65×10^{-137}	3.88×10^{-69}	5.32×10^{-70}	2.03×10^{-71}	2.19×10^{-68}
2	4.97×10^{-51}	9.30×10^{-94}	6.35×10^{-50}	1.37×10^{-48}	1.59×10^{-27}	7.76×10^{-33}	1.71×10^{-30}	3.88×10^{-23}
2.5	9.84×10^{3}	7.73×10^{3}	3.56×10^{6}	3.05×10^{7}	5.55×10^{2}	2.22×10^{1}	6.24×10^{23}	1.37×10^{56}
3	2.57×10^{4}	1.49×10^{6}	1.65×10^{7}	3.21×10^{7}	9.64×10^{46}	6.20×10^{3}	1.36×10^{51}	8.57×10^{85}
3.5	3.11×10^{4}	1.81×10^{6}	3.13×10^{7}	1.71×10^{7}	1.28×10^{2}	8.89×10^{20}	3.13×10^{54}	6.99×10^{114}
4	1.75×10^{4}	4.89×10^{5}	3.15×10^{7}	3.25×10^{8}	9.51×10^{40}	8.14×10^{1}	4.71×10^{56}	1.76×10^{117}
4.5	3.11×10^{4}	1.67×10^{6}	2.57×10^{7}	3.25×10^{8}	1.97×10^{41}	6.22×10^{18}	3.65×10^{54}	3.96×10^{59}
5	1.19×10^{4}	3.26×10^{6}	3.10×10^{7}	3.26×10^{8}	2.33×10^{47}	6.70×10^{18}	3.93×10^{53}	1.99×10^{113}

* : LR stands for learning rates.
** : No. stands for the scenario number.

This experiment assesses ICPSO's optimization performances across eight scenarios while varying learning rates from 0.5 to 5.0 in increments of 0.5. The results are presented in Table 5.3. As in most PSO studies, I do not differentiate between the two learning-rate coefficients, C_1 and C_2. Table 5.3 yields the same pattern observed in Table 5.2: as the test fitness function becomes more intricate, its dimensionality grows, or the search space widens, ICPSO's optimization performance deteriorates.

Focusing on the learning-rate coefficients, it is easy to find that when $C_1 = C_2 \geq 2.5$ the resulting solutions are unacceptable; indeed, at $C_1 = C_2 \geq 4$ the algorithm fails to evolve at all, and its final output mirrors the random initialization. By contrast, when $C_1 = C_2 \leq 2$ every solution meets the acceptance criterion, with $C_1 = C_2 = 1$ producing the outcome closest to the theoretical optimum. Hence, the learning rate's stable operating range can be placed in $[0.5, 2]$.

5.6 Numerical Examples: Validation of the Proposed Solution Algorithms

Section 5.5 has shown that the ICPSO developed in this study can attain satisfactory optimal solutions. In the present section, two computational study will be conducted to demonstrate that the refinements introduced to both ICPSO and its adaptive variant, ACPSO, are effective—specifically, that these algorithms surpass the benchmark methods in their ability to reach the global optimum.

5.6.1 Computational Study 1: Validation of ICPSO under Benchmark Fitness Functions

This section examines the capability of ICPSO to obtain satisfactory near–optimal solutions by benchmarking its performance on standard fitness functions against other established PSO algorithms.

Experimental Settings

a. Benchmark fitness function

In this study, eight canonical benchmark fitness functions [191] are adopted to evaluate the proposed ICPSO. Their key properties are summarized in Table 5.4, in which n= problem dimension, Ss=Searching space.

As what have reviewed in Section 2.3.4, benchmark fitness functions can be classified in terms of features like modality, basins, valleys, separability and dimensionality. Therefore, to furnish the algorithms under evaluation with a fair and comprehensive testbed, the selected benchmark fitness functions should, as far as possible, embody diverse facets of the aforementioned features.

Specifically, functions f_1 to f_3 are unimodal with distinct features, f_4 and f_6 are step functions which have one minimum and are discontinuous. Function f_5 is a non-separable and scalable singular function. Function f_7 is a dimensional sensitive quartic function while function f_8 is a continuous and multimodal function. Furthermore, for every function in the set, the global minimum equals 0, which represents the theoretical optimal fitness level that all algorithms seek to achieve.

Table 5.4: Benchmark fitness functions in Computational Study 1.

Test function	n	Ss
$f_1(x) = \sum_{i=1}^{n} x_i^2$	60	$[-100, 100]^n$
$f_2(x) = \sum_{i=1}^{n} \lvert x_i \rvert + \prod_{i=1}^{n} \lvert x_i \rvert$	30	$[-10, 10]^n$
$f_3(x) = \sum_{i=1}^{n}(\sum_{j=1}^{i} x_j^2)$	30	$[-100, 100]^n$
$f_4(x) = max\{\lvert x_i \rvert, 1 \leq i \leq n\}$	30	$[-30, 30]^n$
$f_5(x) = \sum_{i=1}^{n-1}[100(x_{i+1} - x_i)^2 + (x_i - 1)^2]$	30	$[-30, 30]^n$
$f_6(x) = \sum_{i=1}^{n}(\lfloor x_i + 0.5 \rfloor)^2$	30	$[-100, 100]^n$
$f_7(x) = \sum_{i=1}^{n} ix_i^4$	30	$[-1.28, 1.28]^n$
$f_8(x) = \sum_{i=1}^{n}[x_i^2 - 10cos(2\pi x_i) + 10]$	30	$[-5.12, 5.12]^n$

b. Selected algorithms for comparison

To evaluate the effectiveness of the proposed method, three established algorithms are chosen as baselines for all selected benchmark objective functions:

1. PSO [11]. A classical swarm–intelligence technique that emulates the collective behavior of bird flocks to search for solutions.

2. IMOPSO (Improved multi-objective PSO) [162]. Wang et al. devised IMOPSO to boost iterative efficiency and curb premature convergence by embedding the concepts of escape speed and particle restart location into the search dynamics.

3. AGLDPSO (Adaptive granularity learning distributed PSO) [181]. Employing a master–slave, multi–sub-swarm distributed framework, this approach divides the overall swarm into several sub-swarms and, at each iteration, updates solely the particle that currently occupies the worst position.

Each of the three benchmark methods belongs to evolutionary intelligence and has a documented record of producing accurate, well–suited solutions across a broad spectrum of optimization problems. Accordingly, contrasting the proposed ICPSO with these baselines is appropriate for gauging whether ICPSO exhibits superior or inferior performance relative to the three alternatives.

c. Parameter settings for Computational Study 1

Algorithmic hyperparameters critically influence PSO performance. For a fair head-to-head assessment, all parameters common to the four algorithms are assigned identical values, as reported in Table 5.5. Each of these values is determined through a series of preliminary trials to ensure equitable comparison. Moreover, in this experiment, the inertia weight and learning rates settings are chosen in accordance with the sensitivity analysis findings; selected values lie within their respective stability ranges.

Table 5.5: Parameter settings for Computational Study 1.

Parameter	Description	value
τ	Inertia weight	0.5
C_1	Learning weight	2
C_2	Learning weight	2
N	Entire population size	100
$\mathcal{T}$	Iteration step	1000
M	Sub-swarm number	10

Results and Analysis of Computational Study 1

To evaluate the algorithms' performance, each chosen benchmark fitness function was executed across 100 independent trials. At every iteration, the average fitness was computed and displayed in Figure 5.3. As visible in Figure 5.3, the fitness curves of all methods decrease over iterations—consistent with the behavior of these algorithms. Across nearly all test functions, PSO ranks among the two weakest performers, motivating numerous enhancements to this baseline. On most functions, IMOPSO achieves performance comparable to PSO; however, on the test functions $f_1(x)$, $f_4(x)$, and $f_5(x)$, IMOPSO clearly outperforms PSO. Hence, the modifications embodied in IMOPSO can be regarded as effective improvements over the standard PSO.

AGLDPSO and ICPSO employ cooperative–coevolution frameworks that divide the population into multiple sub–swarms, with iterations guided by information exchange among sub–swarms. Figure 5.3 shows that these two methods achieve the best performance on nearly all benchmark functions, indicating that cooperative coevolution is advantageous when addressing complex optimization tasks. Focusing on ICPSO, the fitness trajectories converge the fastest and approach the theoretical optima on most test functions (the sole exception being $f_3(x)$. In addition, for each algorithm collecting the minimal value obtained in every run, computed the averages, and reported them in Table 5.6.

Table 5.6: Mean minima values obtained by algorithms in Computational Study 1.

Algorithm / Test function	PSO	IMOPSO	AGLDPSO	ICPSO
$f_1(x)$	643.603	231.040	0.684	3.6×10^{-46}
$f_2(x)$	4.753×10^{-4}	2.089	0.010	1.036×10^{-14}
$f_3(x)$	6315.150	3639.609	185.334	1.819×10^{-34}
$f_4(x)$	2.228	2.248	0.544	5.971×10^{-23}
$f_5(x)$	63.324	29.073	12.622	1.143×10^{-17}
$f_6(x)$	0	8	319	0
$f_7(x)$	2.740×10^{-10}	0.026	0.003	3.480×10^{-98}
$f_8(x)$	270.998	287.721	50.918	0

From Table 5.6, the average minima delivered by PSO and IMOPSO on $f_1(x)$, $f_3(x)$, $f_5(x)$ and $f_8(x)$ remain far from the theoretical optima, revealing insufficient exploration capability in these two methods. Although IMOPSO does surpass PSO on the aforementioned four functions, it still fails to achieve sufficiently accurate results across all tests, reflecting limited exploitation strength. While AGLDPSO outperforms IMOPSO on all eight functions, its

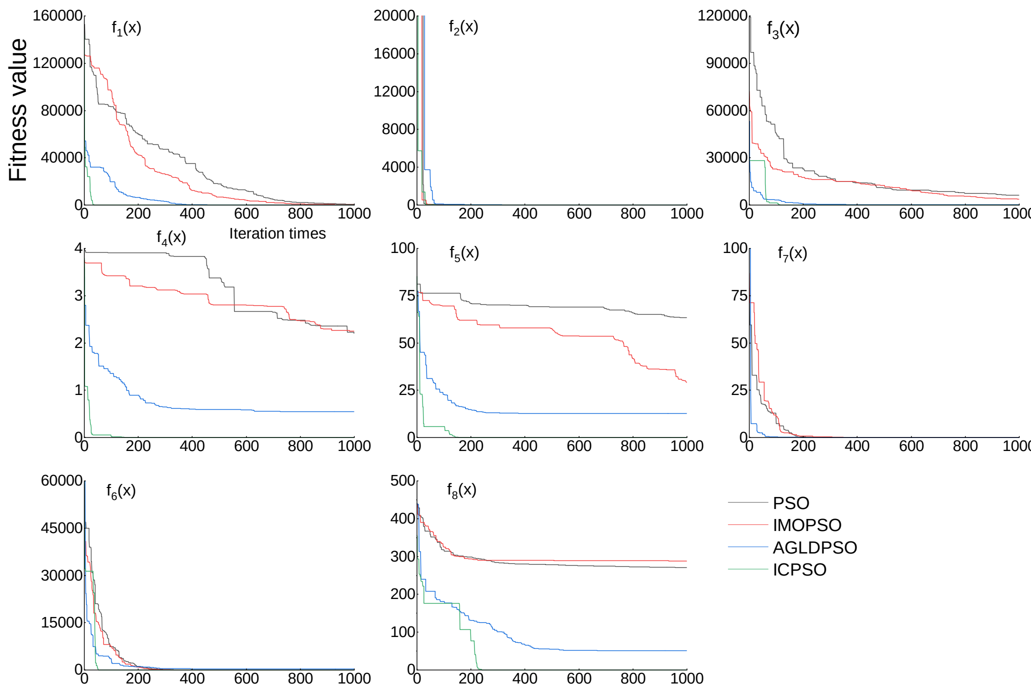

Figure 5.3: Algorithm comparison results under 8 test functions.

outcomes on $f_3(x)$, $f_5(x)$,$f_6(x)$ and $f_8(x)$ are still unsatisfactory. In contrast, ICPSO yields results that are consistently extremely close to the theoretical optima, demonstrating the method's capacity to obtain correct and highly precise solutions.

Overall, the experimental evidence indicates that ICPSO surpasses all other comparison algorithms on every tested fitness function. The method exhibits rapid convergence and reliably finds accurate solutions. Additional experiments exploring the effective dimensional range of ICPSO show that, when the test problem dimension is increased to roughly 1000, the algorithm no longer converges to the true optimum. Since the problem sizes considered in this study are substantially below 1000, it is reasonable to conclude that the solutions obtained with ICPSO for the optimization problems investigated here are dependable.

5.6.2 Computational Study 2: Validation of ACPSO under Benchmark Fitness Functions

The preceding section introduced ICPSO as a method for addressing large–scale, complex optimization tasks. A computational study on eight benchmark functions compared ICPSO with several heuristic baselines, namely PSO [11], IMOPSO [162], and AGLDPSO [181]. Aggregated experimental evidence shows that ICPSO surpasses all comparison methods on every selected fitness function, exhibiting rapid convergence and the ability to locate accurate, dependable solutions. Results also reveal that when the problem dimensionality is increased to around 1000, ICPSO encounters difficulty converging to the global optimum.

In order to address the issue of ICPSO's inability to accurately converge to the optimal solution when facing high-dimensional problems, the adaptive strategy will be introduced into ICPSO. This modified version is referred to ACPSO, which is proposed in this study.

In this section, a computational experiment is conducted to test the effectiveness of adopting adaptive strategy into PSO. In this experiment, 8 benchmark fitness functions [191] were selected as test optimization problems, as listed in Table 5.7. Functions f_1, f_2, f_4 to f_6 are unimodal with distinct structures. Function f_3 is a noisy sextic function. Function f_7

is a step function which has one minimum and is discontinuous. Function f_8 is dimension sensitive quartic function.

Table 5.7: Benchmark fitness functions in Computational Study 2.

Test function	n	Ss
$f_1(x) = \sum_{i=1}^{\mathrm{D}} x_i^2$	1000	[-10, 10]
$f_2(x) = (\sum_{i=1}^{\mathrm{D}} x_i^2)^2$	1000	[-10, 10]
$f_3(x) = \sum_{i=1}^{\mathrm{D}} x_i^6(2 + \sin\frac{1}{x_i})$	1000	[-10, 10]
$f_4(x) = -20\exp(-0.2\sqrt{\frac{1}{\mathrm{D}}\sum_{i=1}^{\mathrm{D}} x_i^2})$	1000	[-10, 10]
$f_5(x) = \sum_{i=1}^{\mathrm{D}} \lvert x_i \rvert + \prod_{i=1}^{\mathrm{D}} \lvert x_i \rvert$	1000	[-10, 10]
$f_6(x) = \sum_{i=1}^{\mathrm{D}} \sum_{j=1}^{i} x_j^2$	1000	[-10, 10]
$f_7(x) = \sum_{i=1}^{\mathrm{D}} (\lfloor x_i + 0.5 \rfloor)^2$	1000	[-10, 10]
$f_8(x) = \sum_{i=1}^{\mathrm{D}} i x_i^4$	1000	[-10, 10]

The first step of this experiment is to find the optimal serial values of learning rates C_1 and C_2 by Algorithm 2. The benchmark fitness function for Algorithm 2 was selected as $f_1(x) = \sum_{i=1}^{D} x_i^2$, $D = 100$. The iteration time T_b was set as 1000, it should be noted that the iteration time T_o in Algorithm 3 and in ICPSO were also set as 1000. After executing Algorithm 2 1000 times, the mean values of optimal serial C_1 and C_2 were depicted in Figure 5.4.

It could be observed from Figure 5.4 that learning rates C_1 and C_2 decrease in the iteration process. In previous research, it has also been demonstrated that employing larger learning rates during the early stages of iteration in PSO can enhance the algorithm's exploration capability, while using smaller learning rates in the later stages of iteration can strengthen its exploitation capability. The optimal serial values of C_1 and C_2 are contained in the input parameters of Algorithm 3.

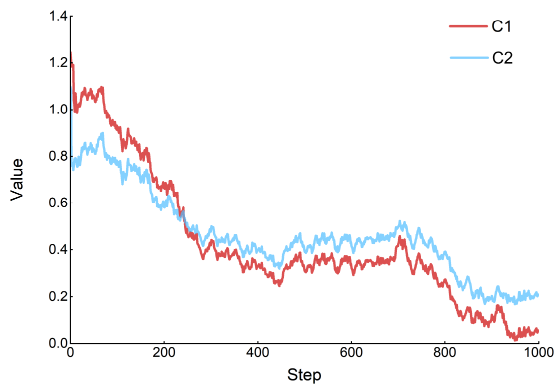

Figure 5.4: Optimal serial values of learning rates.

The setting of parameter values significantly impacts this experimental results. Therefore, to ensure the fairness in the experiments, the common parameters of ICPSO and ACPSO have been set to the same values, and certain unique parameters have also been set to the optimal performance values of the respective algorithms. All parameter values are listed in Table 5.8. Furthermore, in this experiment the inertia weight is chosen in accordance with the sensitivity analysis results and kept within its identified stability range. To safeguard the algorithm's effectiveness, the learning rates' initial value and upper bound are likewise set within the stable range indicated by the sensitivity study.

Table 5.8: Parameter settings for Computational Study 2.

Parameter	Description	Value
τ	Velocity coefficient in Equation 5.11	0.5
ω	Inertia weight	0.5
N	Population size	1000
T_o	Iteration time	1000
M	Sub-swarm number	10
D	Problem dimension	1000
C_1	Learning weight in ICPSO	2
C_2	Learning weight in ICPSO	2

To assess the performance of ICPSO and ACPSO, each algorithm will solve the minimum value of each selected test fitness function 100 times, and the experiments results were recorded in Table 5.9 and Table 5.10. It should be noted the theoretical minimal value for the first to 8th selected test fitness function are all 0.

Table 5.9: Test results of ICPSO in Computational Study 2.

No.	Best	Worst	Median	Mean	Std
1	3.62×10^{-37}	2.58×10^{-15}	6.78×10^{-28}	2.90×10^{-16}	8.11×10^{-16}
2	7.46×10^{-77}	1.33×10^{-38}	1.31×10^{-60}	1.13×10^{-39}	3.57×10^{-39}
3	1.23×10^{-116}	6.93×10^{-68}	1.38×10^{-97}	6.97×10^{-69}	2.19×10^{-68}
4	4.44×10^{-16}	6.81	4.00×10^{-15}	0.68	2.15
5	7.36×10^{-21}	2.96×10^{-10}	1.74×10^{-14}	3.16×10^{-11}	9.31×10^{-11}
6	497.54	498.96	498.79	498.55	0.52
7	0	0	0	0	0
8	4.29×10^{-88}	5.36×10^{-59}	5.20×10^{-66}	5.36×10^{-60}	1.69×10^{-59}

Table 5.10: Test results of ACPSO in Computational Study 2.

No.	Best	Worst	Median	Mean	Std
1	4.88×10^{-49}	3.87×10^{-41}	1.08×10^{-44}	4.4×10^{-42}	1.22×10^{-41}
2	1.26×10^{-97}	7.45×10^{-84}	3.30×10^{-91}	7.50×10^{-85}	2.35×10^{-84}
3	3.99×10^{-155}	6.42×10^{-136}	9.40×10^{-145}	6.42×10^{-137}	2.03×10^{-136}
4	7.33×10^{-9}	4.50×10^{-5}	3.56×10^{-7}	1.71×10^{-5}	2.144×10^{-5}
5	4.27×10^{-25}	1.30×10^{-20}	8.82×10^{-23}	1.69×10^{-21}	4.25×10^{-21}
6	8.94×10^{-49}	3.71×10^{-40}	5.29×10^{-45}	3.72×10^{-41}	1.17×10^{-40}
7	0	0	0	0	0
8	1.50×10^{-90}	4.71×10^{-84}	2.25×10^{-86}	6.62×10^{-85}	1.49×10^{-84}

From Table 5.9, it can be observed that ICPSO achieves results very close to the theoretical optimal value of 0 for most of the test functions, demonstrating the effectiveness of ICPSO in solving optimization problems. But for the 4th test function, the result obtained in the worst scenario is almost considered unusable. Additionally the results obtained for the sixth test function deviate significantly from the theoretical optimal value, making them also unusable. These limitations highlight the constraint of ICPSO.

The obtained results show low standard deviations, indicating the stability of ICPSO. I speculate that this may be attributed to the algorithm's structure and a relatively large population size of the particle swarm.

It can be observed from Table 5.10 that ACPSO achieves results very close to the theoretical value 0 for all test functions and scenarios. These results are considered acceptable solutions. All solutions obtained by ACPSO exhibit higher accuracy compared to ICPSO. Therefore, it can be considered that ACPSO is a more accurate and efficient optimization algorithm than ICPSO. Utilizing DDPG to obtain the optimal learning rates serial values within the PSO proves to be an effective strategy for enhancing the algorithm's solving performance.

Another important metric to evaluate the performance of the algorithm is the convergence speed. To test the convergence performance of these algorithms, the average number of iterations required are recorded for the algorithm to reach the precision levels ($100,\ 1, 10^{-2},\ 10^{-4},\ 10^{-6}$) for all solutions obtained. These results are presented in Table 5.11 and Table 5.12 below.

Table 5.11: Convergence speed of ICPSO in Computational Study 2.

No.	10^2	1	10^{-2}	10^{-4}	10^{-6}
1	187	239	383	466	558
2	203	224	350	358	415
3	140	185	203	227	297
4	1	175	N.A.	N.A.	N.A.
5	27	136	257	513	613
6	N.A.	N.A.	N.A.	N.A.	N.A.
7	178	255	255	255	255
8	167	170	205	249	258

Table 5.12: Convergence speed of ACPSO in Computational Study 2.

No.	10^2	1	10^{-2}	10^{-4}	10^{-6}
1	325	344	368	384	408
2	337	345	362	369	378
3	12	284	296	303	311
4	1	639	686	745	N.A.
5	273	339	382	414	449
6	311	335	361	383	399
7	330	350	350	350	350
8	350	358	366	379	393

From Table 5.11 and Table 5.12, it can be observed that ICPSO take less iteration time to convergence to low precision results (100, 1) compared to ACPSO. But in most cases, ACPSO converges to higher-precision results (10^{-6}) in less iteration time than ICPSO. This phenomenon may be attributed to maintaining higher learning rates, which prevents ICPSO's exploratory nature from being weakened but also hinders the exploitation process, making it difficult for the algorithm to achieve higher precision results.

In conclusion, from this experiment it can be inferred that, in the iterative process of PSO, the use of higher learning rates in the early stage can enhance the exploratory capabilities of the algorithm and accelerate convergence. On the other hand, utilizing lower learning rates in the later stage can enhance the algorithm's exploitation capabilities and improve the precision of the solutions obtained.

This experiment has demonstrated that using DDPG can yield optimal learning rate serial values, which in turn enables the ACPSO to converge faster to higher precision solutions. Considering the complexity of the mathematical model established in this study and the scale of the variables used, the using of ACPSO for model optimization is reliable.

Chapter 6

FINDINGS AND DISCUSSIONS

In this chapter, I will provide a detailed discussion of the findings and corresponding limitations identified in this study, spanning from the portfolio selection robustness in various market context to the reference point dependency in prospect theory and disappointment theory, and finally the tractability of behaviorally-based portfolio models.

6.1 Robustness of the Models in Various Market Contexts

In this study, to establish a comprehensive framework for characterizing investor decision-making behaviors, two novel portfolio selection models were proposed and empirically validated through four real-market case studies. Specifically, Case Studies 1 and 2 were designed to assess the efficacy of the multi-objective portfolio selection model proposed in Chapter 3, while Case Studies 3 and 4 evaluated the performance of the multiple reference points prospect theory-based portfolio selection model proposed in Chapter 4 under varying market conditions. Notably, the effectiveness of portfolio strategies is influenced not only by their structural design and parameterization but also critically by the market environments in which they are implemented. Consequently, this section undertakes a systematic examination of the market contexts underpinning these case studies—an analysis essential for verifying the robustness and generalizability of the proposed models. Section 6.1.1 focuses on robustness testing for the multi-objective portfolio selection model , whereas Section 6.1.2 evaluates the robustness of the multi-reference-point portfolio framework. By contextualizing model performance within distinct market regimes (e.g., bull-bearish markets, volatility clusters, and transaction volumes), this dual analysis provides critical insights into the adaptability of behavioral portfolio models to heterogeneous financial environments, thereby strengthening their theoretical validity and practical relevance.

6.1.1 Robustness of the Multi-Objective Model

In order to validate the effectiveness of the proposed multi-objective portfolio selection framework which integrates multiple behavioral decision theories, this research adopts two real-market data case studies. Data in Case Study 1 is collected from SSE 50 Index 2023 quarter 1, while data in Case Study 2 is collected from NYSE Composite Index from the given period. To further validate the robustness of the proposed portfolio multi-objective portfolio model under different market conditions, comparing the performance of the SSE 50 Index during 2023 Q1 which are plotted as a candlestick chart in Figure 6.1 with that of NYSE over the given period as shown in Figure 6.2.

In a candlestick chart, a candlestick compresses a scenario's price story. Its body spans the open-to-close range – red for a price rise, green for a drop – and its length gauges momentum. The upper and lower shadows records the day's high and low; elongated shadows flag intraday moves that were later rejected, hinting at volatility and potential reversals.

Based on the comparative analysis of the two candlestick charts provided, several key characteristics of the two capital markets can be identified in terms of returns, volatility, and overall market behavior.

The first market (SSE 50 Index 2023 Q1) displays significantly higher volatility. The price trajectory does not exhibit a clear upward or downward trend; rather, it fluctuates

Figure 6.1: Shanghai Stock Exchange 50 Index 2023 quarter 1.

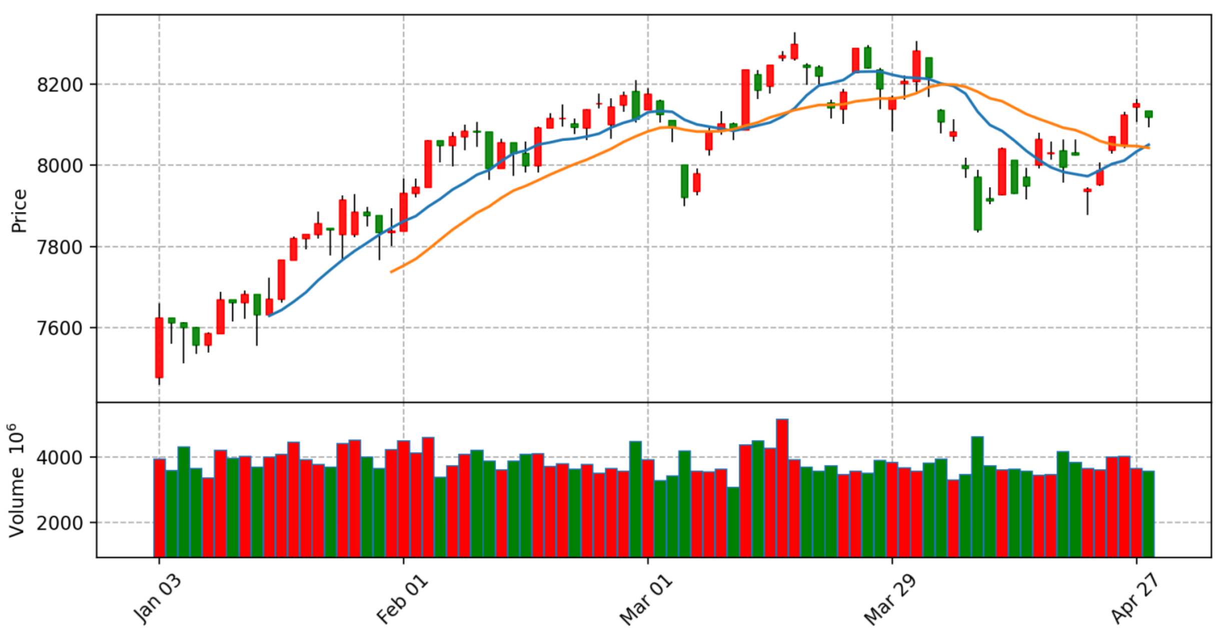

Figure 6.2: New York Stock Exchange Composite Index 2012.

within a broader range. The candlesticks in this market frequently display longer shadows and larger bodies, reflecting heightened intraday price swings and greater uncertainty among investors. Both bullish and bearish candles appear with comparable frequency, suggesting the absence of a dominant trend and the presence of frequent market reversals. Consequently, the cumulative returns in this market are likely lower or more unstable compared to the second market (NYSE Composite Index 2012), and the higher volatility indicates elevated risk exposure for investors.

In contrast, the second market (NYSE Composite Index 2012) demonstrates a relatively stable upward trend over the observed period. Despite short-term fluctuations, the overall price movement indicates consistent gains, suggesting that investors in this market experienced positive cumulative returns. The candlestick patterns show moderate daily price changes, with relatively small upper and lower shadows, indicating limited intraday volatility. Furthermore, the distribution of bullish (increasing) candles appears more frequent than bearish (decreasing) candles, reinforcing the impression of a sustained positive momentum. Overall, this market exhibits characteristics of a steadily growing market with controlled risk levels, appealing to investors seeking moderate but consistent returns.

A comparison of Tables 3.5: Performance under selected criteria at the end of the given period in Case Study 1, and Table 3.7: Performance under selected criteria at the end of the given period in Case Study 2, shows that the proposed multi-objective portfolio model which integrates multiple behavioral decision theories—designed to accommodate diverse decision preferences—yields markedly lower returns in Case Study 1 than in Case Study 2. The same pattern emerges for the two risk-adjusted return criteria, Sharpe Ratio, and Calmar Ratio: Both indicators place Case Study 1 well behind Case Study 2. Such cross-market discrepancies stem not only from differences in market performance but also from differences in market structure. As noted in Section 2.1, retail investors account for a far larger share of holdings and trading volume in the Chinese stock market than in the U.S. market; consequently, behavioral factors tied to retail participation exert a stronger influence in China. This claim is borne out by the superior showing of the proposed multi-objective model relative to its peers in both tables.

Conversely, the Expected Utility-CVaR model delivers solid returns in both cases, implying that the return predictions reported in Tables 3.2 and Table 3.6 are reasonably accurate. That said, the finding also highlights a key limitation of the present study. Although the proposed framework is more robust than traditional models and better able to manage risk, it still relies—at least partially—on accurate return predictions. If those predictions turn out to be wrong, or if unforeseen events (e.g., black-swan shocks) occur, the model's performance could deteriorate sharply. Accordingly, future research should focus on improving the precision of return projections and on developing portfolio strategies that remain effective when forecasts are noisy or erroneous.

6.1.2 Robustness of the Multiple Reference Points Model

In order to validate the effectiveness of the proposed multiple reference point portfolio selection framework, this research adopts two real-market data case studies. Data in Case Study 3 is collected from SSE 50 Index 2022 quarter 4, while data in Case Study 4 is collected from NYSE Composite Index and NASDAQ Composite Index from the given period. To further validate the robustness of the proposed portfolio multi-objective portfolio model under different market conditions, comparing the performance of the SSE 50 Index during 2022 Q4 which are plotted as a candlestick chart in Figure 6.3 with that of NYSE and NASDAQ over the given period as shown in Figure 6.4 and 6.5.

As presented in Figure 6.3, the cumulative wealth for the SSE 50 Index 2022 Q4 could be calculated as 1.0354, corresponding to an annualized yield of 15.75%, which significantly outperforms the comparison market index in Case Study 4.

However, this superior return from the SSE 50 Index 2022 Q4 comes at the cost of higher volatility and downside risk. Specifically, the SSE 50 Index exhibits an annualized volatility of 23.21% and a maximum drawdown of 11.20%, compared to 7.40% and 7.30% respectively

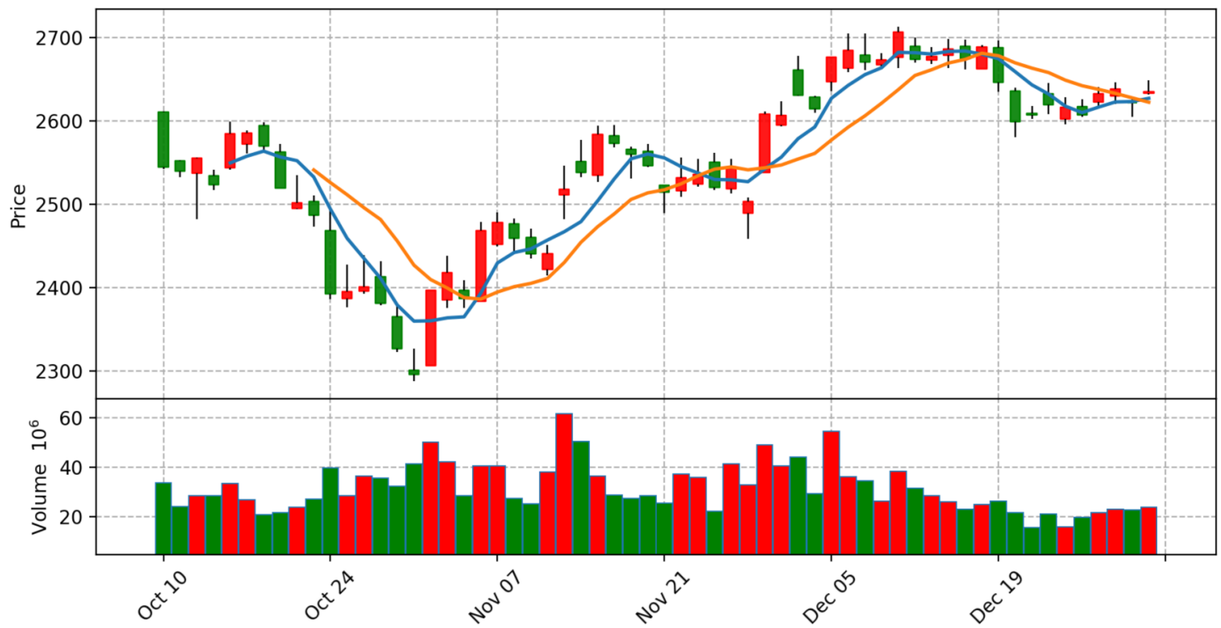

Figure 6.3: Shanghai Stock Exchange 50 Index 2022 quarter 4.

Figure 6.4: New York Stock Exchange Composite Index 2016.

Figure 6.5: NASDAQ Composite Index 2016.

for the comparison market index in Case Study 4. Despite the increased risk exposure, the SSE 50 Index demonstrates a stronger risk-adjusted performance. The Sharpe ratio and Calmar ratio reach 0.679 and 1.406 respectively, markedly surpassing the comparison's corresponding values of 0.311. These results suggest that while the SSE 50 Index entails higher market fluctuations, it also delivers superior excess returns per unit of risk. This indicates a more favorable risk-reward trade-off and a higher risk premium embedded in the SSE 50 Index during the observed period. In contrast, the benchmark index exhibits a more stable yet conservative return pattern, making it more suitable for risk-averse investors.

Drawing on Table 4.5: Performance under selected criteria at the end of the given period in Case Study 3, and Table 4.7: Performance under selected criteria at the end of the given period in Case Study 4, it is easy to conclude that the proposed multiple reference points portfolio selection model outperforms its single-reference-point counterpart by curbing investment risk when market volatility is high. Large price swings often trigger decision-making that departs from strict rationality; by embedding these behavioral patterns into the model, the proposed approach dampens that risk.

That said, both Case Study 3 and Case Study 4 unfold against a backdrop of only moderate volatility. Consider instead a far more turbulent episode—China's 2015 equity boom and bust. In such an extreme environment, retail investors incurred widespread losses as herd behavior amplified the market's violent gyrations. Extending the present framework to markets that experience even sharper shocks would therefore be a valuable avenue for future work, as it could bolster portfolio robustness and better equip investors to navigate severe risk.

Finally, retrospective analysis of the four case studies conducted in this research reveals the inherent difficulty in precisely predicting stock price fluctuations, thereby necessitating the validation of the proposed models across multiple distinct market regimes. Notably, Chinese equity markets (represented as SSE 50 Index) have historically exhibited significantly higher volatility compared to their U.S. counterparts (represented as NYSE and NASDAQ Composite Index) across various time horizons, a phenomenon consistent with prior scholarly observations and statistical analyses. This heightened volatility has been widely attributed to the prevalence of retail investors in Chinese markets, who demonstrate greater trading activity (as evidenced by higher trading volume participation) and distinct behavioral patterns [6, 192, 193, 194] (You may refer to Section 2.2.2 for detailed discussions). Within investment environments characterized by coexisting opportunities and risks, these retail investors exhibit well-documented behavioral tendencies under uncertainty, including bounded rationality, loss aversion, and return chasing. Consequently, predicting potential investor behaviors across differing market rhythms and providing corresponding investment guidance has emerged as a critical research objective within this study.

6.2 Static Reference Point

This study proposes two prospect theory-based portfolio selection models. Prospect theory, widely observed and documented as reference-dependent, underpins these frameworks. The reference-dependent nature of prospect theory and disappointment theory underscores a critical yet underappreciated challenge in behavioral finance: the inherent dynamic instability of reference points.

6.2.1 Intrinsic Fluidity of Reference Points: beyond Static Assumptions

The reference-dependent frameworks of prospect theory and disappointment theory inherently challenge the conventional paradigm of static reference points in behavioral finance [87]. While traditional models often simplify reference points as fixed parameters—such as initial wealth levels or exogenously defined aspiration thresholds—empirical studies increasingly highlight their endogenous adaptability to both cognitive and contextual factors. For instance, reference points in prospect theory are not merely anchored to historical data (e.g., purchase prices or past returns) but are dynamically recalibrated through adaptive expectations shaped by: 1. Recency bias: investors disproportionately weigh recent market performance, leading to upward/downward adjustments during bull/bear markets. 2. Social Contagion: Peer comparisons and social media trends amplify shifts in aspiration levels, particularly among retail investors. 3. Regulatory or macroeconomic shocks: Sudden policy changes (e.g., interest rate hikes) or geopolitical events (e.g., trade wars) can reset reference points abruptly.

The model developed in Chapter 4 extends classical prospect theory by introducing dual fuzzy reference points, capturing both minimum requirements and goal-seeking behavior. Compared to conventional prospect-theory-based models that rely on a fixed reference point, such as the one proposed by [175], our dual-point model demonstrates improved adaptability to investor preferences, as shown in Case Study 3. Table 4.5: Performance under selected criteria at the end of the given period in Case Study 3 shows that, when all other portfolio selection models' features are held constant, adopting uncertain interval-based reference points—rather than fixed values—effectively reduces investment risk. This interval specification represents our first attempt to incorporate non-static reference points into the framework, and Case Studies 3 and 4 together confirm that such non-static benchmarks both reflect actual investor behavior more faithfully and demonstrably curb risk in real markets. The enhanced expressiveness and flexibility help reflect nuanced investor behaviors in highly volatile markets, which is not fully captured by single-reference models.

This fluidity undermines the validity of cross-sectional studies that assume temporal invariance, as reference points exhibit time-varying heterogeneity influenced by evolving market conditions and investor learning processes. For example, a longitudinal study by [195] demonstrated that reference points for S&P 500 investors shifted by 15–20% annually, correlating with macroeconomic volatility indices.

6.2.2 Adaptive Feedback Mechanisms and Path Dependencies

The interplay between reference points and market cycles introduces nonlinear feedback loops that static models fail to capture. During bullish phases, investors often escalate reference points due to: 1. Overconfidence: Successive gains reinforce beliefs in personal forecasting ability, raising risk tolerance. 2. Goal gradient effects: As portfolios approach aspirational thresholds (e.g., target retirement savings), investors may increase risk exposure to "close the gap."Conversely, in bear markets, downward rigidity emerges: 1. Loss aversion: Investors resist lowering reference points to avoid acknowledging losses, perpetuating conservative strategies. 2. Regret aversion: Fear of further underperformance relative to peers locks reference points at unrealistically high levels.

This study proposes two approaches to depict retail investors' tendencies in different market phases, the first model-driven approach introduced in Chapter 3 and the other theory-centric approach introduced in Chapter 5. Compared to other models [13, 7, 15, 61, 175], this study validates that the incorporation of reference points' dynamic and uncertainty is effective and robust. These dynamics create path dependencies where prior outcomes recursively shape future behavior. For instance, post-2008 crisis data reveals that investors who experienced severe losses maintained elevated reference points for over a decade, amplifying risk aversion despite market recovery—a phenomenon termed "financial scarring."

6.2.3 Implications for Portfolio Selection Models

The failure to incorporate dynamic reference points risks specification bias with cascading consequences:

Tail risk mispricing: Static models underestimate extreme losses during regime shifts (e.g., COVID-19 market crash), as reference points lag behind rapid sentiment changes.

Ecological validity erosion: High-frequency trading algorithms relying on fixed reference points generate suboptimal orders, evidenced by the 2020 "Flash Crash" anomalies.

Policy design flaws: Pension funds using static thresholds may overestimate risk capacity, jeopardizing long-term solvency.

The failure to account for these dynamics carries profound implications. Portfolio selection models predicated on static reference points risk specification bias, wherein the assumed mathematical structures become misaligned with real-world decision heuristics. For instance, a model assuming fixed reference points may systematically underestimate tail risks during market regime shifts, as it cannot adapt to sudden changes in investor sentiment. This misalignment not only undermines predictive accuracy but also erodes the ecological validity of prospect theory- and disappointment theory-based frameworks, particularly in high-frequency trading contexts where decision cycles are compressed.

6.3 Model Tractability

The behavioral portfolio selection frameworks developed in this study, while rich in psychological realism, inherit profound mathematical complexities that challenge the very foundations of tractable optimization. These complexities arise not merely from algorithmic limitations but are intrinsic to the models' theoretical architecture, rooted in the nonlinear, non-convex, and recursive structures demanded by prospect theory and disappointment theory.

This study adopts the two PSO algorithms proposed in Chapter 6 to find solutions of the portfolio selection models, the adoption of heuristic algorithm is a balance between solution time and accuracy. Scholars have employed methodological approaches—such as mathematical transformations or convex relaxation techniques—to convert non-convex objective functions or constraints into directly solvable forms [14, 59, 45, 48, 196, 50]. While these methods yield precise solutions under reformulated problem structures, the inherent discrepancy between such solutions and the theoretical optima of the original model remains non-negligible. This divergence arises from approximation errors in problem reformulation, computational simplifications, or inherent limitations in relaxation strategies. Ultimately, regardless of the specific methodology adopted, the solvability of a model—defined as its capacity to generate solutions that faithfully preserve the original problem's theoretical properties—is paramount to obtaining reliable and behaviorally consistent outcomes. This underscores the critical need for optimization frameworks that balance computational tractability with minimal deviation from global optimality, particularly in high-dimensional, behaviorally complex portfolio selection contexts.

6.3.1 Non-Convex, Discontinuous Objective Landscapes

In Section 5.5, I conducted a sensitivity analysis experiment to examine how problem characteristics - namely, structure, dimensionality and searching space - affect algorithmic performances. The experimental results summarized in Table 5.2 and Table 5.3 further reveal that, with all other experimental settings unchanged, a more complex objective function sharply degrades the solution accuracy of the optimization algorithm. For example, when the inertia weight is 0.1, the best solution in Scenario 1 is 8.56×10^{-245}, whereas Scenario 5 yields 3.15×10^{-85}—even though Scenario 5 involves only 100 decision variables compared with 1,000 in Scenario 1. The added structural complexity of objective function

$f_2(x) = \sum_1^n |x_i| + \prod_i^n |x_i|$, as opposed to $f_1(x) = \sum_1^n x_i^2$, is therefore the leading cause of this deterioration. It is also noteworthy that prospect theory—the theoretical cornerstone of this study—introduces numerous discontinuities that make the objective landscape distinctly more challenging than that of traditional expected-utility models. Prospect theory's S-shaped value function introduces kinked utility surfaces with discontinuous first derivatives at reference points. Mathematically, this creates:

Non-differentiable regions. The abrupt shift from risk-averse (concave) to risk-seeking (convex) utility around reference points invalidates gradient-based optimization, which requires smooth, differentiable objective functions.

Non-convex Pareto frontiers. The coexistence of multiple risk-return equilibrial—some corresponding to local optima—renders convex relaxation techniques (e.g., Lagrange multipliers) ineffective. For instance, portfolios near a reference point may exhibit radically different risk sensitivities compared to those far from it, fracturing the solution space into disjoint basins of attraction.

Disappointment theory compounds these challenges through asymmetric, nonlinear penalty functions that amplify disutility for outcomes below expectations. The resulting objective landscape resembles a high-dimensional "quasi-concave" terrain punctuated by cliffs and valleys, where even minor perturbations in parameters can collapse entire regions of feasible solutions.

6.3.2 Curse of Dimensionality in Dynamic Reference Points

The dynamic nature of reference points transforms portfolio optimization into a time-recursive stochastic control problem. Unlike static models, where reference points are fixed parameters, adaptive frameworks require continuous recalibration of:

Endogenous thresholds. Reference points evolve as functions of past portfolio performance, introducing memory-dependent variables that exponentially expand the state space.

Exogenous interactions: Market-wide shocks (e.g., interest rate changes) and social influences (e.g., herd behavior) couple reference point dynamics to external stochastic processes, necessitating high-dimensional partial differential equations for exact solutions.

For a portfolio selection scheme with n assets optimized over T periods, the resulting dimensionality scales as $\mathcal{O}(n \times T^2)$, as each period's reference point depends on all prior states. This combinatorial explosion rapidly exceeds the computational capacity of deterministic solvers—even for modest $n = 10$ and $T = 12$, the problem involves $\sim 10^4$ interdependent variables, far beyond the reach of exact dynamic programming.

6.3.3 Absence of Closed-Form Solutions

Unlike the Markowitz mean-variance framework, which admits analytical solutions under quadratic utility, behavioral models lack closed-form expressions due to:

Non-quadratic utility: Prospect theory's piecewise-defined value functions and disappointment theory's exponential disutility penalties preclude symbolic integration.

Non-Gaussian returns: Behavioral frameworks inherently accommodate skewed and fat-tailed distributions, rendering moment-based approximations (e.g., mean-variance) statistically inconsistent.

This forces reliance on numerical methods, which are inherently approximate and sensitive to discretization errors. For instance, discretizing continuous reference point adjustments into a finite grid introduces quantization artifacts, where optimal portfolios artificially cluster around grid points, distorting risk-return trade-offs.

The mathematical intractability of behavioral portfolio models is not a transient limitation but a structural consequence of their psychological realism. These frameworks demand non-convex, high-dimensional, and recursive formulations that lie beyond the reach of both classical optimization and modern heuristics. While computational workarounds like PSO enable provisional solutions, they cannot surmount the fundamental tension between behavioral accuracy and mathematical tractability—a trade-off that defines the frontier of contemporary financial modeling.

Chapter 7

CONCLUSIONS, CONTRIBUTIONS TO KNOWLEDGE AND FUTURE WORK

This final chapter concludes the key findings and theoretical contributions presented in this dissertation, offering a comprehensive reflection on the behavioral portfolio optimization models and solution algorithms proposed throughout. The chapter begins by drawing conclusions from the main developments introduced in Chapters 3 through 5, where multi-objective models, advanced prospect theory frameworks, and enhanced PSO algorithms were explored in depth. It then identifies the knowledge contributions of the research in the fields of behavioral finance, computational optimization, and decision science. Finally, several promising directions for future research are outlined, aimed at enhancing the adaptability, efficiency, and theoretical robustness of portfolio decision-making models under uncertainty.

7.1 Conclusions

This section summarizes the core contributions of the dissertation and reflects on how the proposed models and methodologies address the research gaps identified earlier. The conclusion is organized into three thematic subsections. The first subsection revisits the problem of portfolio selection, concludes the first research objective, the development of a multi-objective portfolio selection model by integrating multiple retail investor behavioral decision theories to address the research gap of behavioral-based models' incompleteness and narrowness. The second subsection focuses on prospect theory, concludes the second research objective, enhancement of prospect theory by encompassing diverse decision biases to address the research gap of behavioral-based models' incompleteness and narrowness. The final subsection evaluates the role of PSO in solving complex, behavior-based portfolio optimization problems, concludes the third research objective, optimization of the architecture and parameters of PSO to address the research gap of premature and local minima in solution algorithms.

7.1.1 Portfolio Selection: Markowitz to Behavioral-based Models

Portfolio selection is the process of choosing a mix of investment assets that aligns with an investor's goals and risk tolerance. Traditional models, rooted in Markowitz's mean-variance framework, aim to balance risk and return via diversification. Over time, this classical approach has evolved to include considerations such as transaction costs, multi-period decision-making, and non-normal return distributions. Despite these advancements, a significant gap remains in capturing how retail investors behave under market uncertainty, especially when asset values drop below psychological thresholds. Existing models often rely on expected utility theory, assuming rational decision-making and static market conditions. However, retail investors—who dominate markets like China's—exhibit behavior that deviates from this rationality, particularly during extreme market fluctuations.

This dissertation addresses this gap by introducing a structurally refined, behaviorally grounded portfolio selection model, which is the first research objective. The first research objective is development of multi-objective portfolio selection model by integrating multiple retail investor behavioral decision theories. The proposed model adopts a multi-objective approach to balance profitability and risk while reflecting retail investors' preferences, including risk aversion and behavioral inconsistencies. The proposed model aims to better explain real-world investment decisions and provide more robust portfolio solutions under market stress. Three benchmark portfolio selection methods are used as baselines against the proposed multi-objective portfolio selection framework under conditions of market stress. Two case studies based on real market data are conducted to assess the effectiveness of the proposed approach. The experimental evidence shows that the proposed model delivers steadier profits than the three alternatives, when judged by criteria of return, risk, and risk-adjusted return. Moreover, Section 6.1.1 examines the robustness of the model. The empirical results indicate that it delivers consistently favorable returns across diverse market environments and regimes. Therefore, the conclusion can be drawn that the proposed multi-objective portfolio selection model - integrating multiple retail investor behavioral decision theories - effectively balances return and risk, and that this strategy remains effectively across different markets.

7.1.2 Prospect Theory and Retail Investor Portfolios

Prospect theory, developed by Kahneman and Tversky, describes how individuals make decisions under risk by evaluating potential gains and losses relative to reference points rather than final outcomes. A central concept is loss aversion—investors react more intensely to losses than to gains. While this theory has been applied in portfolio modeling, most models still emphasize loss aversion, often leading to conservative investment strategies. However, behaviors such as return chasing, where investors prefer assets with recent high returns, are underexplored. The literature also lacks clarity on how reference points are selected or how investors adjust to market volatility. To fill this gap, this research develops prospect theory by encompassing diverse decision biases, which is the second research objective. The second research objective is enhancement prospect theory by encompassing diverse decision biases. And a portfolio selection model based on this enhanced prospect theory is proposed.

This model captures dynamic behaviors like return chasing and overcomes the static nature of loss-averse models. By embedding behavioral features within risk-constrained portfolio optimization, this study offers a more nuanced framework that reflects how retail investors respond to real-time changes. This approach aims to enhance the explanatory power of prospect theory in financial decision-making and provide actionable insights for developing adaptive investment strategies in uncertain markets.

In order to reflect the phenomenon of return-chasing where investors disproportionately favor assets with recent positive performance, a portfolio selection model which incorporates a variant of prospect theory that uses two reference points is proposed. This model is designed to address the dynamic nature of investor behavior, ensuring that overly conservative strategies, which are common in models focused only on loss aversion, are avoided. By using the mean-absolute deviation as a risk constraint, this model also improves risk control and diversification in the portfolio.

In comparison to existing works, this two reference points portfolio selection model closely aligns with real-world investor behavior patterns and demonstrates robust risk resilience. Simultaneously, it amalgamates the advantages of expected utility theory and prospect theory, achieving a balance between risk and return. It does not err on the side of excessive conservatism, avoiding missing opportunities, nor does it become overly aggressive, leading to excessive volatility. Two case studies based on real-market data validates the incorporation of two reference points empowers the model to attain higher returns while reference points with uncertain interval bolster its risk resilience to a certain extent. Furthermore, Section 6.1.2 evaluates the robustness of the proposed multiple reference points portfolio selection model. The empirical results indicate that it delivers consistently favorable returns across diverse market environments and regimes. Therefore, the conclusion can be drawn that the proposed multiple reference points portfolio selection model - encompassing diverse decision biases - effectively balances return and risk, and that this strategy remains effectively across different markets.

7.1.3 Particle Swarm Optimization for Behavioral-based Portfolios

PSO is a heuristic optimization technique inspired by the social behavior of flocks and swarms. It is valued for its simplicity, parallelizability, and suitability for solving high-dimensional, non-convex problems. In the context of portfolio optimization, PSO has been employed to navigate complex objective landscapes where traditional solvers struggle. However, classical PSO suffers from premature convergence and entrapment in local optima, especially in high-stakes financial applications involving behavioral models and real-world constraints. This research identifies these limitations as a second key gap in the literature. To overcome them, this dissertation proposes two improved PSO algorithms that incorporate collaborative-adaptive mechanisms to better explore the solution space and avoid stagnation, which is the third research objective. These enhancements allow for more accurate and robust optimization in complex portfolio models that integrate behavioral theories like prospect theory. The improved PSO algorithms not only serve as effective solvers for the proposed models but also contribute a generalizable tool for addressing similar high-dimensional, non-smooth optimization challenges in finance and engineering.

Compared with conventional PSO variants, the proposed improved cooperative PSO partitions the population into multiple sub–swarms, and applies an evolution/update rule to the sub–swarm's incumbent best particle that is deliberately different from the rule used for the other particles in that sub–swarm. In experiments conducted on eight classical benchmark test functions, the obtained results show clear advances in exploring the entire search space and in locating global optima, relative to the comparison algorithms. These findings suggest that the method's effectiveness can inspire new directions for enhancing heuristic optimizers. In addition, due to its straightforward implementation, the algorithm is amenable to solving a wide variety of other optimization problems.

Compared with established PSO variants, the proposed ICPSO partitions the entire swarm into multiple sub-swarms. Within each sub-swarm, the particle attaining the best fitness is updated by a distinct evolution strategy, whereas the remaining particles follow a different update rule. A computational study employing eight classical benchmark functions was conducted; the empirical results confirm that, relative to the comparison algorithms, the proposed method achieves substantial advances in exploring the full search space and in locating global optima. The demonstrated effectiveness of the approach can inspire the design of stronger heuristic algorithms, and—owing to its straightforward implementation—it is suitable for addressing a wide range of other optimization problems.

Moreover, the other proposed novel PSO algorithms, adaptive cooperative PSO algorithm, incorporates adaptive and cooperative strategies, whereby the optimal learning rate sequences is derived via the deep deterministic policy gradient algorithm to achieve the best adaptive strategy. The optimal cooperative strategy is attained by decomposing the entire swarm randomly into multiple sub-swarms. An computational study, based on test fitness functions, verifies the capability of this algorithm to rapidly yield solutions of sufficient precision.

7.2 Contributions to Knowledge

This study makes significant theoretical, methodological, and practical contributions to the fields of portfolio selection, behavioral finance, and optimization algorithms. By integrating behavioral insights with advanced computational techniques, it addresses critical gaps in existing frameworks and offers novel solutions tailored to the complexities of modern financial markets.

7.2.1 Advancing Behavioral Portfolio Selection Models

The research contributes to portfolio theory by bridging the divide between classical Markowitz-based models and behavioral finance. Traditional portfolio optimization frameworks often assume rational decision-making and static risk preferences, failing to account for cognitive biases such as loss aversion, return chasing, and psychological lower bounds. This study introduces a multi-objective behavioral portfolio model that systematically incorporates these biases into the optimization process. By formalizing concepts like the "psychological lower bound"—the threshold below which investors react irrationally to losses—the model captures how extreme market conditions amplify behavioral distortions. Additionally, the integration of dynamic risk constraints and multiple reference points (e.g., financial goals, status quo) enables a more nuanced representation of retail investor behavior under volatility. These innovations enhance the predictive accuracy of portfolio strategies during market stress, offering a robust alternative to overly conservative or aggressive traditional approaches. Empirical validation through case studies demonstrates the model's ability to balance risk-return trade-offs while aligning with real-world investor psychology, thereby enriching the theoretical foundations of behavioral portfolio management.

7.2.2 Refining Prospect Theory for Financial Decision-Making

The study advances prospect theory by addressing its limitations in modeling dynamic and multi-faceted investor behavior. While prospect theory has been widely adopted to explain deviations from rationality, existing applications often rely on static reference points and oversimplified loss-aversion parameters. This research proposes a prospect theory-based multiple reference points framework, which incorporates financial, social, and aspirational benchmarks to reflect the evolving priorities of investors. For instance, the multiple reference points model distinguishes between short-term survival thresholds (e.g., avoiding losses below a psychological floor) and long-term aspirational targets (e.g., wealth accumulation goals), enabling a granular analysis of how investors reallocate assets during market shifts. Furthermore, the framework integrates return-chasing behavior—a phenomenon where investors disproportionately favor recently outperforming assets—into loss-aversion calculations, mitigating the conservatism inherent in traditional prospect theory models. By validating these enhancements through computational experiments, the study demonstrates their capacity to explain paradoxical behaviors, such as simultaneous risk aversion and speculative trading, thereby expanding the scope of prospect theory in financial contexts.

7.2.3 Enhancing Computational Tools for High-Dimensional Optimization

Methodologically, the study addresses the computational challenges of solving high-dimensional, non-convex portfolio optimization problems with behavioral components. While PSO is a popular heuristic, its efficacy is hindered by premature convergence and local optima traps in complex scenarios. This research develops a collaborative-adaptive PSO variant that introduces two key innovations: (1) dynamic inertia weights adjusted via real-time fitness feedback to balance exploration and exploitation, and (2) cooperative sub-swarms that share information across partitioned search spaces to prevent stagnation. These modifications enable the algorithm to navigate non-smooth, high-dimensional objective functions efficiently, as evidenced by benchmark tests and case studies on behavioral portfolio models. The improved PSO not only achieves faster convergence but also maintains solution diversity, making it a scalable tool for real-world applications. By open-sourcing the algorithm and validating its performance across diverse market regimes, the study provides a replicable framework for solving complex optimization problems in finance and beyond.

7.2.4 Practical Implications for Investors and Institutions

Beyond theoretical and algorithmic contributions, this research offers actionable insights for practitioners. The behavioral portfolio models equip financial advisors with tools to design personalized investment strategies that account for clients' cognitive biases and risk thresholds. For instance, the MRP framework helps institutions tailor products (e.g., target-date funds) to align with investors' aspirational goals while safeguarding against extreme losses. Similarly, the enhanced PSO algorithm enables asset managers to solve large-scale optimization problems—such as multi-asset rebalancing under transaction costs—with greater precision and speed. By bridging behavioral insights with computational robustness, the study fosters a more resilient approach to portfolio management in volatile markets, ultimately enhancing investor trust and financial system stability.

Overall, this research contributes valuable insights into portfolio management and optimization, offering practical tools and methodologies that can be adapted for various optimization challenges. The findings underscore the potential for these innovative models and algorithms to inspire further advancements in financial engineering and computational optimization. By providing a comprehensive framework that integrates theoretical insights with practical applications, this study lays the groundwork for future research and development in the field, paving the way for more resilient and effective financial decision-making strategies.

7.3 Proposed Future Work

The limitations identified in this study—ranging from the dynamic nature of reference points to the computational inefficiencies of heuristic optimization algorithms—provide a robust foundation for defining transformative future research trajectories. Building on these challenges, the following directions outline pathways to advance both the theoretical rigor and practical applicability of behavioral portfolio optimization frameworks.

7.3.1 Dynamic Reference Point Calibration Frameworks

As discussed in Section 6.2, the static nature of reference points in prospect theory and disappointment theory represents a critical vulnerability in dynamic financial environments. Future research should prioritize the development of adaptive reference point calibration systems that integrate real-time data streams and behavioral feedback loops. Key innovations could include:

Real-Time Sentiment Analysis: Leveraging natural language processing (NLP) to extract investor sentiment from social media, news, and earnings calls, enabling continuous updates to reference points based on collective psychological shifts.

Regime-Switching Models: Incorporating Markov regime-switching mechanisms to adjust reference points across distinct market states (e.g., "normal," "stressed," "euphoric"). These models would re-estimate parameters conditional on volatility clusters, liquidity conditions, or macroeconomic indicators.

Demographic-Aware Calibration: Using unsupervised learning techniques (e.g., k-means clustering) to segment investors by behavioral profiles and dynamically adjust reference points for each cohort. This approach would account for generational and cultural differences in risk perception and decision-making.

By embedding these adaptive mechanisms, portfolio models can better align with the fluid realities of investor psychology, enhancing their robustness during market regime shifts and structural breaks.

7.3.2 Hybrid Optimization Architectures for Theoretical and Practical Balance

As discussed in Section 6.3.3, the adoption of PSO to seek optimal solutions in this study because behavioral portfolio selection models are mathematically intractable - an enduring, structural consequence of their psychological realism rather than a transient limitation. The reliance on PSO introduces inherent trade-offs between computational efficiency and theoretical validity. Future work should explore hybrid optimization architectures that combine the exploratory strengths of heuristic algorithms with the rigorous convergence properties of mathematical programming. Potential innovations include:

Convergence Scaffolding: Embedding gradient-based or convex optimization techniques within heuristic frameworks to guide search trajectories toward globally optimal regions. For instance, trust-region methods could be used to refine solutions identified by PSO.

Certifiable Heuristics: Developing theoretical guarantees for heuristic-derived solutions by integrating Lyapunov stability analysis or regret-bound formulations. These frameworks would provide confidence intervals for solution quality, addressing the reproducibility challenges of stochastic algorithms.

Quantum-Inspired Optimization: Exploring quantum annealing or variational quantum algorithms to enhance the scalability and efficiency of high-dimensional portfolio optimization. These methods could significantly reduce computational overhead while maintaining heuristic flexibility.

Such hybrid architectures would bridge the gap between heuristic adaptability and mathematical rigor, making portfolio models more reliable for institutional applications.

7.3.3 Adaptive Computational Resource Allocation and Lightweight Adaptation

The computational inefficiencies of static subgroup coordination and reinforcement learning-driven adaptation highlight the need for resource-aware optimization frameworks. Future research should focus on:

Dynamic Subgroup Coordination: Transitioning from static to adaptive subgroup partitioning, where sub-swarms autonomously merge or split based on real-time convergence diagnostics. This approach would reduce redundant computations while preserving population diversity.

Lightweight Reinforcement Learning: Simplifying DDPG workflows by replacing deep neural networks with interpretable surrogate models (e.g., random forests, symbolic regression) for policy evaluation. Episodic adaptation strategies—triggered by optimization milestones rather than continuous updates—could further reduce computational demands.

Hardware-Software Co-Design: Leveraging hardware acceleration (e.g., FPGA/GPU) and edge computing architectures to distribute optimization tasks across networked devices. This would enable real-time portfolio rebalancing in latency-sensitive applications.

By optimizing resource allocation and reducing algorithmic overhead, these innovations would enhance the operational feasibility of behavioral portfolio models in high-frequency trading and dynamic asset allocation scenarios.

References

[1] H. Markowitz, "Portfolio selection," *The Journal of Finance*, 1952.

[2] B. Li, R. Zhang, and Y. Sun, "Multi-period portfolio selection based on uncertainty theory with bankruptcy control and liquidity," *Automatica*, vol. 147, p. 110751, 2023.

[3] H. Shefrin and M. Statman, "Behavioral capital asset pricing theory," *Journal of Financial and Quantitative Analysis*, vol. 29, no. 3, pp. 323–349, 1994.

[4] M. Leković, *Behavioral portfolio theory and behavioral asset pricing model as an alternative to standard finance concepts*. Faculty of Economics, University of Kragujevac, Kragujevac, 2019.

[5] M. Akkaya, "Behavioral portfolio theory," in *Applying Particle Swarm Optimization: New Solutions and Cases for Optimized Portfolios*. Springer, 2021, pp. 29–48.

[6] W. Chen, S. Liang, and D. Shi, "Who chases returns? evidence from the chinese stock market," *Evidence from the Chinese Stock Market (June 30, 2022)*, 2022.

[7] G. Curtis, "Modern portfolio theory and behavioral finance," *The Journal of Wealth Management*, vol. 7, no. 2, pp. 16–22, 2004.

[8] C. M. Jones, A. V. Reed, and W. Waller, "When brokerages restrict retail investors, does the game stop?" *Columbia Business School Research Paper Forthcoming*, 2021.

[9] J. Fu, J. Wei, and H. Yang, "Portfolio optimization in a regime-switching market with derivatives," *European Journal of Operational Research*, vol. 233, no. 1, pp. 184–192, 2014.

[10] H. Markowitz, P. Todd, G. Xu, and Y. Yamane, "Computation of mean-semivariance efficient sets by the critical line algorithm," *Annals of Operations Research*, vol. 45, pp. 307–317, 1993.

[11] J. Kennedy and R. Eberhart, "Particle swarm optimization," in *Proceedings of the IEEE International Conference on Neural Networks*, vol. 4. IEEE, 1995, pp. 1942–1948.

[12] Y. Zhang, H. Lin, X. Yang, and W. Long, "Combining expert weights for online portfolio selection based on the gradient descent algorithm," *Knowledge-Based Systems*, vol. 234, p. 107533, 2021.

[13] H. Mi and Z. Q. Xu, "Optimal portfolio selection with var and portfolio insurance constraints under rank-dependent expected utility theory," *Insurance: Mathematics and Economics*, vol. 110, pp. 82–105, 2023.

[14] H.-Q. Li and Z.-H. Yi, "Portfolio selection with coherent investor's expectations under uncertainty," *Expert Systems with Applications*, vol. 133, pp. 49–58, 2019.

[15] J. Hao, X. Gao, X. Yang, Y. Liu, and Z. Han, "A decision-making method for design schemes based on intuitionistic fuzzy sets and prospect theory," *Symmetry*, vol. 15, no. 8, p. 1570, 2023.

[16] J. Gu, Y. Zheng, X. Tian, and Z. Xu, "A decision-making framework based on prospect theory with probabilistic linguistic term sets," *Journal of the Operational Research Society*, vol. 72, no. 4, pp. 879–888, 2021.

[17] G. Guo, Y. Xiao, and C. Yao, "Multi-period uncertain portfolio selection model with prospect utility function," *Plos One*, vol. 17, no. 9, p. e0274625, 2022.

[18] T. Hens and J. Mayer, "Cumulative prospect theory and mean variance analysis: A rigorous comparison," *Swiss Finance Institute Research Paper*, no. 14-23, 2014.

[19] D. Kahneman and A. Tversky, "Prospect theory: an analysis of decisions under risk." *Econometrica*, vol. 47, pp. 263–291, 1979.

[20] A. O. Hoffmann, H. Shefrin, and J. M. Pennings, "Behavioral portfolio analysis of individual investors," *Available at SSRN 1629786*, 2010.

[21] P. N. Kolm, R. Tütüncü, and F. J. Fabozzi, "60 years of portfolio optimization: Practical challenges and current trends," *European Journal of Operational Research*, vol. 234, no. 2, pp. 356–371, 2014.

[22] J. J. Choi, D. Laibson, and B. C. Madrian, "Mental accounting in portfolio choice: Evidence from a flypaper effect," *American Economic Review*, vol. 99, no. 5, pp. 2085–2095, 2009.

[23] D. Li and W.-L. Ng, "Optimal dynamic portfolio selection: Multiperiod mean-variance formulation," *Mathematical Finance*, vol. 10, no. 3, pp. 387–406, 2000.

[24] R. D. Harris and M. Mazibas, "Portfolio optimization with behavioural preferences and investor memory," *European Journal of Operational Research*, vol. 296, no. 1, pp. 368–387, 2022.

[25] R. Storn and K. Price, "Differential evolution–a simple and efficient heuristic for global optimization over continuous spaces," *Journal of Global Optimization*, vol. 11, pp. 341–359, 1997.

[26] M. Ghasemi, E. Akbari, A. Rahimnejad, S. E. Razavi, S. Ghavidel, and L. Li, "Phasor particle swarm optimization: a simple and efficient variant of pso," *Soft Computing*, vol. 23, pp. 9701–9718, 2019.

[27] F. J. Fabozzi, D. Huang, and G. Zhou, "Robust portfolios: contributions from operations research and finance," *Annals of Operations Research*, vol. 176, pp. 191–220, 2010.

[28] M. Dai, Y. Jia, and H. Jin, "Dynamic mean-variance portfolio selection with transaction costs," *Available at SSRN*, 2024.

[29] S. Guo, J.-W. Gu, and W.-K. Ching, "Adaptive online portfolio selection with transaction costs," *European Journal of Operational Research*, vol. 295, no. 3, pp. 1074–1086, 2021.

[30] S. Ceria, A. Saxena, and R. A. Stubbs, "Factor alignment problems and quantitative portfolio management," *Journal of Portfolio Management*, vol. 38, no. 2, p. 29, 2012.

[31] M. Borkovec, I. Domowitz, B. Kiernan, and V. Serbin, "Portfolio optimization and the cost of trading," *The Journal of Investing*, vol. 19, no. 2, pp. 63–76, 2010.

[32] C. Fu, A. Lari-Lavassani, and X. Li, "Dynamic mean–variance portfolio selection with borrowing constraint," *European Journal of Operational Research*, vol. 200, no. 1, pp. 312–319, 2010.

[33] X. Li, A. S. Uysal, and J. M. Mulvey, "Multi-period portfolio optimization using model predictive control with mean-variance and risk parity frameworks," *European Journal of Operational Research*, vol. 299, no. 3, pp. 1158–1176, 2022.

[34] H. Yao, Z. Li, and D. Li, "Multi-period mean-variance portfolio selection with stochastic interest rate and uncontrollable liability," *European Journal of Operational Research*, vol. 252, no. 3, pp. 837–851, 2016.

[35] J. Mossin, "Optimal multiperiod portfolio policies," *The Journal of Business*, vol. 41, no. 2, pp. 215–229, 1968.

[36] P. A. Samuelson, "Lifetime portfolio selection by dynamic stochastic programming," *Stochastic Optimization Models in Finance*, pp. 517–524, 1975.

[37] N. Gârleanu and L. H. Pedersen, "Dynamic trading with predictable returns and transaction costs," *The Journal of Finance*, vol. 68, no. 6, pp. 2309–2340, 2013.

[38] S. Boyd, E. Busseti, S. Diamond, R. N. Kahn, K. Koh, P. Nystrup, J. Speth *et al.*, "Multi-period trading via convex optimization," *Foundations and Trends® in Optimization*, vol. 3, no. 1, pp. 1–76, 2017.

[39] X. Cui, J. Gao, Y. Shi, and S. Zhu, "Time-consistent and self-coordination strategies for multi-period mean-conditional value-at-risk portfolio selection," *European Journal of Operational Research*, vol. 276, no. 2, pp. 781–789, 2019.

[40] C. H. Chiu and X. Y. Zhou, "The premium of dynamic trading," *Quantitative Finance*, vol. 11, no. 1, pp. 115–123, 2011.

[41] H. Konno and H. Yamazaki, "Mean-absolute deviation portfolio optimization model and its applications to tokyo stock market," *Management Science*, vol. 37, no. 5, pp. 519–531, 1991.

[42] J. Kettunen and M. A. Lejeune, "Data-driven project portfolio selection: Decision-dependent stochastic programming formulations with reliability and time to market requirements," *Computers & Operations Research*, vol. 143, p. 105737, 2022.

[43] F. Z. Xing, E. Cambria, and R. E. Welsch, "Intelligent asset allocation via market sentiment views," *IEEE Computational Intelligence Magazine*, vol. 13, no. 4, pp. 25–34, 2018.

[44] F. Z. Xing, E. Cambria, and Y. Zhang, "Sentiment-aware volatility forecasting," *Knowledge-Based Systems*, vol. 176, pp. 68–76, 2019.

[45] F. Z. Xing, E. Cambria, L. Malandri, and C. Vercellis, "Discovering bayesian market views for intelligent asset allocation," in *Joint European Conference on Machine Learning and Knowledge Discovery in Databases.* Springer, 2018, pp. 120–135.

[46] P. Jorion, *Value at risk: the new benchmark for controlling market risk.* New York: The McGraw-Hill Companies, 1997.

[47] T. J. Linsmeier and N. D. Pearson, "Value at risk," *Financial Analysts Journal*, vol. 56, no. 2, pp. 47–67, 2000.

[48] P. Artzner, "Thinking coherently," *Risk*, vol. 10, pp. 68–71, 1997.

[49] R. T. Rockafellar and S. Uryasev, "Conditional value-at-risk for general loss distributions," *Journal of Banking & Finance*, vol. 26, no. 7, pp. 1443–1471, 2002.

[50] G. C. Pflug, "Some remarks on the value-at-risk and the conditional value-at-risk," *Probabilistic Constrained Optimization: Methodology and Applications*, pp. 272–281, 2000.

[51] C. Ren, Z. Wei, Y. Zhou, S. Chen, H. Han, G. Sun, H. Zang, and W. Ji, "Distributionally robust cvar optimization for resilient distribution system planning with consideration for long-term and short-term uncertainties," *Reliability Engineering & System Safety*, vol. 251, p. 110378, 2024.

[52] Q. Zhang, S. Leng, X. Ma, Q. Liu, X. Wang, B. Liang, Y. Liu, and J. Yang, "Cvar-constrained policy optimization for safe reinforcement learning," *IEEE Transactions on Neural Networks and Learning Systems*, 2024.

[53] R. Bedoui, R. Benkraiem, K. Guesmi, and I. Kedidi, "Portfolio optimization through hybrid deep learning and genetic algorithms vine copula-garch-evt-cvar model," *Technological Forecasting and Social Change*, vol. 197, p. 122887, 2023.

[54] A. Biglova, S. Ortobelli, S. T. Rachev, and S. Stoyanov, "Different approaches to risk estimation in portfolio theory," *The Journal of Portfolio Management*, vol. 31, no. 1, pp. 103–112, 2004.

[55] X. Gong, C. Yu, L. Min, and Z. Ge, "Regret theory-based fuzzy multi-objective portfolio selection model involving dea cross-efficiency and higher moments," *Applied Soft Computing*, vol. 100, p. 106958, 2021.

[56] W. Chen, D. Li, S. Lu, and W. Liu, "Multi-period mean–semivariance portfolio optimization based on uncertain measure," *Soft Computing*, vol. 23, pp. 6231–6247, 2019.

[57] L. Dymova, K. Kaczmarek, and P. Sevastjanov, "A new approach to the bi-criteria multi-period fuzzy portfolio selection," *Knowledge-Based Systems*, vol. 234, p. 107582, 2021.

[58] Y.-J. Liu, W.-G. Zhang, and W.-J. Xu, "Fuzzy multi-period portfolio selection optimization models using multiple criteria," *Automatica*, vol. 48, no. 12, pp. 3042–3053, 2012.

[59] M. K. Mehlawat, P. Gupta, and A. Z. Khan, "Multiobjective portfolio optimization using coherent fuzzy numbers in a credibilistic environment," *International Journal of Intelligent Systems*, vol. 36, no. 4, pp. 1560–1594, 2021.

[60] N. Mansour, M. S. Cherif, and W. Abdelfattah, "Multi-objective imprecise programming for financial portfolio selection with fuzzy returns," *Expert Systems with Applications*, vol. 138, p. 112810, 2019.

[61] H. Xu, P. Liu, and F. Teng, "Two prospect theory-based decision-making models using data envelopment analysis with hesitant fuzzy linguistic information," *Information Sciences*, vol. 582, pp. 415–438, 2022.

[62] A. Gu and H. I. Yoo, "Prospect theory and mutual fund flows," *Economics Letters*, vol. 201, p. 109776, 2021.

[63] R. E. Bellman and L. A. Zadeh, "Decision-making in a fuzzy environment," *Management Science*, vol. 17, no. 4, pp. B–141, 1970.

[64] W. Zimmermann, "Reduction in the number of coupling parameters," *Communications in Mathematical Physics*, vol. 97, pp. 211–225, 1985.

[65] Q. Wu, X. Liu, J. Qin, L. Zhou, A. Mardani, and M. Deveci, "An integrated generalized todim model for portfolio selection based on financial performance of firms," *Knowledge-Based Systems*, vol. 249, p. 108794, 2022.

[66] A. Tversky and D. Kahneman, "Advances in prospect theory: Cumulative representation of uncertainty," *Journal of Risk and Uncertainty*, vol. 5, pp. 297–323, 1992.

[67] H. Shefrin and M. Statman, "Behavioral portfolio theory," *Journal of Financial and Quantitative Analysis*, vol. 35, no. 2, pp. 127–151, 2000.

[68] A. D. Roy, "Safety first and the holding of assets," *Econometrica: Journal of the econometric society*, pp. 431–449, 1952.

[69] L. G. Telser, "Safety first and hedging," *The Review of Economic Studies*, vol. 23, no. 1, pp. 1–16, 1955.

[70] L. L. Lopes, "Between hope and fear: The psychology of risk," in *Advances in Experimental Social Psychology.* Elsevier, 1987, vol. 20, pp. 255–295.

[71] S. Das, H. Markowitz, J. Scheid, and M. Statman, "Portfolio optimization with mental accounts," *Journal of Financial and Quantitative Analysis*, vol. 45, no. 2, pp. 311–334, 2010.

[72] B. Mandelbrot, "New methods in statistical economics," *Journal of Political Economy*, vol. 71, no. 5, pp. 421–440, 1963.

[73] H. Levy and M. Levy, "Prospect theory and mean-variance analysis," *Review of Financial Studies*, vol. 17, no. 4, pp. 1015–1041, 2004.

[74] H. Levy, E. G. De Giorgi, and T. Hens, "Two paradigms and nobel prizes in economics: a contradiction or coexistence?" *European Financial Management*, vol. 18, no. 2, pp. 163–182, 2012.

[75] D. Kahneman and A. Tversky, "Prospect theory: An analysis of decision under risk," in *Handbook of the fundamentals of financial decision making: Part I*. World Scientific, 2013, pp. 99–127.

[76] X. Wang, B. Wang, S. Liu, H. Li, T. Wang, and J. Watada, "Fuzzy portfolio selection based on three-way decision and cumulative prospect theory," *International Journal of Machine Learning and Cybernetics*, vol. 13, no. 1, pp. 293–308, 2022.

[77] X. Zhou, L. Wang, H. Liao, S. Wang, B. Lev, and H. Fujita, "A prospect theory-based group decision approach considering consensus for portfolio selection with hesitant fuzzy information," *Knowledge-Based Systems*, vol. 168, pp. 28–38, 2019.

[78] G. M. Ferro, T. Kovalenko, and D. Sornette, "Quantum decision theory augments rank-dependent expected utility and cumulative prospect theory," *Journal of Economic Psychology*, vol. 86, p. 102417, 2021.

[79] K. Gao, L. Sun, Y. Yang, F. Meng, and X. Qu, "Cumulative prospect theory coupled with multi-attribute decision making for modeling travel behavior," *Transportation Research Part A: Policy and Practice*, vol. 148, pp. 1–21, 2021.

[80] A. Grant, D. Johnstone, and O. K. Kwon, "A cumulative prospect theory explanation of gamblers cashing-out," *Journal of Mathematical Psychology*, vol. 102, p. 102534, 2021.

[81] C. Fulga, "Portfolio optimization under loss aversion," *European Journal of Operational Research*, vol. 251, no. 1, pp. 310–322, 2016.

[82] X. Tian, Z. Xu, J. Gu, and E. Herrera-Viedma, "How to select a promising enterprise for venture capitalists with prospect theory under intuitionistic fuzzy circumstance?" *Applied Soft Computing*, vol. 67, pp. 756–763, 2018.

[83] R. A. Krohling and T. T. de Souza, "Combining prospect theory and fuzzy numbers to multi-criteria decision making," *Expert Systems with Applications*, vol. 39, no. 13, pp. 11 487–11 493, 2012.

[84] A. Baillon, H. Bleichrodt, and V. Spinu, "Searching for the reference point," *Management Science*, vol. 66, no. 1, pp. 93–112, 2020.

[85] G. A. Akerlof and W. T. Dickens, "The economic consequences of cognitive dissonance," *The American Economic Review*, vol. 72, no. 3, pp. 307–319, 1982.

[86] F. Gul, "A theory of disappointment aversion," *Econometrica: Journal of the Econometric Society*, pp. 667–686, 1991.

[87] G. Loomes and R. Sugden, "Disappointment and dynamic consistency in choice under uncertainty," *The Review of Economic Studies*, vol. 53, no. 2, pp. 271–282, 1986.

[88] M. K. Brunnermeier and J. A. Parker, "Optimal expectations," *American Economic Review*, vol. 95, no. 4, pp. 1092–1118, 2005.

[89] C. Gollier and A. Muermann, "Optimal choice and beliefs with ex ante savoring and ex post disappointment," *Management Science*, vol. 56, no. 8, pp. 1272–1284, 2010.

[90] M. J. Best and R. R. Grauer, "Prospect theory and portfolio selection," *Journal of Behavioral and Experimental Finance*, vol. 11, pp. 13–17, 2016.

[91] X. D. He and M. S. Strub, "How endogenization of the reference point affects loss aversion: a study of portfolio selection," *Operations Research*, vol. 70, no. 6, pp. 3035–3053, 2022.

[92] D. E. Bell, "Disappointment in decision making under uncertainty," *Operations Research*, vol. 33, no. 1, pp. 1–27, 1985.

[93] A. Cillo and P. Delquié, "Mean-risk analysis with enhanced behavioral content," *European Journal of Operational Research*, vol. 239, no. 3, pp. 764–775, 2014.

[94] A. A. Marley and R. D. Luce, "Independence properties vis-à-vis several utility representations," *Theory and Decision*, vol. 58, pp. 77–143, 2005.

[95] M. H. Birnbaum, "New paradoxes of risky decision making." *Psychological Review*, vol. 115, no. 2, p. 463, 2008.

[96] P. C. Fishburn, "Ssb utility theory: An economic perspective," *Mathematical Social Sciences*, vol. 8, no. 1, pp. 63–94, 1984.

[97] J. M. Miyamoto and P. Wakker, "Multiattribute utility theory without expected utility foundations," *Operations Research*, vol. 44, no. 2, pp. 313–326, 1996.

[98] H. Zank, "On probabilities and loss aversion," *Theory and Decision*, vol. 68, pp. 243–261, 2010.

[99] H. Bleichrodt and J. Miyamoto, "A characterization of quality-adjusted life-years under cumulative prospect theory," *Mathematics of Operations Research*, vol. 28, no. 1, pp. 181–193, 2003.

[100] A. M. Eltamaly, "A novel strategy for optimal pso control parameters determination for pv energy systems," *Sustainability*, vol. 13, no. 2, p. 1008, 2021.

[101] K. R. Harrison, A. P. Engelbrecht, and B. M. Ombuki-Berman, "Optimal parameter regions and the time-dependence of control parameter values for the particle swarm optimization algorithm," *Swarm and Evolutionary Computation*, vol. 41, pp. 20–35, 2018.

[102] P. N. Suganthan, "Particle swarm optimiser with neighbourhood operator," in *Proceedings of the 1999 Congress on Evolutionary Computation*, vol. 3. IEEE, 1999, pp. 1958–1962.

[103] J.-J. Liang and P. N. Suganthan, "Dynamic multi-swarm particle swarm optimizer," in *Proceedings 2005 IEEE Swarm Intelligence Symposium*. IEEE, 2005, pp. 124–129.

[104] C.-C. Peng and C.-H. Chen, "Compensatory neural fuzzy network with symbiotic particle swarm optimization for temperature control," *Applied Mathematical Modelling*, vol. 39, no. 1, pp. 383–395, 2015.

[105] W.-D. Chang, "A modified particle swarm optimization with multiple subpopulations for multimodal function optimization problems," *Applied Soft Computing*, vol. 33, pp. 170–182, 2015.

[106] B. Al-Kazemi and C. K. Mohan, "Multi-phase generalization of the particle swarm optimization algorithm," in *Proceedings of the 2002 Congress on Evolutionary Computation*, vol. 1. IEEE, 2002, pp. 489–494.

[107] C. Yang and D. Simon, "A new particle swarm optimization technique," in *18th International Conference on Systems Engineering*. IEEE, 2005, pp. 164–169.

[108] A. Leontitsis, D. Kontogiorgos, and J. Pagge, "Repel the swarm to the optimum!" *Applied Mathematics and Computation*, vol. 173, no. 1, pp. 265–272, 2006.

[109] N. Himanshu and A. Burman, "Determination of critical failure surface of slopes using particle swarm optimization technique considering seepage and seismic loading," *Geotechnical and Geological Engineering*, vol. 37, pp. 1261–1281, 2019.

[110] G. A. F. Alfarisy, W. F. Mahmudy, and M. H. Natsir, "Optimizing laying hen diet using multi-swarm particle swarm optimization," *TELKOMNIKA (Telecommunication Computing Electronics and Control)*, vol. 16, no. 4, pp. 1712–1723, 2018.

[111] A. P. Piotrowski, J. J. Napiorkowski, and A. E. Piotrowska, "Population size in particle swarm optimization," *Swarm and Evolutionary Computation*, vol. 58, p. 100718, 2020.

[112] D. Wang, D. Tan, and L. Liu, "Particle swarm optimization algorithm: an overview," *Soft Computing*, vol. 22, pp. 387–408, 2018.

[113] Z. Beheshti and S. M. H. Shamsuddin, "Capso: centripetal accelerated particle swarm optimization," *Information Sciences*, vol. 258, pp. 54–79, 2014.

[114] E. Koessler and A. Almomani, "Hybrid particle swarm optimization and pattern search algorithm," *Optimization and Engineering*, vol. 22, pp. 1539–1555, 2021.

[115] Z. Yang and A. Wu, "A non-revisiting quantum-behaved particle swarm optimization based multilevel thresholding for image segmentation," *Neural Computing and Applications*, vol. 32, pp. 12 011–12 031, 2020.

[116] R. C. Eberhart and Y. Shi, "Tracking and optimizing dynamic systems with particle swarms," in *Proceedings of the 2001 Congress on Evolutionary Computation (IEEE Cat. No. 01TH8546)*, vol. 1. IEEE, 2001, pp. 94–100.

[117] A. Ratnaweera, S. K. Halgamuge, and H. C. Watson, "Self-organizing hierarchical particle swarm optimizer with time-varying acceleration coefficients," *IEEE Transactions on Evolutionary Computation*, vol. 8, no. 3, pp. 240–255, 2004.

[118] R. Poli, J. Kennedy, and T. Blackwell, "Particle swarm optimization: An overview," *Swarm Intelligence*, vol. 1, pp. 33–57, 2007.

[119] P. J. Angeline, "Evolutionary optimization versus particle swarm optimization: Philosophy and performance differences," in *International Conference on Evolutionary Programming*. Springer, 1998, pp. 601–610.

[120] ——, "Using selection to improve particle swarm optimization," in *1998 IEEE International Conference on Evolutionary Computation Proceedings. IEEE World Congress on Computational Intelligence*. IEEE, 1998, pp. 84–89.

[121] M. Lovbjerg, T. K. Rasmussen, T. Krink *et al.*, "Hybrid particle swarm optimiser with breeding and subpopulations," in *Proceedings of the Genetic and Evolutionary Computation Conference*, vol. 2001. San Francisco, USA, 2001, pp. 469–476.

[122] Y. Chen, Y. Feng, and X. Li, "A parallel system for adaptive optics based on parallel mutation pso algorithm," *Optik*, vol. 125, no. 1, pp. 329–332, 2014.

[123] S. Tsafarakis, C. Saridakis, G. Baltas, and N. Matsatsinis, "Hybrid particle swarm optimization with mutation for optimizing industrial product lines: An application to a mixed solution space considering both discrete and continuous design variables," *Industrial Marketing Management*, vol. 42, no. 4, pp. 496–506, 2013.

[124] H. Wang, Z. Wu, S. Rahnamayan, Y. Liu, and M. Ventresca, "Enhancing particle swarm optimization using generalized opposition-based learning," *Information Sciences*, vol. 181, no. 20, pp. 4699–4714, 2011.

[125] A. Meng, Z. Li, H. Yin, S. Chen, and Z. Guo, "Accelerating particle swarm optimization using crisscross search," *Information Sciences*, vol. 329, pp. 52–72, 2016.

[126] K. E. Parsopoulos and M. N. Vrahatis, "On the computation of all global minimizers through particle swarm optimization," *IEEE Transactions on Evolutionary Computation*, vol. 8, no. 3, pp. 211–224, 2004.

[127] Y.-X. Jin, H.-Z. Cheng, J.-Y. Yan, and L. Zhang, "Local optimum embranchment based convergence guarantee particle swarm optimization and its application in transmission network planning," in *2005 IEEE/PES Transmission & Distribution Conference & Exposition: Asia and Pacific*. IEEE, 2005, pp. 1–6.

[128] R. Brits, A. P. Engelbrecht, and F. van den Bergh, "Scalability of niche pso," in *Proceedings of the 2003 IEEE Swarm Intelligence Symposium. SIS'03 (Cat. No. 03EX706)*. IEEE, 2003, pp. 228–234.

[129] R. Brits, A. Engelbrecht, and F. Van den Bergh, "Solving systems of unconstrained equations using particle swarm optimization," in *IEEE International Conference on Systems, Man and Cybernetics*, vol. 3. IEEE, 2002, pp. 6–pp.

[130] I. Schoeman and A. Engelbrecht, "A parallel vector-based particle swarm optimizer," in *Adaptive and Natural Computing Algorithms: Proceedings of the International Conference in Coimbra, Portugal, 2005*. Springer, 2005, pp. 268–271.

[131] M. Lovbjerg and T. Krink, "Extending particle swarm optimisers with self-organized criticality," in *Proceedings of the 2002 Congress on Evolutionary Computation*, vol. 2. IEEE, 2002, pp. 1588–1593.

[132] M. Clerc, "The swarm and the queen: towards a deterministic and adaptive particle swarm optimization," in *Proceedings of the 1999 Congress on Evolutionary Computation*, vol. 3. IEEE, 1999, pp. 1951–1957.

[133] W. Fang, J. Sun, H. Chen, and X. Wu, "A decentralized quantum-inspired particle swarm optimization algorithm with cellular structured population," *Information Sciences*, vol. 330, pp. 19–48, 2016.

[134] Narendra and Fukunaga, "A branch and bound algorithm for feature subset selection," *IEEE Transactions on Computers*, vol. 100, no. 9, pp. 917–922, 1977.

[135] B. H. Nguyen, B. Xue, and M. Zhang, "A survey on swarm intelligence approaches to feature selection in data mining," *Swarm and Evolutionary Computation*, vol. 54, p. 100663, 2020.

[136] Q. Al-Tashi, H. M. Rais, S. J. Abdulkadir, and S. Mirjalili, "Feature selection based on grey wolf optimizer for oil & gas reservoir classification," in *2020 International Conference on Computational Intelligence (ICCI)*. IEEE, 2020, pp. 211–216.

[137] B. Ji, X. Lu, G. Sun, W. Zhang, J. Li, and Y. Xiao, "Bio-inspired feature selection: An improved binary particle swarm optimization approach," *IEEE Access*, vol. 8, pp. 85 989–86 002, 2020.

[138] B. Xiong, Y. Li, M. Huang, W. Shi, M. Du, and Y. Yang, "Feature selection of input variables for intelligence joint moment prediction based on binary particle swarm optimization," *IEEE Access*, vol. 7, pp. 182 289–182 295, 2019.

[139] J. Too, A. R. Abdullah, and N. Mohd Saad, "A new co-evolution binary particle swarm optimization with multiple inertia weight strategy for feature selection," in *Informatics*, vol. 6, no. 2. MDPI, 2019, p. 21.

[140] ——, "Hybrid binary particle swarm optimization differential evolution-based feature selection for emg signals classification," *Axioms*, vol. 8, no. 3, p. 79, 2019.

[141] B. Xia, T. Liu, T. Ding, and Z. Wang, "An improved pso localization algorithm for uwb sensor networks," *Wireless Personal Communications*, vol. 117, pp. 2207–2223, 2021.

[142] Z.-J. Teng, L.-Y. Xie, H.-L. Chen, and H. Zhang, "Application research of chaotic binary particle swarm optimization algorithm in dynamic spectrum allocation," *Journal of Computers*, vol. 31, no. 4, pp. 288–299, 2020.

[143] V. D. P. Souto, R. D. Souza, B. F. Uchoa-Filho, A. Li, and Y. Li, "Beamforming optimization for intelligent reflecting surfaces without csi," *IEEE Wireless Communications Letters*, vol. 9, no. 9, pp. 1476–1480, 2020.

[144] X. Chen, J. Zhang, B. Lin, Z. Chen, K. Wolter, and G. Min, "Energy-efficient offloading for dnn-based smart iot systems in cloud-edge environments," *IEEE Transactions on Parallel and Distributed Systems*, vol. 33, no. 3, pp. 683–697, 2021.

[145] J. S. Priya, M. Femina, and R. Samuel, "Apso-mvs: an adaptive particle swarm optimization incorporating multiple velocity strategies for optimal leader selection in hybrid manets," *Soft Computing*, vol. 24, pp. 18 349–18 365, 2020.

[146] S. Jiang, Y. Wang, and Z. Ji, "A new design method for adaptive iir system identification using hybrid particle swarm optimization and gravitational search algorithm," *Nonlinear Dynamics*, vol. 79, pp. 2553–2576, 2015.

[147] X. Zhang, D. Lu, X. Zhang, and Y. Wang, "Antenna array design by a contraction adaptive particle swarm optimization algorithm," *EURASIP Journal on Wireless Communications and Networking*, vol. 2019, pp. 1–7, 2019.

[148] R. V. Kulkarni and G. K. Venayagamoorthy, "Particle swarm optimization in wireless-sensor networks: A brief survey," *IEEE Transactions on Systems, Man, and Cybernetics, Part C (Applications and Reviews)*, vol. 41, no. 2, pp. 262–267, 2010.

[149] J. Chen, S. Huang, H. Li, X. Lv, and Y. Cai, "Pso-based agent cooperative spectrum sensing in cognitive radio networks," *IEEE Access*, vol. 7, pp. 142 963–142 973, 2019.

[150] G. Eappen and T. Shankar, "Hybrid pso-gsa for energy efficient spectrum sensing in cognitive radio network," *Physical Communication*, vol. 40, p. 101091, 2020.

[151] S. K. Ghosh, B. Biswas, and A. Ghosh, "A novel approach of retinal image enhancement using pso system and measure of fuzziness," *Procedia Computer Science*, vol. 167, pp. 1300–1311, 2020.

[152] M. M. S. Rani and P. Chitra, "A hybrid medical image coding method based on haar wavelet transform and particle swarm optimization technique," *International Journal of Pure and Applied Mathematics*, vol. 118, no. 8, pp. 3056–3067, 2018.

[153] X. Kang, Y. Chen, F. Zhao, and G. Lin, "Multi-dimensional particle swarm optimization for robust blind image watermarking using intertwining logistic map and hybrid domain," *Soft Computing*, vol. 24, pp. 10 561–10 584, 2020.

[154] M. Jamil and X.-S. Yang, "A literature survey of benchmark functions for global optimisation problems," *International Journal of Mathematical Modelling and Numerical Optimisation*, vol. 4, no. 2, pp. 150–194, 2013.

[155] V. S. Gordon and D. Whitley, "Serial and parallel genetic algorithms as function optimizers," in *ICGA*, 1993, pp. 177–183.

[156] D. Whitley, S. Rana, J. Dzubera, and K. E. Mathias, "Evaluating evolutionary algorithms," *Artificial Intelligence*, vol. 85, no. 1-2, pp. 245–276, 1996.

[157] P. H. Winston, *Artificial intelligence*. Addison-Wesley Longman Publishing Co., Inc., 1992.

[158] C.-J. Chung and R. G. Reynolds, "Caep: An evolution-based tool for real-valued function optimization using cultural algorithms," *International Journal on Artificial Intelligence Tools*, vol. 7, no. 03, pp. 239–291, 1998.

[159] D. Ortiz-Boyer, C. Hervás-Martínez, and N. Garcia-Pedrajas, "Cixl2: A crossover operator for evolutionary algorithms based on population features," *Journal of Artificial Intelligence Research*, vol. 24, pp. 1–48, 2005.

[160] X. Yao and Y. Liu, "Fast evolutionary programming." *Evolutionary Programming*, vol. 3, pp. 451–460, 1996.

[161] R. Shang, Y. Wang, J. Wang, L. Jiao, S. Wang, and L. Qi, "A multi-population cooperative coevolutionary algorithm for multi-objective capacitated arc routing problem," *Information Sciences*, vol. 277, pp. 609–642, 2014.

[162] B. Wang, Y. Li, S. Wang, and J. Watada, "A multi-objective portfolio selection model with fuzzy value-at-risk ratio," *IEEE Transactions on Fuzzy Systems*, vol. 26, no. 6, pp. 3673–3687, 2018.

[163] M. A. Potter and K. A. D. Jong, "Cooperative coevolution: An architecture for evolving coadapted subcomponents," *Evolutionary Computation*, vol. 8, no. 1, pp. 1–29, 2000.

[164] X. Wang, Y. Ouyang, Y. Li, S. Liu, L. Teng, and B. Wang, "Multi-objective portfolio selection considering expected and total utility," *Finance Research Letters*, vol. 58, p. 104552, 2023.

[165] L. A. Zadeh, "Fuzzy sets," *Information and Control*, 1965.

[166] D. Dubois and H. Prade, "Possibility theory," in *Granular, Fuzzy, and Soft Computing.* Springer, 1988.

[167] Z. Wang and T. He, "Multi-period portfolio with a dynamic reference point considering disappointment feelings," *Journal of the Operational Research Society*, vol. 73, no. 5, pp. 1073–1084, 2022.

[168] X. Wang, B. Wang, L. Teng, and Y. Wu, "Prospect theory-based portfolio selection using multiple fuzzy reference intervals," *IEEE Transactions on Systems, Men and Cybernetics: Systems*, Accepted, to be appear soon.

[169] R. Oprea, "Simplicity equivalents," *Working Paper*, 2022.

[170] J. Chapman, E. Snowberg, S. W. Wang, and C. Camerer, "Looming large or seeming small? attitudes towards losses in a representative sample," National Bureau of Economic Research, Tech. Rep., 2022.

[171] X. T. Wang, "Decision heuristics as predictors of public choice," *Journal of Behavioral Decision Making*, vol. 21, no. 1, pp. 77–89, 2008.

[172] G. J. Koop and J. G. Johnson, "The use of multiple reference points in risky decision making," *Journal of Behavioral Decision Making*, vol. 25, no. 1, pp. 49–62, 2012.

[173] M. Pfiffelmann, T. Roger, and O. Bourachnikova, "When behavioral portfolio theory meets markowitz theory," *Economic Modelling*, vol. 53, pp. 419–435, 2016.

[174] X. T. Wang and J. G. Johnson, "A tri-reference point theory of decision making under risk." *Journal of Experimental Psychology: General*, vol. 141, no. 4, p. 743, 2012.

[175] S. Srivastava, A. Aggarwal, and A. Mehra, "Portfolio selection by cumulative prospect theory and its comparison with mean-variance model," *Granular Computing*, vol. 7, no. 4, pp. 903–916, 2022.

[176] X. Wang, B. Wang, T. Li, H. Li, and J. Watada, "Multi-criteria fuzzy portfolio selection based on three-way decisions and cumulative prospect theory," *Applied Soft Computing*, vol. 134, p. 110033, 2023.

[177] B. Liu and K. Iwamura, "Chance constrained programming with fuzzy parameters," *Fuzzy Sets and Systems*, vol. 94, no. 2, pp. 227–237, 1998.

[178] B. Liu and Y.-K. Liu, "Expected value of fuzzy variable and fuzzy expected value models," *IEEE Transactions on Fuzzy Systems*, vol. 10, no. 4, pp. 445–450, 2002.

[179] Z. Qin and X. Ji, "Logistics network design for product recovery in fuzzy environment," *European Journal of Operational Research*, vol. 202, no. 2, pp. 479–490, 2010.

[180] I. Blecic, A. Cecchini, and G. A. Trunfio, "Fast and accurate optimization of a gpu-accelerated ca urban model through cooperative coevolutionary particle swarms," *Procedia Computer Science*, vol. 29, pp. 1631–1643, 2014.

[181] Z. Wang, Z. Zhan, S. Kwong, H. Jin, and J. Zhang, "Adaptive granularity learning distributed particle swarm optimization for large-scale optimization," *IEEE Transactions on Cybernetics*, vol. 51, no. 3, pp. 1175–1188, 2020.

[182] T. P. Lillicrap, J. J. Hunt, A. Pritzel, N. Heess, T. Erez, Y. Tassa, D. Silver, and D. Wierstra, "Continuous control with deep reinforcement learning," in *International Conference on Learning Representations*, 2016.

[183] R. Munos and A. Moore, "Variable resolution discretization in optimal control," *Machine Learning*, vol. 49, pp. 291–323, 2002.

[184] K. He, X. Zhang, S. Ren, and J. Sun, "Deep residual learning for image recognition," in *Proceedings of the IEEE Conference on Computer Vision and Pattern Recognition*, 2016, pp. 770–778.

[185] L. Deng and D. Yu, "Deep learning: methods and applications," *Foundations and Trends® in Signal Processing*, vol. 7, no. 3–4, pp. 197–387, 2014.

[186] K. Hornik, M. Stinchcombe, and H. White, "Universal approximation of an unknown mapping and its derivatives using multilayer feedforward networks," *Neural Networks*, vol. 3, no. 5, pp. 551–560, 1990.

[187] D. Silver, G. Lever, N. Heess, T. Degris, D. Wierstra, and M. Riedmiller, "Deterministic policy gradient algorithms," in *International Conference on Machine Learning.* Pmlr, 2014, pp. 387–395.

[188] R. Nian, J. Liu, and B. Huang, "A review on reinforcement learning: Introduction and applications in industrial process control," *Computers & Chemical Engineering*, vol. 139, p. 106886, 2020.

[189] G. E. Uhlenbeck and L. S. Ornstein, "On the theory of the brownian motion," *Physical Review*, vol. 36, no. 5, p. 823, 1930.

[190] S. Fujimoto, H. Hoof, and D. Meger, "Addressing function approximation error in actor-critic methods," in *International Conference on Machine Learning.* PMLR, 2018, pp. 1587–1596.

[191] K. Tang, X. Li, P. N. Suganthan, Z. Yang, and T. Weise, "Benchmark functions for the cec'2010 special session and competition on large-scale global optimization," *Nature Inspired Computation and Applications Laboratory, USTC, China, Tech. Rep*, 2009.

[192] J. Ammer, J. H. Rogers, G. Wang, and Y. Yu, "Visible hands: Professional asset managers' expectations and the stock market in china," *International Finance Discussion Paper*, no. 1362, 2022.

[193] W. Chen, S. Liang, and D. Shi, "What drives stock prices in a bubble?" *Available at SSRN 4449905*, 2023.

[194] S. Liang, *Essays on Retail Investor Behavior in Financial Markets.* Harvard University, 2023.

[195] N. Barberis, L. J. Jin, and B. Wang, "Prospect theory and stock market anomalies," *The Journal of Finance*, vol. 76, no. 5, pp. 2639–2687, 2021.

[196] R. T. Rockafellar, S. Uryasev *et al.*, "Optimization of conditional value-at-risk," *Journal of Risk*, vol. 2, pp. 21–42, 2000.

Appendix: Pseudocode of Algorithms

Algorithm 1 Improved Cooperative Particle Swarm Optimization algorithm

Input: $N, M, K, J(\cdot), \tau, C_1, C_2, \mathcal{T}$, constraints

for $i = 1$ to N **do**
  generate random $\mathcal{P}_i$
  $\mathcal{P}value_i = J(\mathcal{P}_i)$
  $\mathcal{P}best_i = \mathcal{P}_i$
end for
for $m = 1$ to M **do**
  $\mathcal{S}value_m = \min\{\mathcal{P}value_i, i \text{ in } m\text{th sub} - \text{swarm}\}$
  $\mathcal{S}best_m = \arg\min_{\mathcal{P}best_i}\{J(\mathcal{P}best_i), i \text{ in } m\text{th sub} - \text{swarm}\}$
end for
$\mathcal{G}value = \min\{\mathcal{P}value_i, i = 1, 2, \cdots N\}$
$\mathcal{G}best = \arg\min_{\mathcal{P}best_i}(J(\mathcal{P}best_i), i = 1, 2, \cdots N)$
for $t = 1$ to $\mathcal{T}$ **do**
  for $i = 1$ to N **do**
    if $\mathcal{P}_i$ and $\mathcal{S}best_m$ are different, **then**
      Iterate $\mathcal{P}_i$ using Equation 5.5
    else
      Iterate $\mathcal{P}_i$ using Equation 5.6
    end if
    if $J(\mathcal{P}_i) < \mathcal{P}value_i$ **then**

$\mathcal{P}best_i = \mathcal{P}_i$

$\mathcal{P}value_i = J(\mathcal{P}_i)$

end if

if $J(\mathcal{P}_i) < \mathcal{S}value_m$ **then**

$\mathcal{S}best_m = \mathcal{P}_i$

$\mathcal{S}value_m = J(\mathcal{P}_i)$

end if

if $J(\mathcal{P}_i) < \mathcal{G}value$ **then**

$\mathcal{G}best = \mathcal{P}_i$

$\mathcal{G}value = J(\mathcal{P}_i)$

end if

end for

end for

Output: $\mathcal{G}value$, $\mathcal{G}best$ =0

Algorithm 2 Updating learning rates by DDPG.

Input: $F_b(\cdot)$, D_b, N_b, T_b

Randomly initialize actor and critic network $\mu(s|\theta^\mu)$, $Q(s,a|\theta^Q)$ with weights θ^μ, θ^Q

Initialize target network μ' and Q' with weights $\theta^{\mu'} \leftarrow \theta^\mu, \theta^{Q'} \leftarrow \theta^Q$

Initialize replay buffer D_b

Initialize OU noise process $\mathcal{M}$

for episode= 1 to E, **do**

for $i = 1$ to N_b, **do**

Randomly generate position P_i and velocity V_i

$Pvalue_i \leftarrow F(P_i)$

$Pbest_i \leftarrow P_i$

end for

$Gvalue \leftarrow min\{Pvalue_i, i = 1, 2, \cdots, N_b\}$

$Gbest \leftarrow \underset{Pbest_i}{argmin}\{F_b(Pbest_i), i = 1, 2, \cdots, N_b\}$

for $t = 1$ to T_b, **do**

State $s_t \leftarrow Pbest$

Action $a_t \leftarrow \mu(s_t|\theta^{\mu}) + \mathcal{M}_t$

for $j = 1$ to N_b, **do**

Iterate V_j and P_j by rules in Equation 5.12

if $F_b(P_j) < Pvalue_j$ **then**

$Pbest_j = P_j$

$Pvalue_j = F_b(P_j)$

end if

end for

$Gvalue \leftarrow min\{Pvalue_j, i = 1, 2, \cdots, N_b\}$

$Gbest \leftarrow \underset{Pbest_i}{argmin}\{F_b(Pbest_i), i = 1, \cdots, N_b\}$

Reward $r_t \leftarrow -\Delta(Gvalue + \frac{1}{N}\sum_{i=1}^{N_b} Pvalue_i)$, and scale r to $[-0.1, 0.1]$

$s_{t+1} \leftarrow Pbest$

Store experience (s_t, a_t, r_t, s_{t+1}) into D_b

Randomly sample a minibatch of n experiences (s_i, a_i, r_i, s_{i+1}) from D_b

$y_i \leftarrow r_i + \gamma Q'(s_{i+1}, \mu'(s_{i+1}|\theta^{\mu'})|\theta^{Q'})$

Update the critic network by minimizing the loss by Equation 5.13.

Update the actor network by using the sampled policy gradient by Equation (5.14).

Update the target networks delayed and softly by Equation 5.15.

end for

end for

Output: a_t =0

Algorithm 3 Adaptive Cooperative Particle Swarm Optimization algorithm

Input: $F_o(\cdot)$, N_o, M, D_o, τ, C_1, C_2, T_o, constraints

for $i = 1$ to N **do**

generate random P_i

$Pvalue_i = J(P_i)$

$Pbest_i = P_i$

end for

for $m = 1$ to M **do**

$Svalue_m = \min\{Pvalue_i, i \text{ in } m_{\text{th}} \text{ sub} - \text{swarm}\}$

$Sbest_m = \underset{Pbest_i}{\arg\min}\{J(Pbest_i), i \text{ in } m_{\text{th}} \text{ sub} - \text{swarm}\}$

end for

$Gvalue = \min\{Pvalue_i, i = 1, 2, \cdots N_o\}$

$Gbest = \underset{Pbest_i}{\arg\min}(J(Pbest_i), i = 1, 2, \cdots N_o)$

for $t = 1$ to T_o **do**

for $i = 1$ to N_o **do**

if P_i and $Sbest_m$ are different, **then**

Iterate P_i using Equation 5.10

else

Iterate P_i using Equation 5.11

end if

if $F_o(P_i) < Pvalue_i$ **then**

$Pbest_i = P_i$

$Pvalue_i = F_o(P_i)$

end if

if $F_o(P_i) < Svalue_m$ **then**

$Sbest_m = P_i$

$Svalue_m = F_o(P_i)$

end if

if $F_o(P_i) < Gvalue$ **then**

$Gbest = P_i$

$Gvalue = F_o(P_i)$

end if

end for

end for

Output: $Gvalue$, $Gbest$ =0